QEX

$5

November/December 2015

www.arrl.org

A Forum for Communications Experimenters

Issue No. 293

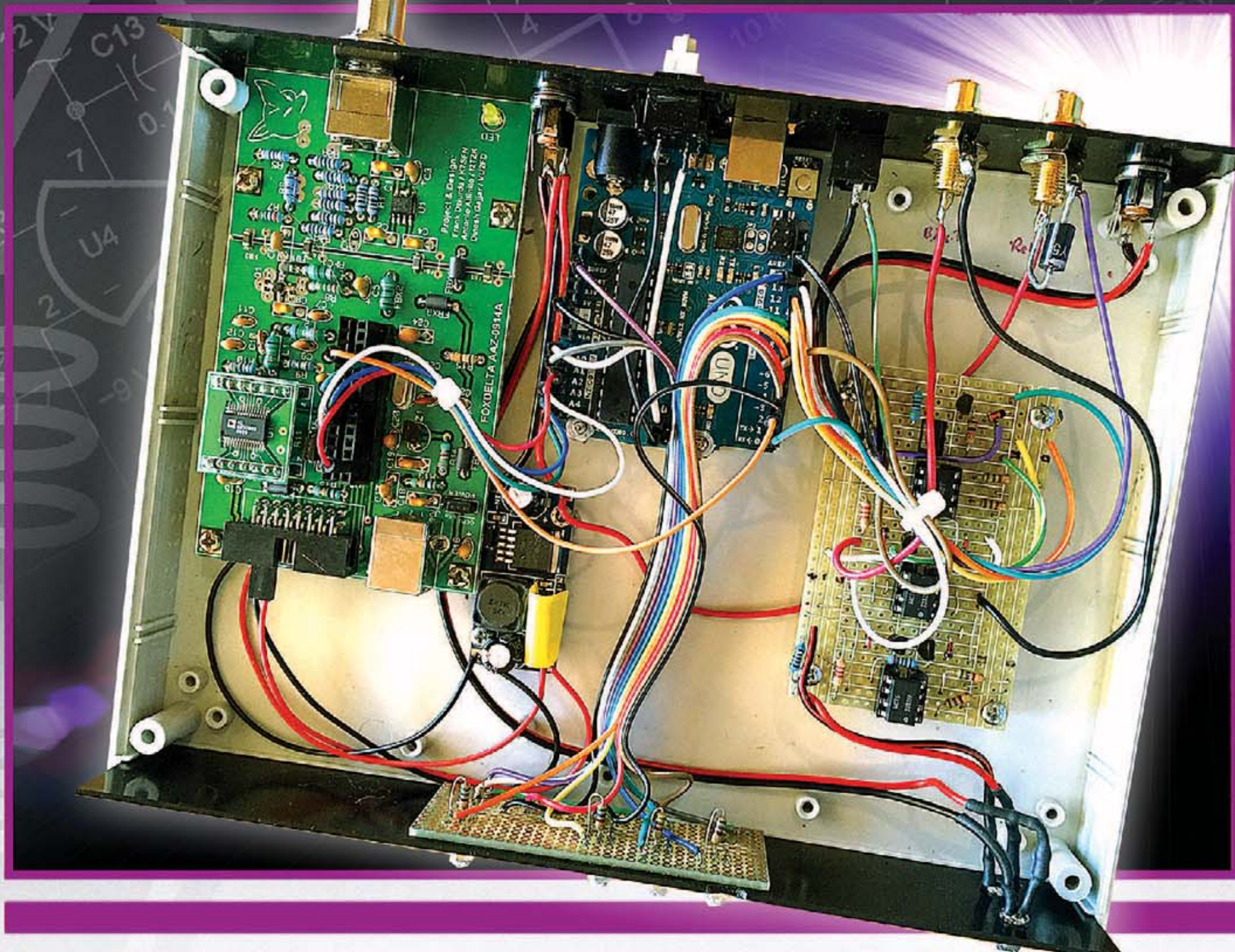

WBØOEW wanted to automatically tune his MFJ-1788 Magnetic Loop Antenna when operating with his Elecraft KX3 transceiver. His controller, shown here, could be adapted to other applications.

ARRL The national association for AMATEUR RADIO™
225 Main Street
Newington, CT USA 06111-1494

F/50MHz ALL MODE TRANSCEIVER TS-590

Nothing But Performance

The TS-590S

Kenwood has essentially redefined HF performance with the TS-590S compact HF transceiver. The TS-590S RX section sports IMD (intermodulation distortion) characteristics that are on par with those "top of the line" transceivers, not to mention having the best dynamic range in its class when handling unwanted, adjacent off-frequency signals.*

- **HF-50MHz 100W**
- **Digital IF Filters**
- **Built-in Antenna Tuner**
- **Advanced DSP from the IF stage forward**
- **500Hz and 2.7KHz roofing filters included**
- **Heavy duty TX section**

- **2 Color LCD**

KENWOOD

Customer Support: (310) 639-4200
Fax: (310) 537-8235

Scan with your phone to download TS-590S brochure.

www.kenwoodusa.com

ISO9001 Registered
Professional Systems Business Group
JVC KENWOOD Corporation
ADS#36812

* For 1.8/3.5/7/14/21 MHz Amateur bands, when receiving in CW/FSK/SSB modes, down conversion is automatically selected if the final passband is 2.7KHz or less.

QEX (ISSN: 0886-8093) is published bimonthly in January, March, May, July, September, and November by the American Radio Relay League, 225 Main Street, Newington, CT 06111-1494. Periodicals postage paid at Hartford, CT and at additional mailing offices.

POSTMASTER: Send address changes to: QEX, 225 Main St, Newington, CT 06111-1494
Issue No 293

Harold Kramer, WJ1B
Publisher

Larry Wolfgang, WR1B
Editor

Lori Weinberg, KB1EIB
Assistant Editor

Zack Lau, W1VT
Ray Mack, W5IFS
Contributing Editors

Production Department

Steve Ford, WB8IMY
Publications Manager

Michelle Bloom, WB1ENT
Production Supervisor

Sue Fagan, KB1OKW
Graphic Design Supervisor

David Pingree, N1NAS
Senior Technical Illustrator

Brian Washing
Technical Illustrator

Advertising Information Contact:

Janet L. Rocco, W1JLR
Business Services
860-594-0203 – Direct
800-243-7768 – ARRL
860-594-4285 – Fax

Circulation Department

Cathy Stepina, *QEX Circulation*

Offices

225 Main St, Newington, CT 06111-1494 USA
Telephone: 860-594-0200
Fax: 860-594-0259 (24 hour direct line)
e-mail: **qex@arrl.org**

Subscription rate for 6 issues:

In the US: ARRL Member $24, nonmember $36;

US by First Class Mail:
ARRL member $37, nonmember $49;

International and Canada by Airmail: ARRL member $31, nonmember $43;

Members are asked to include their membership control number or a label from their QST when applying.

In order to ensure prompt delivery, we ask that you periodically check the address information on your mailing label. If you find any inaccuracies, please contact the Circulation Department immediately. Thank you for your assistance.

About the Cover

Elwood Downey, WBØOEW, wanted to automatically tune his MFJ-1788 Magnetic Loop Antenna when operating with his Elecraft KX3 transceiver. His controller, shown on the cover, is described in this issue. You may be able to adapt his solution to other applications. Check it out!

In This Issue

Features

Index of Advertisers

The American Radio Relay League

The purpose of *QEX* is to:

1) provide a medium for the exchange of ideas and information among Amateur Radio experimenters,

2) document advanced technical work in the Amateur Radio field, and

3) support efforts to advance the state of the Amateur Radio art.

All correspondence concerning *QEX* should be addressed to the American Radio Relay League, 225 Main Street, Newington, CT 06111 USA. Envelopes containing manuscripts and letters for publication in *QEX* should be marked Editor, *QEX*.

Both theoretical and practical technical articles are welcomed. Manuscripts should be submitted in word-processor format, if possible. We can redraw any figures as long as their content is clear.
Photos should be glossy, color or black-and-white prints of at least the size they are to appear in *QEX* or high-resolution digital images (300 dots per inch or higher at the printed size). Further information for authors can be found on the Web at **www.arrl.org/qex/** or by e-mail to **qex@arrl.org**.

Larry Wolfgang, WR1B

Empirical Outlook

Reflections on Another Year Gone By

The last issue of the year always seems like a good time to pause and reflect on the past year. I like to think that helps give us some direction for the year to come, and helps set some goals that we can strive to meet in the new year. I want to encourage every one of you to spend a few minutes thinking about your past year, and where you are headed, as well.

For me, personally, I would have to say that 2015 has been a bit of a let-down in terms of Amateur Radio. Of course 2014, as the ARRL Centennial Year, had so many activities to participate in, and it was so much fun to be part of all that activity! I have been on the air more in 2015 than I had been in several years prior to 2014, but there were still times I went several weeks without turning on my radio. Well, that makes it easy to set a goal for 2016, doesn't it? I would strive to never go an entire week without at least one contact in the log.

One highlight for 2015 would have to be putting a new radio together and experiencing the joys of operating that new toy. As always, the time spent assembling a radio from a kit of parts is a lot of fun. There are few thrills in life that are better than putting a new radio on the air and making contacts with it, whether that radio is a commercial product or a homebrew — or perhaps even better, and home designed radio. Wouldn't you agree?

I have had a Raspberry Pi computer for several years. Although I have enjoyed trying some applications and even adding some hardware peripherals to experiment with. I am still frustrated with my lack of knowledge and experience with *Linux*. Several projects that I really want to get working are stuck in a "research" phase where I am trying to figure out what I have done wrong with *Linux*! I was somewhat gratified to have Ray Mack, W5IFS, tell me that he was stuck on some *Linux* question as he worked on a couple of his SDR Simplified columns. Ray seems to be rather familiar with all the *Linux* commands, and yet he ran into problems. Eventually he was able to find help to solve his problems, but I have not been as fortunate. Maybe 2016 will be my year to sort this out.

Speaking of the Raspberry Pi, I have mentioned my desire for some articles about what *you* are doing with this little computer. So far, we have not had any articles to print in *QEX* using these little devices. I know some of our readers have done some neat stuff with them. Write up the details and send it in!

Another one of my "back burner" projects is the implementation of a Broadband Hamnet local area network. I have picked up several of the previously recommended Linksys WRT54G wireless broadband routers, and successfully flashed the new firmware into them. They can talk to each other, and form the Broadband Hamnet network, and computers connected to them can see all of the network nodes. That's as far as I've gotten so far. Add one more goal for 2016 that should be easily within reach!

An article about setting up the hardware for such a network in another of my *QEX* wishes. At one point a local ham friend who has taken this much farther than I have was interested in writing an article, if I would help him put it together. Of course I was more than willing, and excited to collaborate with him. Some changes in his work life seem to have gobbled up the time he may have had to devote to the project, so I am still waiting. Again, I know that some of our readers have accomplished this. Here is a perfect opportunity to share your expertise with your fellow *QEX* readers!

I always enjoy hearing from readers with your thoughts about our articles,you're your suggestions for future *QEX* articles. Most of the correspondence I have received during 2015 has been about the change to a lighter weight paper, as well as using that same paper for the covers of *QEX*. There was a significant savings in paper and printing costs to do that, but there were also some downsides. Many of you have written with your thoughts and suggestions. I can't say that most of the comments were in favor of the savings, and quite a few of you indicated a willingness to pay a higher subscription rate. Obviously there is a lot to consider an any such decisions. As I've told everyone who wrote about the new paper stock, our ARRL Circulation Manager, Yvette Vinci, KC1AIM, has been compiling all of the comments, and they will be considered as any further changes to the publication and printing of *QEX* are considered. Thank you for sharing your thoughts. My crystal ball is still pretty foggy (okay, maybe it is downright broken!) with regard to what the future will bring, so I am not making any predictions for any changes in format for 2016. If I gain any clarity about that, I will be sure to let you know.

Elwood Downey, WBØOEW

8274 Sunset Ranch Loop, Tucson, AZ 85743: **WB0OEW@arrl.net**

Using an Arduino to Automatically Tune an MFJ-1788 Magnetic Loop Antenna and Elecraft KX3 Transceiver

Here is a microprocessor controlled system that continuously monitors the transmit frequency of an Elecraft KX3 transceiver (or similar radio) and automatically keeps an MFJ-1788 magnetic loop antenna in proper tune without any operator interaction with the antenna.

I enjoy using my MFJ 1788 Magnetic Loop Antenna and Elecraft KX3 transceiver together.[1, 2] I appreciate the effort MFJ put into their loop controller and think it is a clever and effective design. Because the loop has a very narrow bandwidth, however, I find it awkward and distracting to frequently retune after even a small frequency change. I was aware that other antennas, such as the SteppIR, connect to the KX3 to monitor the operating frequency and retune automatically as necessary, and I wanted to have the same convenience with my loop.

My goal was to design a new controller for the MFJ-1788 Magnetic Loop Antenna. I wanted to be able to operate my Elecraft KX3 in the normal manner, but if I tuned beyond the bandwidth of the antenna, I wanted the controller system to temporarily reroute the RF in order to measure return loss while rotating the antenna capacitor for a proper match, then return the RF path back to the radio to resume normal operation. No operator action should be required while this tuning was under way. No modifications whatsoever should be required to either the KX3 or the MFJ-1788.

Another motivation was to find a way to tune without transmitting. I was wary of using even low power during the tuning process, because that can take many seconds, and gave me concerns about the stress this might be causing my rig. Plus, since the tuning process is performed so often, it creates QRM, which I prefer to avoid. If I could tune without transmitting, it would work over the full range of the antenna, not just in the ham bands.

This article describes a solution that meets both challenges. I first discuss the design process I went through, then the build process, and then describe how to operate the device. I will close the article with some observations. I hope that there is enough detail included so you can understand the design principles involved but also so you can adapt the design to your own situation.

Disclaimer: While I am happy to share what I have done and will be glad to discuss the project with anyone, if you try this yourself and break anything, including your antenna, your rig or yourself, *you do so entirely at your own risk and I am not responsible*. The design presented here is specifically for the MFJ-1788 and the Elecraft KX3, and has only been tested on my particular units. It may well be that it can be adapted to other similar equipment or even other uses entirely and you are welcome to do so, but all such uses are the sole responsibility of the user. Okay, back to the fun.

[1]Notes appear on page 12

The Design

I will begin by going over the process I went through to design the new antenna controller.

Requirements

Any design should begin with a list of requirements. My list of detailed requirements boil down to the following items.

1) Be able to monitor the KX3 ACC1 serial communication to read the radio transmit frequency in a manner that is transparent to, and thus does not interfere with, its normal usage as a connection to a computer or KXPA100 amplifier. This implies that I wanted the connection to be entirely passive without the need for any polling from the new controller.

2) Be able to tune the antenna without transmitting with the KX3.

3) Use pulse width modulation (PWM) to control the speed and direction of the DC motor that turns the antenna loop capacitor.

4) Be able to sense the antenna motor end-of-travel in case no peak is found in a given direction.

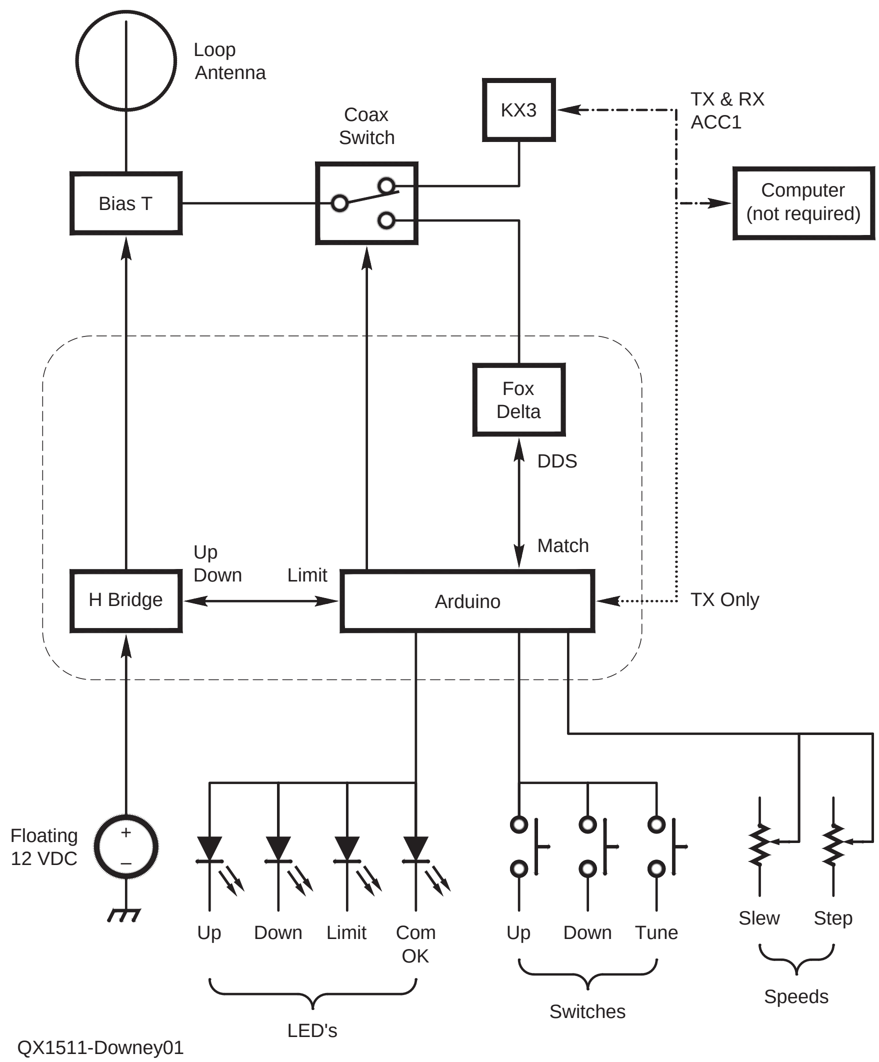

Figure 1 — This combination block diagram and simplified schematic diagram shows the basic construction of the automatic antenna controller.

5) Provide several switches and potentiometers for operator inputs.

6) Provide several status LEDs to keep the operator informed of state information.

7) Include sufficient computing power to monitor the radio frequency on a timely basis, decide when it is necessary to retune, and control the motor to find a peak within several seconds from the start of the search.

8) Include a provision for a coaxial relay to automatically switch the antenna to the tuning controller while searching, and back to the radio when completed without operator intervention.

9) Make no changes whatsoever to either the radio or the antenna so they can be returned to service at any time in their original condition.

Before arriving at these requirements, I explored other approaches. I settled on searching for maximum return loss but I also tried searching for maximum receive noise. This uses much less hardware: no RF generator, bridge or detector; just send the audio to an ADC, but I was never satisfied. It worked very well when in the clear but the main challenge was making it work in the presence of a signal. My best approach was to use an FFT and use only those frequencies with minimal strength (to measure only the noise and avoid the wildly varying modulation content). I got pretty close but, again, was never satisfied. I still think it would be cool if it worked though. I also tried using the SWR meter built into the KX3. The main problem with that is, it's not very repeatable so there were many false nulls.

Choice of Microprocessor

After researching the available options, I settled on an Arduino Uno for the main processor. It is inexpensive, has a rich ecosystem of development tools and supporting information, and is rapidly gaining traction as a preferred platform in Amateur Radio circles. It comes well equipped to address all the requirements listed above with some additional hardware. Figure 1 shows a combination block diagram/simplified schematic diagram of the system.

I wrote the software, called "sketches" in Arduino parlance, in small steps to understand each requirement separately. The tools and techniques for doing so are covered well elsewhere and will not be repeated here.[3]

Monitoring the KX3 Frequency

The new tuner needs to constantly monitor the KX3 frequency coming from its ACC1 connection. I dug into both the KX3 and Uno schematics to see how I could listen to this line without interfering with its normal use with a computer. Once I realized that the polarity between the two units was opposite (the KX3 uses RS232 with mark High whereas the Arduino uses TTL with mark Low) it was a simple matter to wire up a transistor to serve as both an isolation buffer and level inverter (Q6 in the schematic).

In order to share the serial connection for use with the Arduino IDE Serial Monitor at the same time as it listens to the KX3, you must set the IDE to 38400 baud to match the radio. Note that this speed for the Arduino Serial Monitor only became available starting with IDE Version 1.6.1.[4]

After more study of the Arduino (really the Atmel) serial port function and the KX3 Programmers Manual for the command syntax, I had code running that reliably recognized and extracted the operating frequency as I turned the main knob or changed bands on the KX3.

Note that I decided not to use the Arduino Serial class because I wanted a fully interrupt-driver serial mechanism that could effectively run simultaneously "in the background" while my main loop was controlling everything and also because I did not want to poll the radio and worry that any latency in my main loop would risk missing characters. The results are a little more complex, but functionally it is the same, and works fine with the IDE Serial Monitor.

Finally on this topic, with factory default settings, the KX3 only reports its frequency to the ACC1 port when polled but this was counter to my requirement of a non-invasive read-only connection. It turns out that there is an option called AUTO INF in the KX3 menu system, which can be set to ANT CTRL to create exactly the desired behavior — clearly the folks at Elecraft anticipated this use. With this setting, any time the operator changes frequency or switches bands the KX3 automatically sends a new frequency report within a second or so, even when not connected to a computer. If you have your KX3 connected to computer software that gets confused with these unsolicited responses, however, it is pretty safe to assume said software is surely doing its own polling so turn off this menu setting, let the software do its own polling and everything should still work fine.

Controlling the Antenna Motor Speed

The next requirement I tackled was controlling the loop motor. I was familiar with the idea of pulse width modulation, whereby the effective power of a digital signal is controlled by changing the fraction of time during which it remains at a logic High level while maintaining a constant frequency, otherwise known as changing its duty cycle. So that was a simple means to control the speed, but I also needed a way to change direction. After more study, I found this is normally done by an H Bridge. This is a classic circuit that connects the two wires from a DC motor with four SPST switches, arranged in such a way that the proper combination of switch states can connect either side of the motor to power or ground potential, thus providing a means to change the polarity of the motor and thus its direction of rotation. This technique is so common, in fact, that dedicated ICs are available to perform this function with just a few parts. I did not have such an IC, but I had enough parts in my junk box to fabricate an H Bridge from first principles. I built up a circuit and my next trial sketch convinced me I could control both motor speed and direction using two PWM outputs from the Arduino.

Detecting End-of-Travel

The next requirement was to detect the end of travel. Although in principle the capacitor mechanism in the MFJ-1788 controller could rotate endlessly without doing any harm, it is only allowed to rotate one half revolution. I can imagine this design decision was made because the other half rotation does not really provide any new values of capacitance, and because the net capacitance would first increase and then decrease while the motor continues to turn in one direction, which would be quite confusing to any tuning algorithm. The rotation limits are implemented as two physical switches and diodes inside the antenna module. A given switch opens when motion in a given direction reaches its end of travel and yet the diode allows current to flow in the opposite direction even with the switch open.

The MFJ-1788 makes use of a bias-T to provide motor power through the same coax as the RF. This is a clever way to eliminate an extra control cable, but it also means the state of these limit switches is not directly available to the control end of the system. Fortunately, the only function these switches effectively perform is to interrupt the path of current to the motor. Thus, the activation of a limit switch can be detected by simply monitoring the current to the motor and noting if it drops to zero. I did this by using a pair of optoisolators, a pair being required in order to allow for both polarities sent to the motor for direction control. Although it is true this technique does not directly provide the means to know *which* limit switch was activated, this can be reliably inferred by knowing which way the motor is being commanded to move when the current stops.

This method of detecting a travel limit comes with one caveat, however. Using PWM means that the current is intentionally brought down to zero during each cycle. So a means was needed for this frequent occurrence of zero current to not cause a false indication of a limit. The solution turned out to be as simple as adding a timer to the limit detection algorithm. Although the instantaneous current detector circuit still reports no current during each PWM cycle, a *logical* limit is not reported unless the condition persists for some small length of time.

Operator Inputs

In this application, the requirement to provide operator command inputs is sufficiently simple as to be met with some small momentary contact push button switches. I ended up using three.

1) Tap to force an automatic search to commence, if desired.

2) Hold to manually rotate lower in frequency, release to stop.

3) Hold to manually rotate higher in frequency, release to stop.

There are other combinations of switch inputs for lesser used functions, which will be described later. Each switch is connected directly between a digital input and ground, and the Arduino is programmed to provide an internal pullup resistor to the positive supply rail, a handy feature that saves a resistor for each switch. Note that in the code, the logic is inverted, such that a High denotes the switch is idle and a Low denotes the switch is being pressed.

In addition, there are two analog values that must be set based upon your particular antenna characteristics. Even with my single unit, I find it necessary to adjust these whenever the weather, temperature, or humidity changes appreciably, probably because of their effect on the motor lubrication and friction in the simple journal bearings. The operator adjusts these by turning two potentiometers. One is called Slew, which sets the fast slewing rate. The other is called Step, which sets the fine stepping pulse duration time. These will be explained more fully later when we discuss the tuning algorithm. These potentiometers also have specialized applications as explained later.

LED State Indicators

I decided that controller state information can be communicated clearly enough using four colored LEDs. At times during development I found it handy to connect an 8 character 8 × 8 LED matrix array controlled using

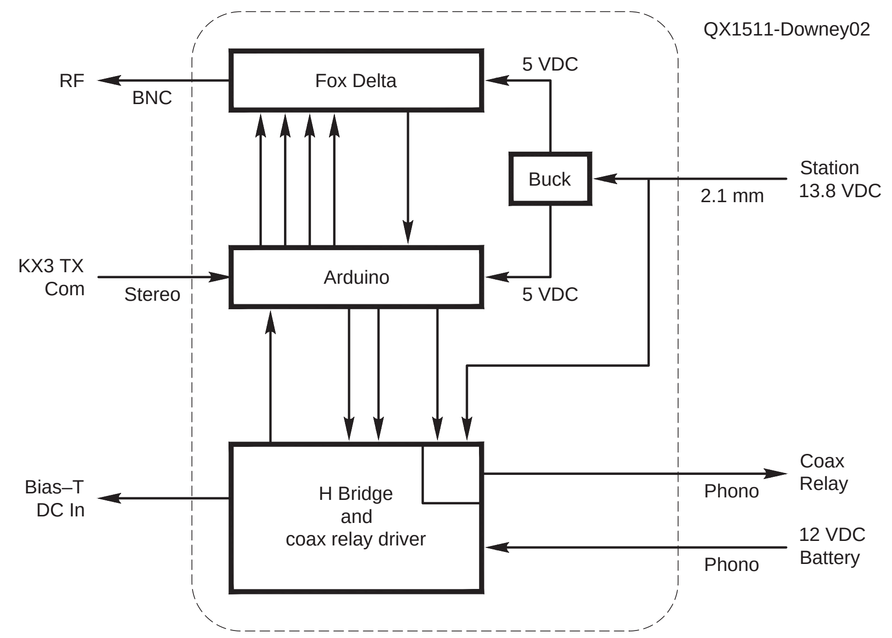

Figure 2 — This is a more detailed block diagram of the antenna tuner.

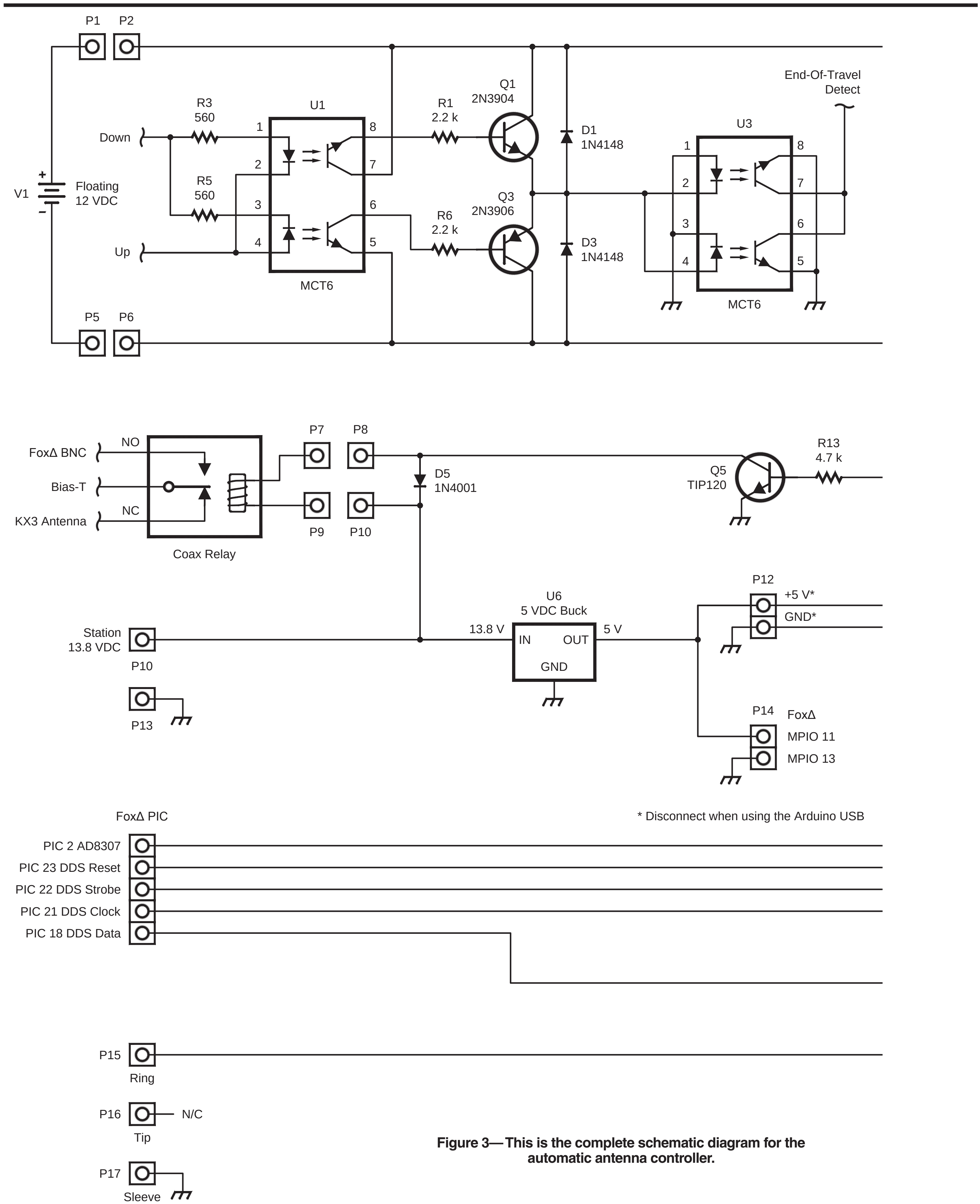

Figure 3—This is the complete schematic diagram for the automatic antenna controller.

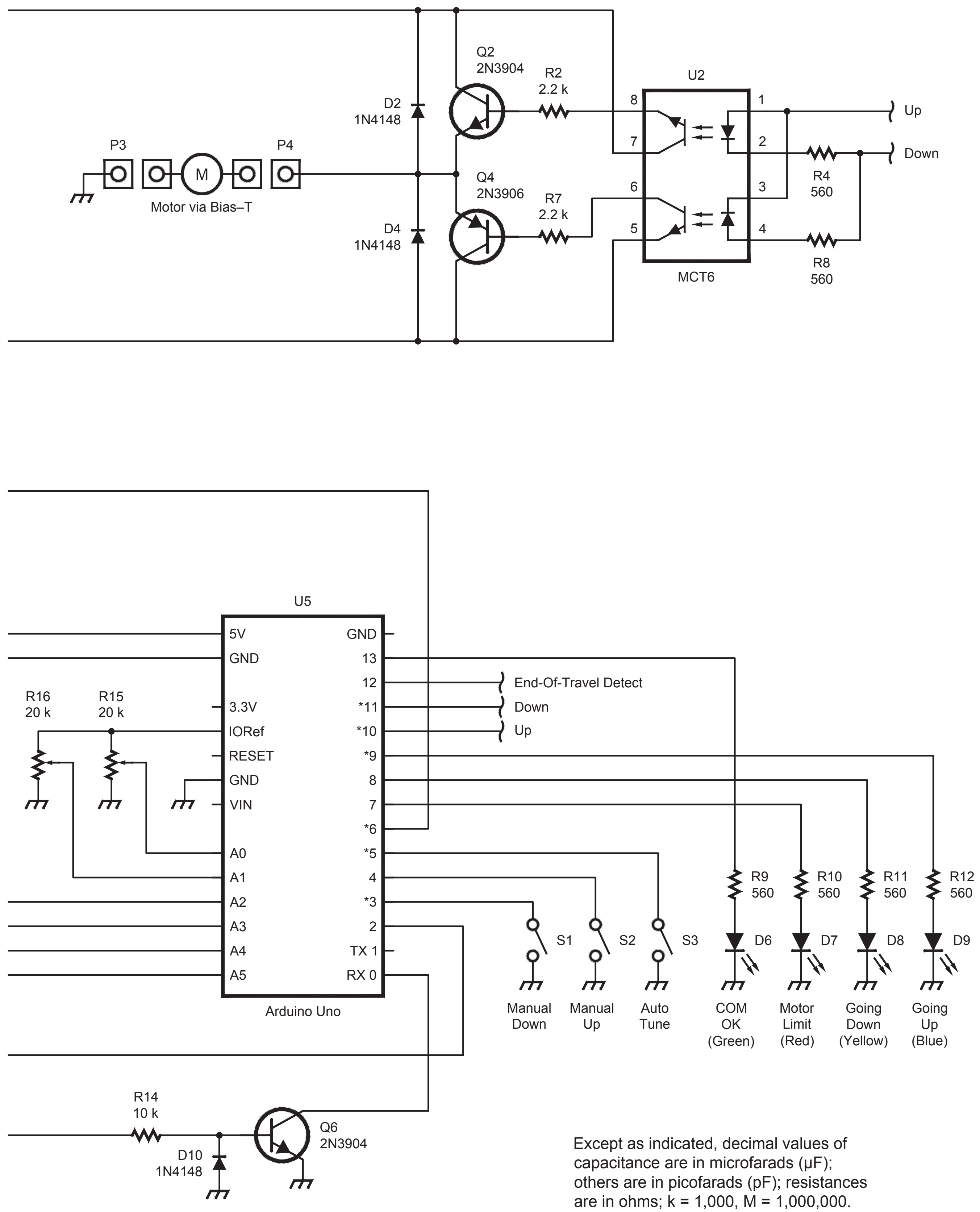

Except as indicated, decimal values of capacitance are in microfarads (µF); others are in picofarads (pF); resistances are in ohms; k = 1,000, M = 1,000,000.

QX1511-Downey03

the SCI bus, but this is not needed for the final system. Each LED is connected to a digital output pin with a series resistor to ground. I chose to define the four LEDs as follows:

• Light a red LED while a logical end-of-travel limit is being detected.

• Light a yellow LED to indicate that the antenna is moving down in frequency.

• Light a blue LED to indicate that the antenna is moving up in frequency.

• Blink a green LED when communication with the KX3 has reliably determined the operating frequency.

As with the switches, other LED combinations are used for lesser used functions, as described later.

Measuring the Antenna Match

The final piece of the puzzle is to find a way to measure the degree of impedance match of the antenna. I considered many approaches but finally settled on using a balanced bridge circuit to sense when the magnitude of the input impedance of the antenna connector was near 50 Ω. The idea is to connect three 50 Ω resistors into a square, with the antenna connect in the place of the fourth resistor. Then connect a signal generator to drive two opposite corners with a reference frequency, and measure the voltage across the two remaining corners. The lower the measured signal across the bridge, the better the antenna impedance agrees with the surrounding resistor values. Such a bridge does not provide the sign of the reactance when not matched, but we can infer that in other ways.

With this design in mind, it remains to choose a signal source and a detector. It turns out there are two ICs from Analog Devices that serve both these goals admirably. The AD8307 log amp is an excellent detector and the AD9851 Direct Digital Synthesizer is a flexible RF signal source.[5, 6] These parts have been RF work horses for some time so the only real decision was how best to proceed with an implementation around them.

A little searching on the Internet finds lots of schematics and tips for using these parts in similar applications. Being an experimenter, I was tempted to start with bare parts and work up my own solution, but then I found a commercial implementation that was just too good to ignore. The FoxDelta AAZ-0914A Antenna Analyzer provides a complete kit for exactly this purpose.[7] For about $50, there was no way I could match this with my own parts and time. All you do is connect the antenna, 5 V DC, a few wires to control the chips and the Arduino has an easy time of measuring the degree of mismatch anywhere in the frequency range of the antenna.

Note that the FoxDelta unit includes a PIC processor to provide a nice USB interface to a host computer. Rather than work through an intermediate control layer, however, I decided to unplug the PIC and attach leads directly from each control chip to some Arduino IO pins. This allowed me to control the Analog Devices chips exactly as I wanted, and also makes the software independent of the AAZ-0914A and thus entirely suitable for others who might want to use a different implementation using these chips.

Tuning Algorithm

Now that we can read the radio frequency, control the motor, interact with the operator, and measure the degree of tuning match it's time to consider the heart of the matter: the automatic tuning algorithm. This involved a large amount of experimenting and carefully observing how the motor reacts to commands. I'll spare you all the false starts but one lesson stands out of paramount importance: there is a large amount of backlash in the drive train and it is not particularly consistent with direction, speed or position. The MFJ design includes a spring that probably reduces this to some extent, but the very low power motor precludes it from providing much in the way of compensating force, and thus its effectiveness is marginal at best.

Dealing with the backlash becomes the primary challenge. The tuning technique I finally settled on is explained in the following steps.

1) Keep comparing the radio frequency with the last known antenna tuning frequency. Using an estimate of the antenna *Q* (which can be easily adjusted in the source

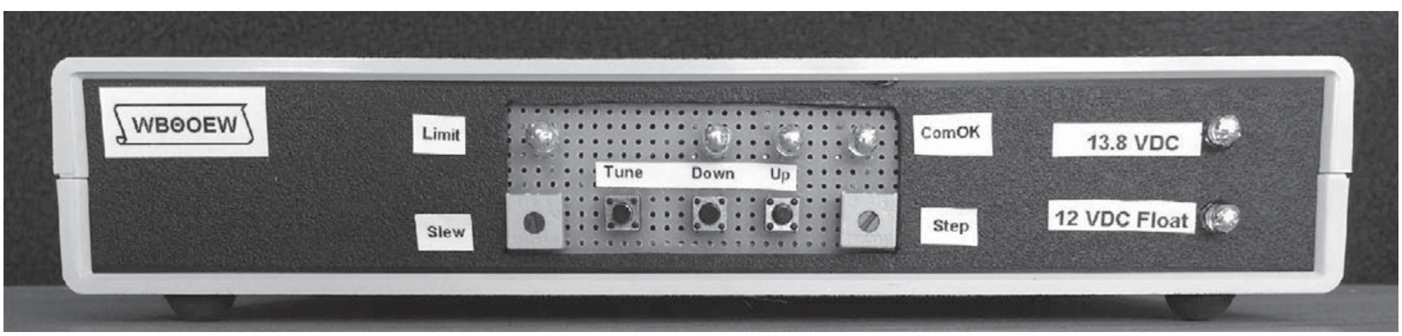

Figure 4 —Here is a photo of the controller front panel. You can see the SLEW **and** STEP **potentiometers, the** TUNE**,** DOWN **and** UP **pushbutton switches and the various indicator LEDs.**

Figure 5 —This photo shows the controller rear panel. The various input and output connections are shown.

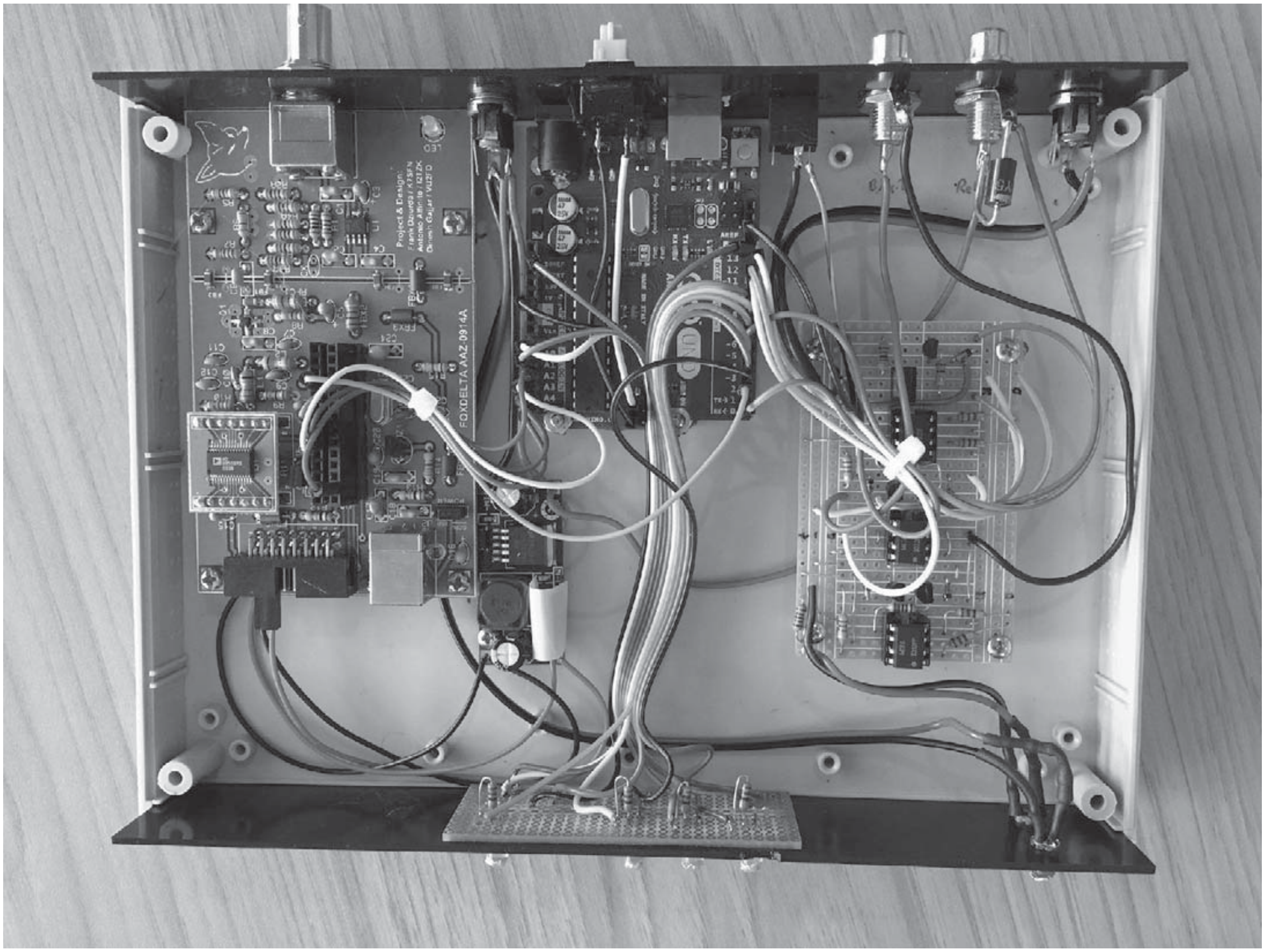

Figure 6 — Here is a photo of the wiring inside the controller cabinet. You can see the Fox Delta Antenna Analyzer boards, the Arduino board and the construction of the rest of the circuit on several perf boards.

code if desired), determine when the two values differ by an amount that is worth correcting. The code takes into account that the useful bandwidth of the loop antenna is smaller at lower frequencies. When the two values are sufficiently far apart, decide which way the motor needs to rotate and go to Step 2.

2) Begin by slewing full speed in the opposite direction for a short while. Yes, you read that right. By going a goodly ways in the wrong direction first, we are assured of always passing through the best match position at full speed, even if it is very close to the starting position. I tried many techniques to approach more slowly but this turned out to be by far the most reliable. After this brief burst, stop, slew at full speed in the other (correct) direction and go to Step 3. It is the SLEW POTENTIOMETER that defines this fast rate of motor rotation.

3) While going full speed toward the desired match position, measure the match as quickly as possible. Given that the match can be read very rapidly, we are assured of a steep and deep dip as we pass through the best match value. As we are performing this search, record the best match value seen so far, to be used later. When the dip is detected, stop the motor. Another benefit of always slewing rapidly through the best match position is that we can be assured the motor has definitely overshot the best position. If we had approached more slowly, we may or may not have passed the best position and so we really would not have learned very much about our target. Now that we know for sure we are stopped just past the best position, go to Step 4.

4) Now the fun begins. We make very small steps and measure the match after making sure the motor has come to a complete stop after each step. The duration that power is applied for each step is controlled by the STEP POTENTIOMETER. It took me days to realize that when power is removed from the motor the capacitor can continue to change aimlessly, even though I had inspected the coupling bushing in the antenna to insure that it is tight. Measuring the antenna match during these uncertain motions is at best meaningless and at worst just adds to the confusion. So, during this procedure, after power is removed for each step, the match is measured repeatedly until it no longer changes. Only then do we believe the motor and capacitor have really stopped moving, and the measurement is meaningful. By insuring a full stop, each of these final measurements are reliable, and we can repeat making small steps looking for the next dip. Step 5 describes exactly what we are looking for.

5) Unlike the dip seen while performing the initial fast slew, in this phase we must minimize the degree of overshoot through the best match condition. This is because since we cannot actually measure position, there is no way to go back to a known position in a reliable fashion. Thus we need a way

to detect that we are just barely past the best match position. To do this, as we make each (stopped) measurement, we look for a match reading that is better than the best reading found during the slew in Step 3, followed by a larger value. This strongly suggests we are exactly one step past the best match position. We could stop here and be pretty close, but we go on to Step 6.

6) To review the work up to this point, we slewed rapidly enough through best match to insure overshoot and we recorded the best value seen during that run. We have turned around and found that same match again but going much more slowly, so we know we are close. What we do now is basically repeat step 5 but at half the step time. We keep doing this until we are all but completely stopped. So in summary, we walk back and forth over the best match going more and more slowly, the plan being that when we go so slow as to be stopped, we should be almost exactly at the best match position.

All the while this is going on, we also watch for the capacitor end-of-travel, in which case we turn around and start over. We also watch for the operator to tap any of the switches, in which case we abort the tuning attempt and stop where we are.

The Build

Now that I had a design and major implementation details worked out, it was time to build it. By the time I had everything working, my bench was pretty much covered with several breadboards and a large number of wires running everywhere, but I love this stuff so that was a feature of the project, not a bug!

Construction

For the following, it is helpful to refer to the schematic diagram, shown in Figure 3.

Many of my component choices and implementation decisions were based simply on using suitable parts that I had on hand as much as possible, even if perhaps there are simpler choices. Looking at the final schematic, you might guess correctly that I had a large number of 2N3904 and 2N3906 transistors, 1N4148 diodes and MCT6 dual optocouplers, so naturally that's what I used. These transistors are rated for only about 200 mA collector current but, remarkably, the MFJ motor draws only about 10 mA, so even these small signal parts work fine in what otherwise would require larger current devices. Even the LEDs in the optocoupler used as a current sense can handle 60 mA of continuous current. I measured about 40 V of back EMF, so the 60 V maximum reverse voltage of the 1N4148 used here as clamping diodes is also adequate, but feel free to use what you prefer.

The most obvious effect of using stuff on hard is that I made my own H Bridge from discrete components. If you have, or want to purchase, an H Bridge chip such as the TI L293D or even a complete Arduino motor control shield, such as those available from Adafruit or Sparkfun, by all means do so. The big point here, however, is to take note that *the Bias-T requires that the power supply for the antenna motor must have both sides isolated from station ground*. The reason is that either side of this isolated supply can, depending on the desired motor direction, be connected to station ground. I could have worked up an isolated supply, or just used a commodity wall-wart, but given the remarkably low current draw of the motor, I just chose to power the H Bridge with batteries adding up to 12 V. I am still using the original set I started with but note that if your unit stops operating reliably, measuring the battery voltage should be a first thing to check. Generous use of the optocouplers made easy work of connecting the grounded Arduino to the floating H Bridge.

Both the Arduino and the Fox Delta require a clean supply of 5 V DC. For this, I found an inexpensive variable buck converter on Amazon that draws from the 13.8 V main supply for the unit.

Two PWM outputs from the Arduino drive the H Bridge. They turn on either Q1 and Q4, thus connecting the left and right leads of the motor to positive and negative supply, respectively, or Q2 and Q3, which provides the opposite polarity to the motor. The motor is off when all four drivers are open. Note that the supply would be shorted if both left or both right drivers were on at the same time, but the logic of the optocoupler wiring, U1 and U2, makes this impossible, thankfully making the design immune at least from this programming error.

Rather than build my own Bias-T, I just purchased the MFJ-4116.[8] I figured since they use the same design within their antenna, their separate product would probably be compatible, and that proved to be the case. Doing so certainly saved some effort and perhaps a little money. My only regret is the poor quality SO-239 connectors they used.

The motion limit sensor uses another pair of optocouplers in U3, wired to connect one Arduino digital input to ground while there is current in either direction, causing the Arduino to read a Low. If there is no current, the coupler outputs will both be open and the Arduino will read a High logic value. As described above, a little extra care is required in the software because the current is also zero in between PWM pulses.

Several IO lines connect to the Fox Delta unit. I did this by carefully removing the original PIC (and packing it for safe keeping if I ever want to use it again) and replacing it with two header strips. I then plugged male breadboard jumper wires into the female header positions. I found it best to lean the two headers toward each other so their tops touch and add a bead of super glue along this junction to form a sort of roof over the socket. I tried using another 28 pin socket as a plug. Although the pins lined up, of course, the body shape was such that it did not firmly seat into the original socket. I also tried to quickly solder wires to this second socket but the plastic melted before anything else. I am open to better ideas that still allow me to replace the original FoxDelta PIC if I ever choose to do so. The digital connections to the AD9851 DDS can probably tolerate a little contact resistance but the analog connection to the AD8307 must be as clean and stable over time as possible. I open my case occasionally and pull out this lead and push it back in a few times and then redo the calibration step to insure best possible performance.

During my experiments, I could see it was going to be important to adjust the Slew and Step rates carefully and adjust them from time to time. Rather than require changing constants in the program to accommodate this, I added two potentiometers to the design, R15 and R16. Suggestions for setting these properly will be discussed later. Figure 4 is a photo of the front panel of my controller. Figure 5 shows the rear panel. Figure 6 shows the wiring inside the cabinet.

The coax relay is not absolutely required for this project but it really makes the controller completely hands-off to operate. There are lots of options here, and several always seem to be available in the used marketplace. The only requirement is that you can find a way to control it with a digital output pin on the Arduino, such that a High switches the antenna to the controller, and a Low switches it back to the radio. The relay I found draws about 100 mA at 13.8 V DC, and generated 120 V of back EMF. See the circuitry surrounding Q5 for my solution.

Checkout

First, a few notes of caution.

1) *Never power the Arduino from the separate 5 V supply and the USB at the same time.* One or the other supply will inevitably be higher, causing current to flow in the reverse direction of the other supply.

2) Although the auto tuner will work fine capturing serial commands from the radio to the computer, *you must disconnect the radio connection temporarily while programming the Arduino*.

For the following, I will assume you have flashed the sample code in your Arduino with the USB connection, built the circuit as per the schematic and connected 5 V to only the Fox Delta. My sample Arduino code is available for download from the ARRL *QEX* files web page.[9] At this point you can connect the antenna Bias-T but do not connect the motor to 12 V.

Upon power up, you will first see all four LEDs light up for a second. This is homage to the tradition of testing all lamps. Then you will see the green COMOK LED slowly flashing. It will remain flashing like this until receipt of the first successful frequency report from the KX3. Ignore it for now.

Hold the DOWN switch for a few seconds and release. The yellow DOWN LED should come on immediately then the red LIMIT LED should come on after a second or so because there is no current to the motor. With an oscilloscope probe on Arduino pin 11 and holding the DOWN switch, you should see a 5 V square wave with a frequency of 490 Hz, and a duty cycle that varies from 0 to 100% as the SLEW potentiometer is adjusted. Repeat this action with the UP switch, except the blue UP LED should come on. Measure the waveform at pin 10.

Now connect 12 V to the H bridge. Repeat the above tests, and measure the high side of the motor connection. It will be similar but it will be a higher voltage and more triangular, reflecting a large time constant because of the motor inductance.

If this works, move on to the KX3 communications. Connect the Ring from the KX3 ACC1 connection to the controller Ring connection point (P15) and the sleeve to ground (P17). The tip is not used. My KX3 is normally connected to a computer while in the shack, so I inserted a stereo "Y" connector to gain access to this signal. Power up the KX3 and check that menu entry AUTO INF is set to ANT CTRL. A slight turn of the main radio knob should cause the green COMOK LED to blink, indicating a valid frequency report was captured.

Calibration

Connect the antenna through the coax relay and the Bias-T. Hold the DOWN switch until the red LIMIT LED comes on. Set the SLEW potentiometer to mid range. Note the time and hold the UP switch. The LIMIT LED will go out then come again many seconds later, after the motor has rotated from one limit to the next. You want to set the SLEW potentiometer so this total travel time is about 20 seconds. Going down is always a few percent faster than going up because the anti-backlash spring is aiding the motor, but the difference is not enough to worry about.

The next step is to calibrate the mismatch value. Remove the antenna connection from the Fox Delta BNC connector. While pressing the TUNE switch, tap the Arduino RESET switch. After a few seconds you will see a steady rolling pattern across all the LEDs. Release the TUNE switch and the pattern should reverse and go somewhat faster. After a few seconds the LEDs go out. This indicates you have successfully calibrated the open circuit mismatch value. Using the Arduino IDE Serial Monitor during this procedure, you will see each measured value reported and the final computed value of BAD_MATCH. On my configuration, the value is near 400 or a little lower. It is a good idea to perform the procedure a few times and confirm it repeats to within a few percent. If the value varies a lot, you probably have a poor connection to the Fox Delta PIC socket, pin 2. The value is stored in EEPROM so it will remain during Arduino power cycles and resets. If for some reason the EEPROM fails to confirm the new value, you will see error code two be reported and you should retry the procedure. If the EEPROM continues to fail, you have a bad Atmel chip and should replace it.

Now to set the STEP potentiometer. This is a little trickier. Too high and it will skip past the best match and continue to the limit in that direction. Too low and it will take a long time to find the best match. After the fast slewing step, you want it to find the first best match candidate in 5 to 10 seconds, turn around, and find it again in 3 to 5 seconds then finally settle on the best position in another few seconds. During this procedure, you will see the yellow and blue LEDs alternate as the algorithm hunts either side of the best match.

The best way to set the STEP potentiometer is to use the IDE Serial Monitor to watch the printed report. Tap the TUNE switch. On the Serial Monitor you will see two lines that begin with Slewing followed by several lines that begin with Stepping. The Slewing lines are reporting each reading during the initial fast scan. Smaller numbers are better matches. As soon as a significant dip is found, the values that qualified as a dip are reported. The center few of these should be well below the value of BAD_MATCH found during calibration. The Stepping lines report the finer moves up and down, hunting for the best match.

Operation

After completing the checkout and calibration, you should have a very good idea how to use the tuner.

1) Power up everything.

2) Change the rig frequency to get the first frequency report, as indicated by a COMOK LED blink. The tuner will never attempt to move the antenna before the first successful rig report. Automatic tuning is not enabled until the TUNE switch is used at least one time.

3) Tune around as desired. You will see the COMOK LED blink each time the rig reports a frequency. Auto tuning will never commence as long you are changing frequency. At some point, stop changing frequency. If you have moved sufficiently far away from the last time the antenna was tuned, a search will commence automatically. If the antenna has never been matched since power up, the tuner will start in a random direction but is smart enough to turn around at the end-of-travel if it guessed wrong.

4) Automatic tuning can be interrupted for any reason at any time by tapping any switch. After doing so, automatic tuning will be disabled until you tap the TUNE switch again.

5) If the fast slewing step fails to stop, and bounces off both limits, try redoing the calibration of the BAD_MATCH value. Also, make sure there is a good connection with the Fox Delta PIC pin 2.

6) If the slower fine stepping phase of the search goes on too long, longer than, say, 30 seconds, tap the TUNE switch to stop the algorithm. Now listen to the audio from the radio and press the same UP or DOWN switch that matches the LED motion that was flashing. Hold the switch for a few seconds and release. If you hear a brief increase in the audio level, you know the match was not yet encountered and you should increase the STEP potentiometer a little. If you can hold the UP or DOWN switch a long time and never hear the audio level increase, you know the step jumped over the best match, so decrease the STEP potentiometer a little.

Error Codes

If the tuner encounters an error during operation, it flashes all LEDs a certain number of times to give a clue to the problem. The error code is repeated four times. The codes are as follows.

1) The transmitter is on when a tune attempt was requested.

2) The EEPROM failed to verify the written value.

3) Radio frequency is still unknown when a tune attempt was requested.

4) Radio frequency is too low for the antenna.

5) Radio frequency is too high for the antenna.

A Few Surprises

There are a few more features available, which you may find useful.

1) **Zero Beat.** During the Tune procedure the DDS frequency may not exactly match the radio frequency, which can cause an annoying heterodyne if there is any leakage through the coax relay from the DDS to the radio. To eliminate this you can calibrate the DDS to zero beat with the radio as follows:

1.1.1.) While holding the UP switch, tap the ARDUINO RESET. After a few seconds you will see the green COMOK LED flashing. Spin the radio knob a little to force it to report the frequency. When a frequency report has been received successfully, the COMOK LED will go out and the blue UP LED will flash. At this point, adjust the STEP potentiometer up and down and confirm you can hear the DDS heterodyne. Tune for zero beat and, finally, release the UP switch. The offset is stored in EEPROM, so it will remain effective across Arduino power cycles and resets until the procedure is repeated.

1.1.2.) Note that this only provides one zero beat setting. It can be set to work with USB/LSB or CW but not both, because of the sidetone offset employed for CW.

2) **Frequency Generator:** The FoxDelta can still be used as a general purpose frequency generator. To enter this mode, tap both UP and DOWN switches at the same time. When successful, both UP and DOWN LEDs will light at the same time. Now the SLEW potentiometer is a coarse frequency control and the STEP potentiometer is a fine control. The resolution is about 15 Hz. The coax relay will connect the antenna to the FoxDelta during this mode, but of course you can ignore that and connect anything you want directly to the FoxDelta. The frequency is reported in the Serial Monitor if you have that visible. Exit this mode by tapping any switch.

3.) **Frequency Sweep:** Hold the UP switch and tap the TUNE switch to start a sweep over the entire auto tuner range. The red LIMIT LED will flash while the sweep is in progress. A table of frequency and mismatch values is printed in the Serial Monitor window. During the sweep the antenna is switched to the FoxDelta. The sweep is finished when the red LIMIT LED stops flashing. The sweep can be aborted at any time by tapping any switch.

Conclusion

I have enjoyed using the loop tuner for several months, and find it meets all the requirements quite well. Once in a while it will miss a match, but I just tap the TUNE switch and it recovers shortly.

Finding a match after a band change typically takes 30 to 40 seconds, tweaking up after a modest QSY takes 10 to 20 seconds. Perhaps I could beat these times a little by hand, but now there's no more remembering to first adjust power level; pressing Tune on the radio; jockeying several lights and switches; manually dealing with end-of-travel; adjusting for overshoot; fighting the temptation to tweak it just a little better; fretting over my finals; or causing QRM to a QSO. Now I just ignore the antenna. I tune the radio around at will, and when I find something I want to listen to I stop. If it is far enough away from the last tuning frequency to matter, the antenna is tweaked for the new frequency in a short while and I'm good to go with no effort at all. It feels almost as though I have a nice broadband antenna. How cool is that?

Elwood Downey, WBØOEW, has held the same call sign since he was first licensed in 1974. He is an ARRL Member. Elwood enjoys software, digital modes, antennas, and experimenting. He graduated with a BSEE cum laude in 1977 from Purdue University. Since then he has focused his career on telescope control systems and related astronomical instrumentation, which he finds very fulfilling. It has taken him to many of the great observatories around the world.

Notes

[1]For information about the MFJ-1788 Magnetic Loop Antenna, go to the MFJ website: **www.mfjenterprises.com/Product.php?productid=MFJ-1788**.

[2]For more information about the Elecraft KX3 transceiver, go to the Elecraft website: **www.elecraft.com/KX3/kx3.htm**.

[3]Glen Popiel, KW5GP, *Ardunio for Ham Radio*, ARRL, 2014, ISBN: 978-1-62595-016-1, ARRL Order No. 0161, $34.95. ARRL publications are available from your local ARRL dealer or from the ARRL Bookstore. Telephone toll free in the US: 888-277-5289, or call 860-594-0355, fax 860-594-0303; **www.arrl.org/shop**; **pubsales@arrl.org**.

[4]The Arduino software is available from: **https://arduino.cc/en/Main/Software**.

[5]Download theAD8307 log amp data sheet from: **www.analog.com/media/en/technical-documentation/data-sheets/AD8307.pdf**.

[6]Download theAD9805 direct digital sythesizer data sheet from: **www.analog.com/media/en/technical-documentation/data-sheets/AD9851.pdf**.

[7]For more information about the Fox Delta Antenna Analyzer, go to: **www.foxdelta.com/products/aaz-0914a.htm**.

[8]See the MFJ website for more information about the MFJ Bias-T: **www.mfjenterprises.com/Product.php?productid=MFJ-4116**.

[9]The author's Arduino code is available for download from the ARRL *QEX* files web page. Go to **www.arrl.org/qexfiles** and look for the file **11X15_Downey.zip**.

John A. Magliacane, KD2BD

1320 Willow Drive, Sea Girt, NJ 08750; **kd2bd@amsat.org**

A Frequency Standard for Today's WWVB

The author shares the design of his frequency standard that's fully compatible with today's WWVB.

For over a half century, the 60 kHz carrier from WWVB has served as a popular and highly respected frequency reference among many scientific, research, and engineering professionals across North America. As GPS-disciplined frequency standards started gaining in popularity, the use of WWVB in frequency reference applications began to decline. With this decline, however, came a tremendous increase in the sale and application of low-cost radio controlled "atomic clocks" that receive time and date information from WWVB on a regular basis. This drastic shift in the use of WWVB by the American public forced a realignment of the priorities set for the station by the National Institute of Standards and Technology (NIST).

With the rapid proliferation of radio-controlled clocks came a realization that reception of the WWVB time code by low-cost consumer products was often unreliable. In the eastern United States where signals from the Fort Collins, Colorado WWVB transmitter are often the weakest, competition from high noise levels and co-channel interference from British radio station MSF made reception especially difficult. Enhancements were made to the WWVB effective radiated power and modulation depth, but reception difficulties continued to persist. Finally, when attempts to commission a second WWVB transmitter to serve the east coast failed to reach fruition by the end of 2009, thoughts turned toward making more aggressive changes to WWVB broadcasts that would help improve reception reliability while maintaining compatibility with the millions of radio-controlled clocks already in operation.

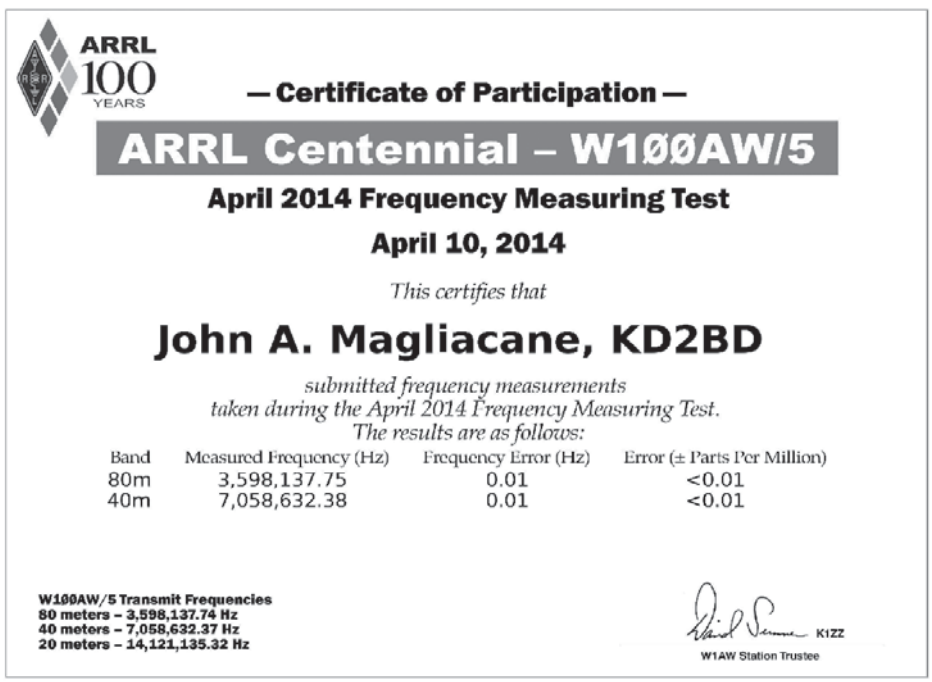

ARRL 100 YEARS

— Certificate of Participation —

ARRL Centennial – W1ØØAW/5

April 2014 Frequency Measuring Test

April 10, 2014

This certifies that

John A. Magliacane, KD2BD

submitted frequency measurements taken during the April 2014 Frequency Measuring Test. The results are as follows:

Band	Measured Frequency (Hz)	Frequency Error (Hz)	Error (± Parts Per Million)
80m	3,598,137.75	0.01	<0.01
40m	7,058,632.38	0.01	<0.01

W1ØØAW/5 Transmit Frequencies
80 meters – 3,598,137.74 Hz
40 meters – 7,058,632.37 Hz
20 meters – 14,121,135.32 Hz

K1ZZ
W1AW Station Trustee

Figure 1 — The author's very successful Frequency Measuring Test results are achieved by using WWVB as a precision frequency reference.

New Modulation Format

NIST Realized that only through a radical change in time code transmission and greater sophistication in receiving techniques would any further improvement in reception reliability be achieved. They decided to add a new time code to the WWVB carrier, modulated by means of binary phase shift keying (BPSK), that next generation radio-controlled clocks could be designed to receive and process with improved reliability. While over-the-air tests conducted in 2012 revealed that the addition of the new BPSK time code had little or no effect on the operation of existing radio-controlled clocks, it caused every WWVB-disciplined frequency standard to lose phase reference with the WWVB carrier, and thus malfunction. With GPS-based frequency standards in wide use and rising steadily in popularity, and commercial WWVB-based frequency standards out of production for years, NIST decided to permanently add its new BPSK time code to WWVB broadcasts beginning on October 29, 2012, and force all previously functioning WWVB-disciplined frequency standards into obsolescence.

Despite this WWVB priority shift toward application in consumer products, and away from the scientific and engineering communities, the WWVB carrier frequency is maintained to within one part in 10^{14}, and continues to be derived from a set of four cesium clocks.[1] As such, provided that BPSK compatible reception techniques are employed, radio station WWVB can continue to serve as a reliable and accurate frequency reference, and can do so with a level of precision that far exceeds that of its time dissemination.

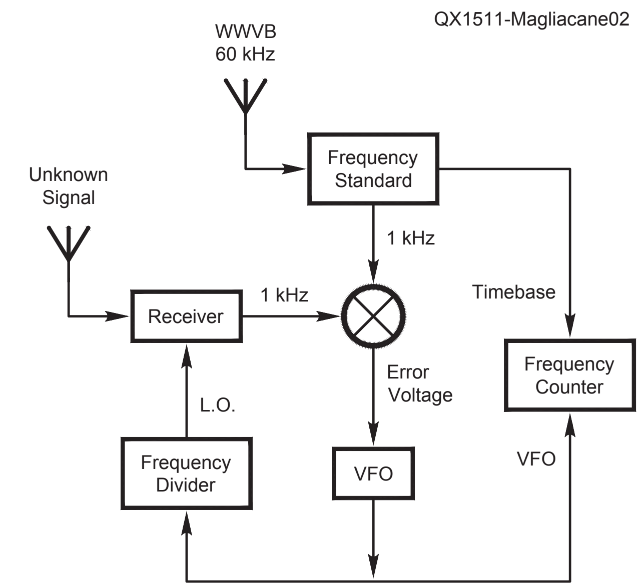

Figure 2 — The author's FMT methodology applies a DC tuning voltage to the local oscillator of a direct conversion receiver to lock its audio output in phase with that of a 1 kHz reference. The frequency of the unknown signal is determined by measuring the frequency of the LO and factoring in the 1 kHz tuning offset.

A BPSK-Compatible Frequency Standard

The frequency standard described here employs a combination of linear signal processing, vector demodulation, and superheterodyne receiving techniques to not only discipline a 10 MHz voltage-controlled, temperature-compensated crystal oscillator (VCTCXO) against the WWVB carrier, but also decode its amplitude modulated time code. A wide variety of calibration signals are available to the user, while an LCD display provides NIST (UTC) date, time, and UT1 offset information. Several audio outputs are provided to help assess reception quality and assist in selecting an optimum antenna placement and orientation. An RS-232 port is also included to provide UTC time and date information to external devices.

Performance

The stability and accuracy of a frequency standard are difficult to assess and quantify without making a direct comparison against another standard of superior precision. Even while lacking a second standard, however, some conclusions can be drawn based on the performance a frequency standard demonstrates while being employed in critical applications over the course of many years. For example, the results achieved while employing this frequency standard during Frequency Measuring Tests over the past decade have consistently equaled or surpassed those of most other participants, many of whom employ advanced digital signal processing techniques, commercial GPS-disciplined frequency standards, rubidium oscillators, and other laboratory grade

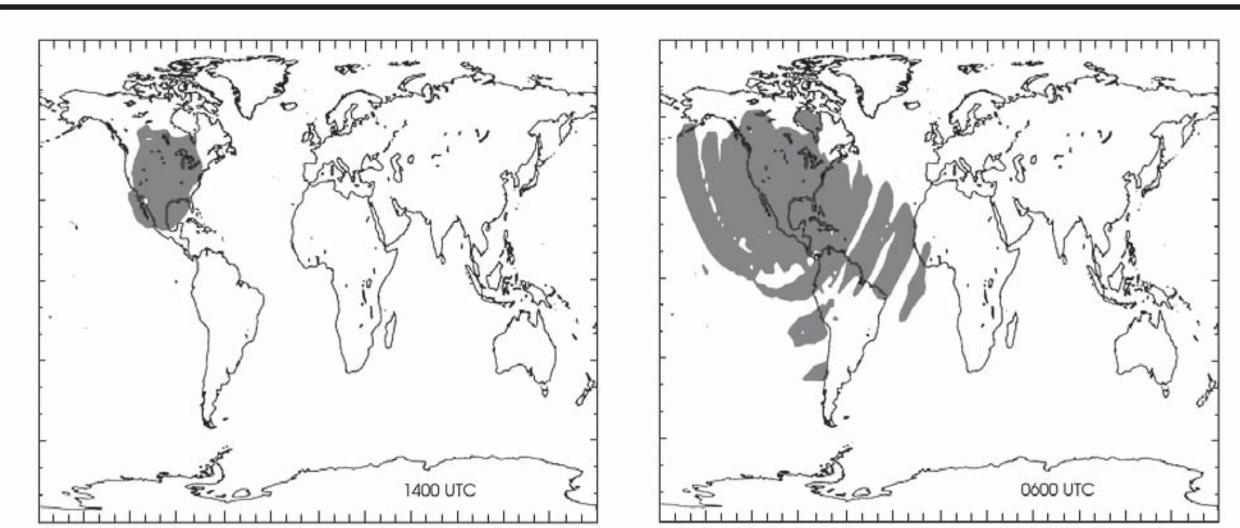

Figure 3 — Space and Naval Warfare Systems (SPAWAR) Command computer simulations illustrate how the WWVB 100 μV/m signal level contours contract during the day and expand during nighttime hours. (Images from NIST website.)

instrumentation. Figure 1 shows a certificate I received for my participation in the April 2014 FMT.

Since the influence of ionospheric perturbations and inaccuracies in frequency measurement methodologies are often the largest consistent sources of error in FMTs, these results alone cannot speak to the full performance of this frequency standard. Using the identical hardware and methodology as those employed in FMTs (Figure 2), I measured the carrier frequencies of many AM broadcast stations received over ground wave paths to a resolution of 312.5 microhertz (less than one part per billion at 1 MHz). During the process, several transmitters were identified as consistently having no measurable frequency error, some of which are known to employ GPS-disciplined rubidium frequency standards for carrier generation. I believe that transmitters exhibiting very small but measurable frequency offsets were likely rubidium controlled but not necessarily GPS-locked, while others that exhibited larger errors that varied over time might have simply been crystal controlled.

Since the GPS-disciplined radio station carriers stood out so clearly among all other stations measured, it follows that the accuracy and stability of this frequency standard probably exceeds the resolution of the measurements taken. In fact, they are possibly several orders of magnitude better based on the known precision to which the WWVB carrier frequency is maintained, and the recognized RF propagation characteristics that exist at low frequencies.

60 kHz Propagation

LF radio propagation is substantially different from that which exists at higher frequencies. Its remarkable stability and reliability have often led to the belief that 60 kHz signals propagate great distances over ground wave paths alone. In reality, a combination of surface wave and D-layer ionospheric paths are responsible for WWVB signal propagation. At night, cosmic background radiation supports a level of D-layer ionization that is sufficient for propagating LF (and lower frequency) radio signals over long distances.[2] Greater D-layer efficiencies and increased effective height with decreased ionization levels contribute to greater signal coverage during the nighttime hours. See Figure 3.

Diurnal shifts in the height of the D-layer cause changes in the RF path length between WWVB and receivers to occur during the time the RF path undergoes sunrise and sunset transitions. While the accompanying Doppler shifts during these periods are generally small, their effects are cyclic and predictable, and can be handled using a priori knowledge. Long-term frequency accuracies very closely approaching those of the WWVB transmitted carrier frequency can be achieved by integrating the diurnal perturbations over a day or more.

WWVB Signal Characteristics

With rare exception, WWVB broadcasts 24 hours a day with a peak envelope effective radiated power of 70 kW. The beginning of every UTC second is identified by a 17 dB reduction in radiated power. See Figure 4. If the carrier amplitude is restored to full power 200 ms later, this represents a "0" bit in the WWVB legacy time code. If it is restored 500 ms later, this represents a "1" bit in the WWVB time code. If it is restored 800 ms later, this represents a "Marker" bit, one of which is sent every 10 seconds to establish frame synchronization in receivers. Two Marker bits transmitted in succession identify the beginning of a new time code frame and the start of a new UTC minute. Over the course of one minute, the individual "1"s and

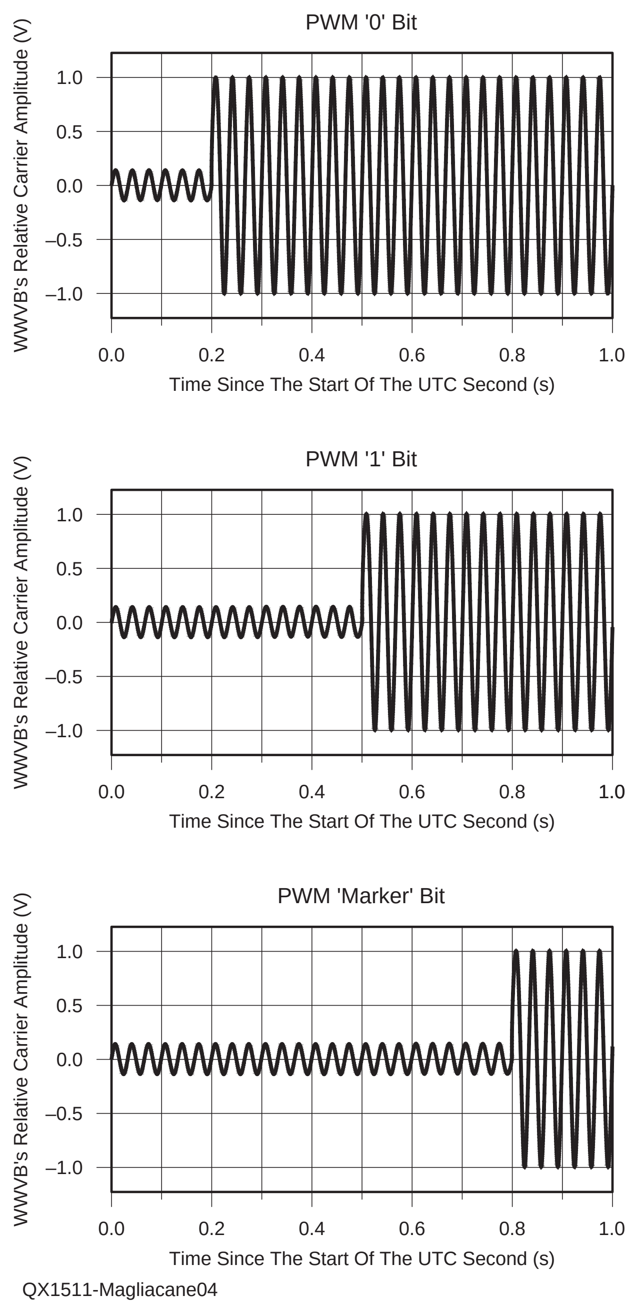

Figure 4 — The WWVB carrier is reduced in amplitude by 17 dB at the beginning of every second. If full power is restored 200 ms later, this represents a "0" bit. If restoration occurs 500 ms later, this represents a "1" bit. If it is restored 800 ms later, this represents a "Marker" bit. The new WWVB BPSK time code is not shown in this illustration.

"0"s produce a pattern that conveys the current date and time, UT1 offset, leap second, and daylight savings time information.

WWVB recently added a secondary time code in the form of BPSK, which co-exists independent of the original amplitude modulated time code. If the phase of the WWVB carrier is reversed 100 ms after the beginning of the UTC second, this represents a "1" bit in the BPSK time code. If no carrier phase reversal takes place at this time, it represents a "0" bit.

The new BPSK time code offers enhanced performance through error detection and correction algorithms, as well as several different modes of operation, not all of which have been fully implemented at this time. While the frequency standard described here possesses BPSK demodulation capability, it is employed solely for the detection and removal of BPSK prior to the carrier phase tracking circuitry that follows.

A Low-Noise WWVB Antenna

Unlike GPS, WWVB reception does not require the use of an outdoor antenna, nor does it require a clear view of the sky. Low-cost consumer grade radio controlled clocks employ electrically small H-Field ferrite loopstick antennas that operate on the same principle as those found in portable AM broadcast band radios. Significantly higher signal levels and noticeably less sensitivity to nearby structures can be realized by using physically larger air-core loop antennas.

While it can take a lot of wire and a lot of labor to wind a 60 kHz resonant air-core loop antenna, just a single turn of multi-conductor ribbon cable can produce an effective multi-turn loop provided that each conductor is connected in series with its adjacent conductor to form a continuous coil. See Figure 5 for an example of how such a coil can be wired. I fabricated an antenna from a 5 meter length of 40 conductor #28 AWG stranded ribbon cable, and supported it from the ceiling of my attic. Figure 6 shows my antenna installation.

Resonance is achieved by introducing an appropriate amount of capacitance in parallel with the loop. Aligning the plane of the loop in the direction of Fort Collins, Colorado allows the WWVB horizontally polarized H-Field to cut through the center of the loop and induce a voltage across its terminals. Along the eastern edge of the 100 mV/meter signal contour in central New Jersey, WWVB typically induces several millivolts (peak-to-peak) of RF across the 40 turn loop.

Antenna Preamplifier

A preamplifier located immediately adjacent to the loop provides an important interface between the high-impedance balanced loop antenna and the unbalanced, ground-referenced circuitry that follows. Figure 7 shows the schematic diagram of the preamplifier. The preamplifier connects to the frequency standard through a length of coaxial cable, and it receives its operating

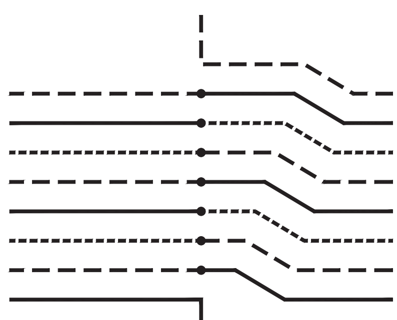

QX1511-Magliacane05

Figure 5 — Loop antenna construction. The ends of the multi-conductor cable are brought together at the bottom of the loop to form a multi-turn coil. After going around once, the end of conductor #1 connects to the beginning of conductor #2, conductor #2 connects to conductor #3, and so on. The uncommitted ends of the first and last conductors form the ends of the coil.

Figure 6 — The author's attic-mounted loop antenna. With the plane of the loop aligned toward Fort Collins, Colorado, the WWVB horizontally polarized H-Field cuts through the center of the loop and induces a voltage across it. The frequency standard amplifies and processes this signal.

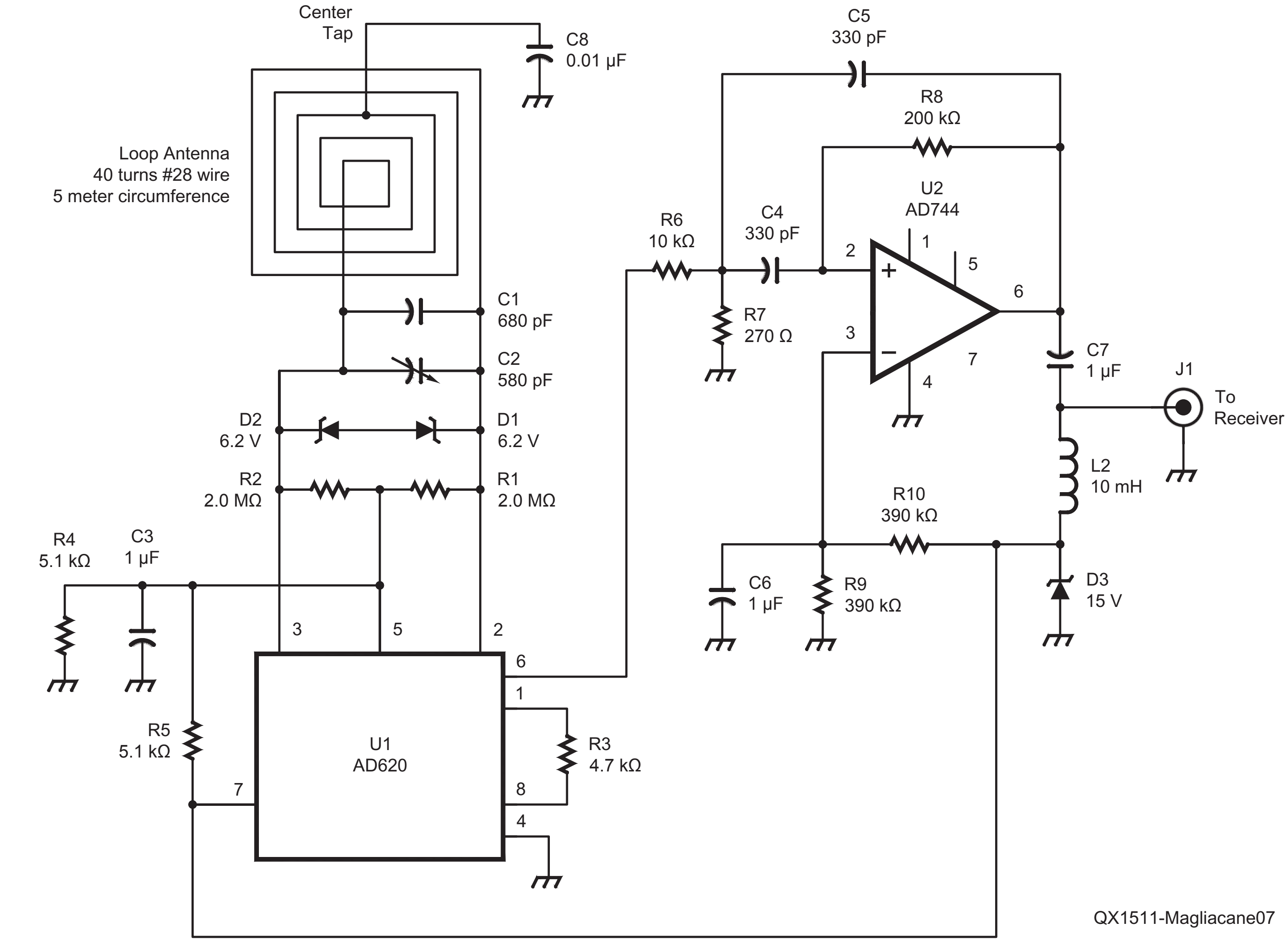

Figure 7 — 60 kHz WWVB loop antenna preamplifier. In addition to providing 40 dB of gain, the preamp properly interfaces the balanced loop antenna with the ground-referenced circuitry in the frequency standard.

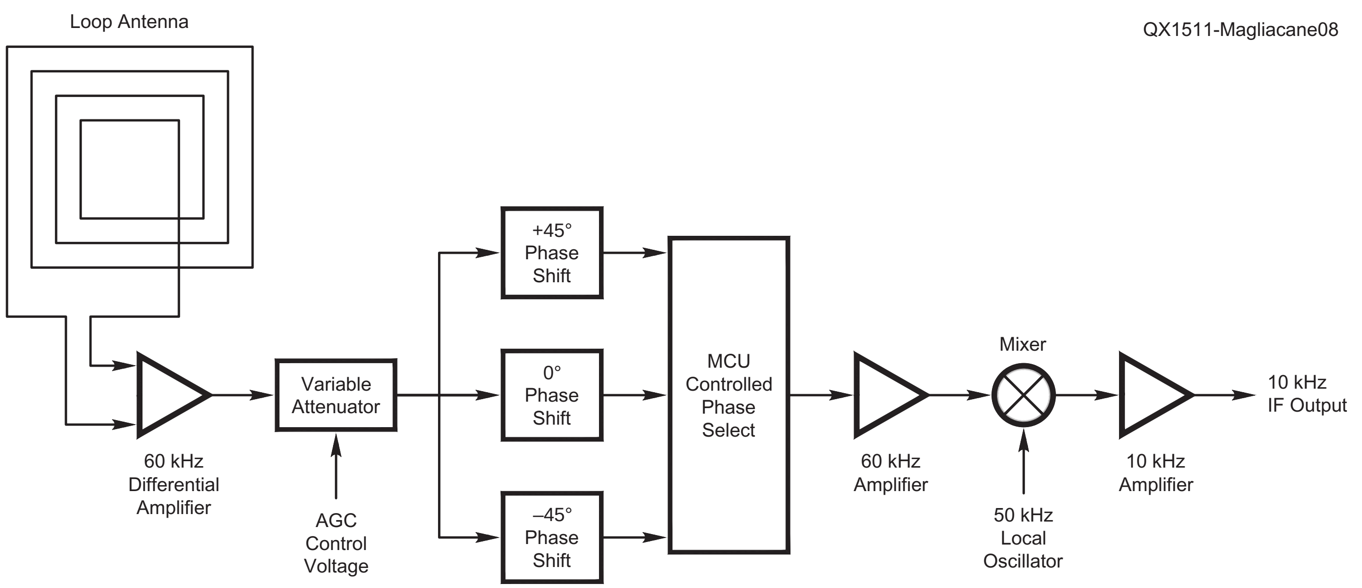

Figure 8 — This block diagram illustrates the overall RF to IF conversion process. The +45° and –45° phase shift networks were used in the past to compensate for the WWVB hourly phase signature, but have not been required since the introduction of BPSK modulation was made in 2012.

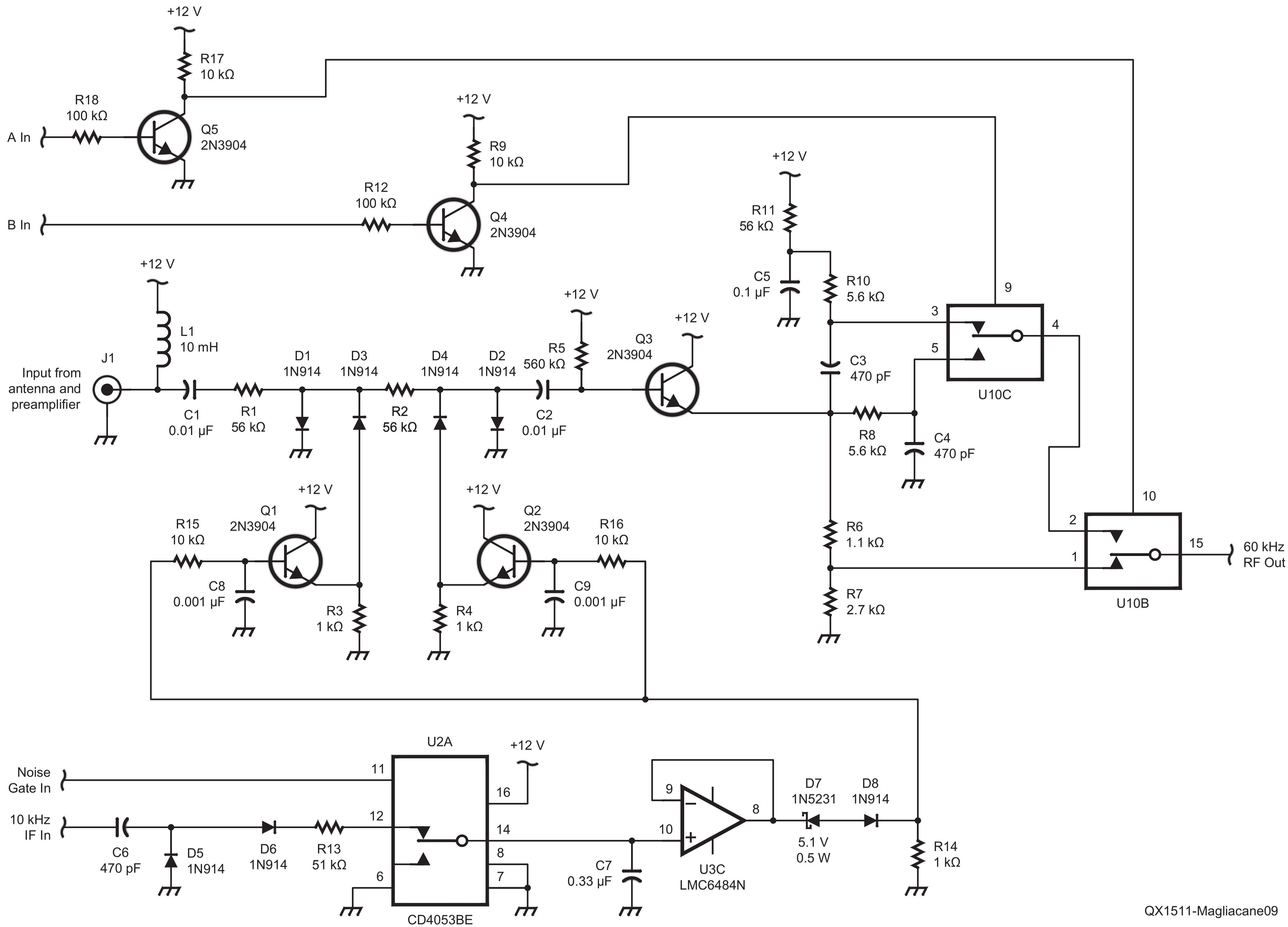

Figure 9 — Details of the RF AGC circuitry and legacy carrier phase shift networks of the frequency standard.

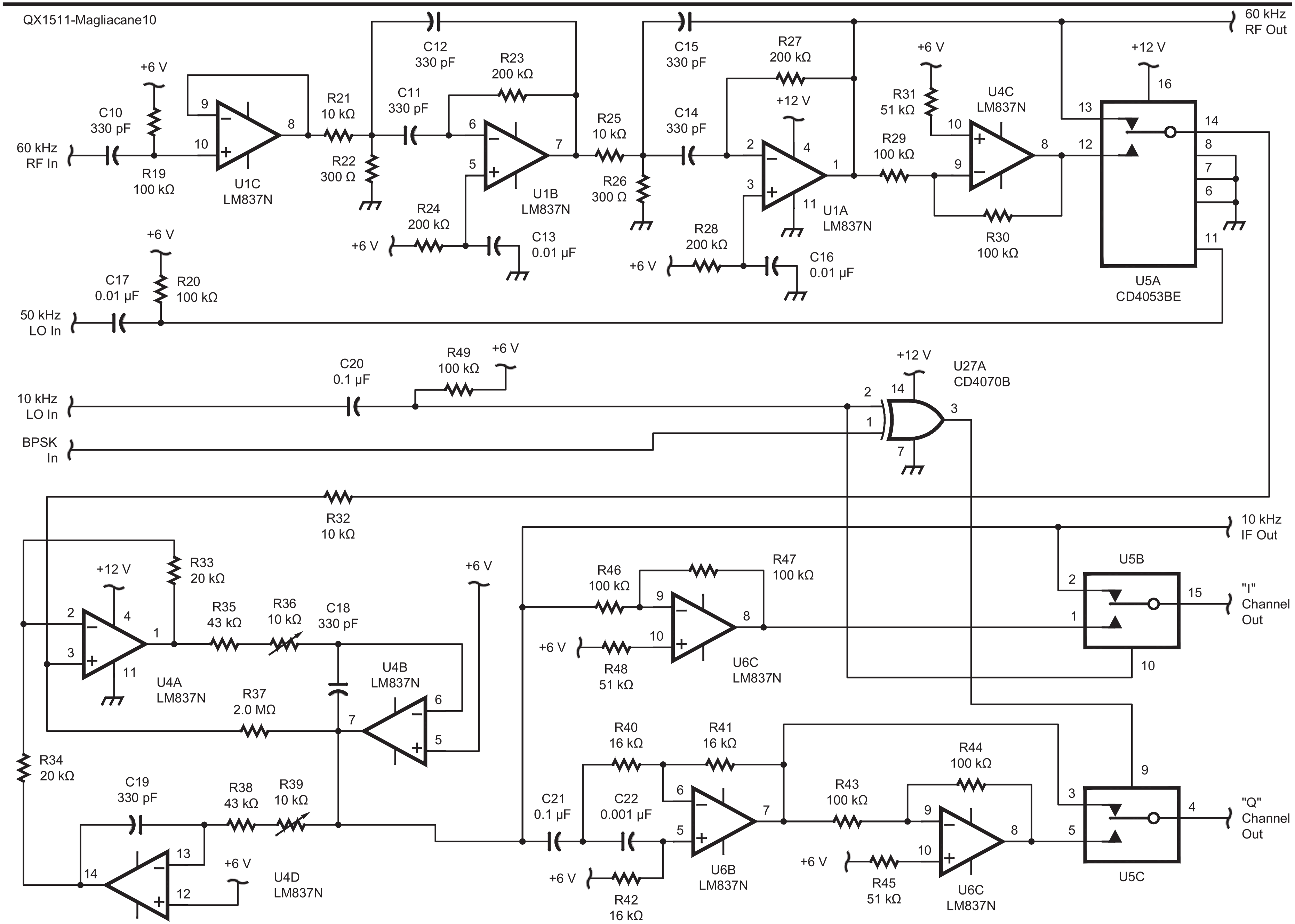

Figure 10 — RF to baseband signal processing. 60 kHz amplification precedes a balanced mixer that downconverts WWVB to a 10 kHz IF, where additional gain and selectivity are provided. A –90° phase shift in the lower IF path drives I and Q demodulators that provide outputs at baseband (DC) levels.

power from the frequency standard through the same length of coax. This connection provides a voltage transfer rather than a power transfer of RF energy between the preamplifier and the frequency standard. Since the length of coax will be small in terms of wavelength, transmission line effects and impedance matching concerns can be ignored, and coaxial cable of any convenient surge impedance can be employed.

The amount of capacitance required in parallel with the loop to achieve resonance at 60 kHz depends on the size, shape, distributed capacitance, and overall inductance of the loop. The 40 turn loop described here required about 1050 pF of capacitance. Capacitor C1 should be a silver mica or similar low-loss, temperature stable capacitor. I used an Elmenco 467 110 pF to 580 pF compression trimmer capacitor at C2 to carefully bring the loop to resonance at 60 kHz.

Signal-to-noise ratios at LF are often enhanced by desensitizing the near-field response of the receiving antenna to E-Field energy. This effect is often accomplished by employing an electrostatic shield around the perimeter of the loop. In this design, E-Field desensitization is achieved by employing a high common-mode-rejection differential amplifier as the first stage of the preamplifier. Capacitor C8 provides an AC ground to the electrical center of the loop, to enhance the preamplifier rejection of out-of-band signals. Zener diodes D1 and D2 help protect the Analog Devices AD620 differential amplifier from damage when nearby lightning strikes induce high voltage impulses across the antenna.

The differential amplifier is followed by a 60 kHz second-order active bandpass filter designed around an AD744 operational amplifier. This stage provides additional RF selectivity beyond that of the loop antenna alone, and raises the overall voltage gain of the preamplifier to 40 dB. The AD744 has the capability of driving capacitive loads, and can deliver output voltages as high as 10 $V_{p\text{-}p}$ without distortion.

Resistor R3 sets the gain of the AD620, and may be increased in value if less preamplifier gain is desired. For best performance, capacitors C4 and C5 should be low-loss, high temperature stability devices (such as silver mica), and all resistors should be within 5% tolerance.

RF Amplitude and Phase Management

Figure 8 illustrates the overall process of converting the WWVB 60 kHz signal down to a 10 kHz IF, where separate amplitude and phase detection takes place. Figure 9 illustrates the frequency standard RF circuitry in greater detail.

Inductor L1 and capacitor C1 form a bias tee network that feeds DC operating voltage to the preamplifier while simultaneously directing RF from the preamplifier into a current controlled RF attenuation network. This network is part of the frequency standard AGC circuitry, and it consists of resistors R1 and R2, and diodes D1 through D4.

Capacitor C6 along with diodes D5 and D6 and resistor R13 charge capacitor C7 to the peak level of the IF voltage. Analog switch U2A is opened when strong atmospheric discharges are detected. This action prevents C7 from charging to the peak level of the noise impulse, which would otherwise engage the AGC more heavily, and desensitize the frequency standard in the moments following the static crash.

The voltage across C7 is buffered by op-amp U3C, level shifted through diodes D7 and D8, and used to control the RF attenuation network through transistors Q1 and Q2.

With no current applied to the network, the dynamic resistance of all four diodes is high, and very little RF signal attenuation takes place across resistors R1 and R2. As the IF signal level begins to rise above the threshold set by diodes D7, D8, and the base-emitter junctions of transistors Q1 and Q2, the DC current passing through diodes D1 through D4 begins to increase. This current decreases the dynamic resistance of the diodes, and causes an increasing amount of RF to be conducted through them to ground. A fairly constant peak RF level remains after the attenuation network, and appears on the emitter of transistor Q3.

For many decades, WWVB employed a method of station identification where its transmitter would advance the phase of its carrier +45° 10 minutes after the start of each hour, and return to normal phase 5 minutes later. These hourly phase shifts were discontinued when BPSK modulation was added in 2012. Nevertheless, the circuitry used to compensate for these phase shifts worked extremely well, and is included here for discussion.

60 kHz RF appearing on the emitter of transistor Q3 is simultaneously applied to a +45° phase shift network (C3, R10), a –45° phase shift network (R8, C4), and a resistive voltage divider (R6, R7) having the same attenuation characteristic as each phase shift network. In the past, the appropriate RF path would be selected by the microcontroller based on the current time of day. The 0° path would normally be selected when the frequency standard was initially powered on. At 10 minutes after the hour, the –45° path would be selected through analog switch U10C and into U10B to compensate for the +45° phase advance that would occur at that time. At 15 minutes after the hour, the 0° path would again be selected through U10B. If the frequency standard were powered on between 10 and 15 minutes past the hour, the WWVB carrier would have already been advanced +45°. Therefore, the frequency standard would continue using the 0° path, and later select the +45° path when WWVB would have shifted back –45° at 15 minutes after the hour.

Converting to a 10 kHz IF

Phase and amplitude conditioned 60 kHz signals are next handled by the circuitry illustrated in Figure 10. Here, additional RF gain and selectivity are provided by active bandpass filters designed around op-amps U1A and U1B. As was the case in the preamplifier, the 330 pF capacitors at C11, C12, C14, and C15 should be of a temperature stable, low-loss chemistry. An AGC conditioned 60 kHz RF sample from the output of U1A is buffered and made available for use outside the frequency standard.

U4C forms a 180° unity gain phase inverter that forms a balanced mixer along with U5A, one section of a CD4053BE triple SPDT analog switch. Driven by a 10 MHz derived 50 kHz local oscillator, this mixer converts the 60 kHz RF signal down to a 10 kHz IF. Op-amps U4A, U4B, and U4D form a 10 kHz biquad active bandpass filter that serves as a high-gain, narrow bandwidth IF amplifier. This amplifier provides 46 dB of gain and a 3 dB bandwidth of 100 Hz. The center frequency of the amplifier is set to 10 kHz through careful alignment of potentiometers R36 and R39. The 330 pF capacitors employed at C18 and C19 must be of a low-loss variety.

Working from within the AGC loop, the IF amplifier provides an output voltage of about 8 $V_{p\text{-}p}$. A sample of the 10 kHz IF is made available for use outside the frequency standard.

Demodulating "I" and "Q"

The 10 kHz IF signal is split between a straight-through path and a path through op-amp U6B that produces a –90° phase shift. A balanced mixer — consisting of op-amp U6C and analog switch U5B — is driven by a 10 MHz derived 10 kHz local oscillator, and forms an in-phase ("I" channel) demodulator. The –90° phase shifted path feeds a second balanced mixer consisting of op-amp U6C and analog switch U5C. This mixer is driven by the same 10 kHz local oscillator after it has passed through exclusive OR gate U27A, and produces a quadrature ("Q" channel) demodulator.

The output of the "I" channel demodulator is a +6 V referenced baseband DC voltage that is linearly proportional to the WWVB carrier phase polarity and modulation amplitude. After the effects of BPSK modulation have been removed by the action of U27A and its associated circuitry, the "Q" channel demodulator produces a +6 V referenced baseband DC voltage that is linearly proportional to a WWVB carrier having no phase modulation.

Figure 11 presents an overview of the signal path taken by the 10 kHz IF. As illustrated in Figure 12, op-amps U3D and U7D function as a 3.685 Hz wide four pole Bessel low-pass filter, and set the frequency standard "I" channel RF bandwidth to 7.37 Hz. Output from the filter drives op-amps U25A and U25B. Using a virtual ground DC reference of +6 V, op-amp U25A acts as a voltage comparator and demodulates the WWVB BPSK into a 12 V_{p-p} square wave. U25B serves as a unity gain phase inverter, and provides an "I" channel waveform that is complementary to the original.

The CD4066B analog switching arrangement that follows is driven by the demodulated BPSK waveform provided by U25A. By selecting the non-inverted "I" channel signal through U26B when the WWVB carrier phase is normal, and selecting the inverted "I" channel signal through U25B and U26C when the WWVB carrier phase is inverted, a BPSK-free "I" channel is produced. U25A's BPSK correction signal is also applied to exclusive OR gate U27A to control the phase of the 10 kHz local oscillator fed to the "Q" channel demodulator, and allows the demodulator to maintain a constant output polarity.

The filtered and BPSK-free "I" channel energy is applied to op-amp U7A and diode D9, and work through analog switch U10A and resistor R57 to charge capacitor C27 to the peak voltage of the demodulated AM time code. This voltage is buffered through U7B, whose output is applied across the R59/R60 voltage divider. The voltage divider sets the threshold of comparator (op-amp) U7C to a level that is midway between the upper (0 dB peak reference) and lower (–17 dB below peak reference) amplitudes of the WWVB detected carrier. The comparator produces a switching waveform that illuminates green Time Code LED, D10, in synchronization with the WWVB amplitude modulation. This waveform is also made available to the microcontroller following a translation to TTL voltage levels by transistor Q6.

Analog switch U10A is briefly opened when high amplitude noise impulses are detected to prevent them from charging C27 and overshooting the decision threshold set by U7C. The demodulated time code pulses and the peak time code voltages are also indicated on a meter mounted on the front panel of the frequency standard's enclosure.

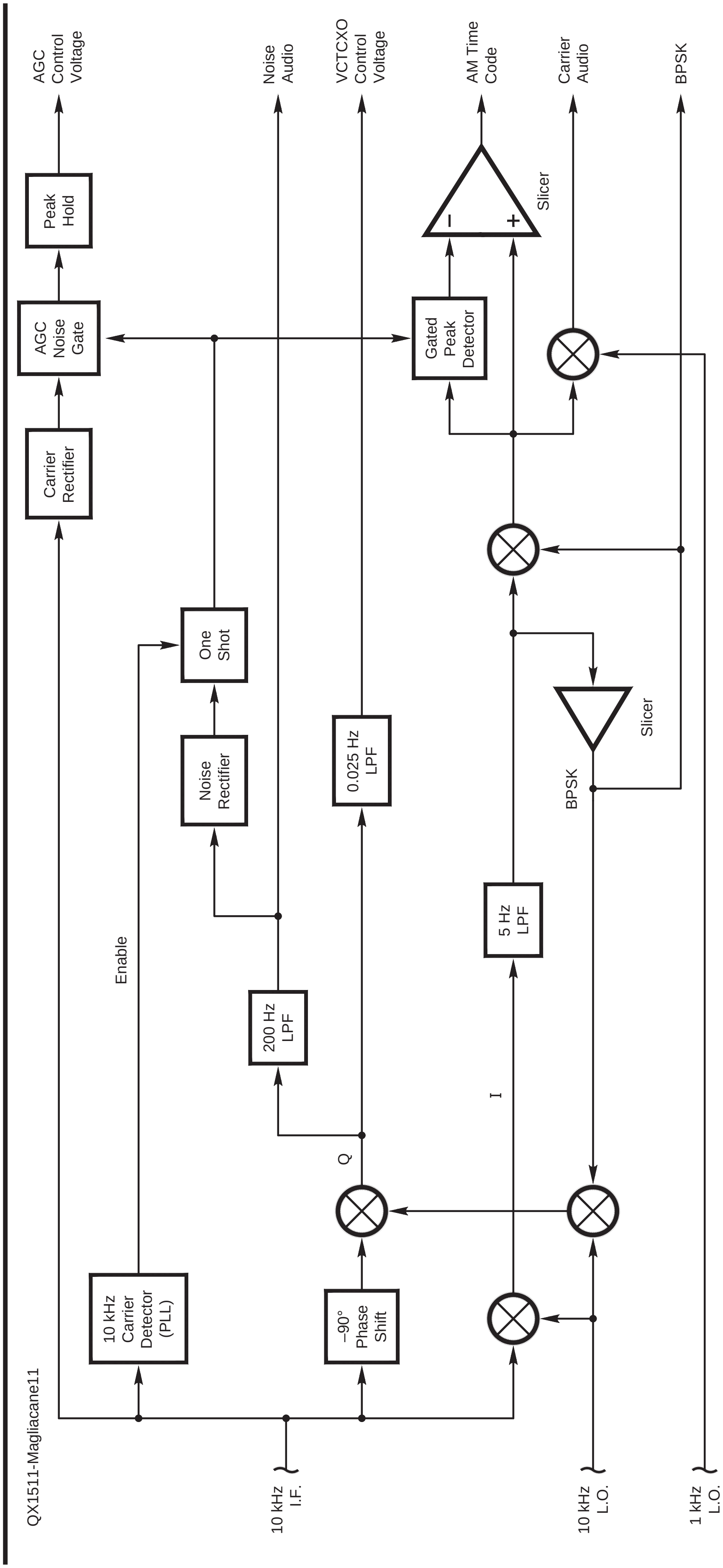

Figure 11 — This block diagram illustrates the post-detection processing. The WWVB amplitude shift keying and phase shift keying are demodulated from the I channel while the Q channel provides tuning voltage for the VCTCXO.

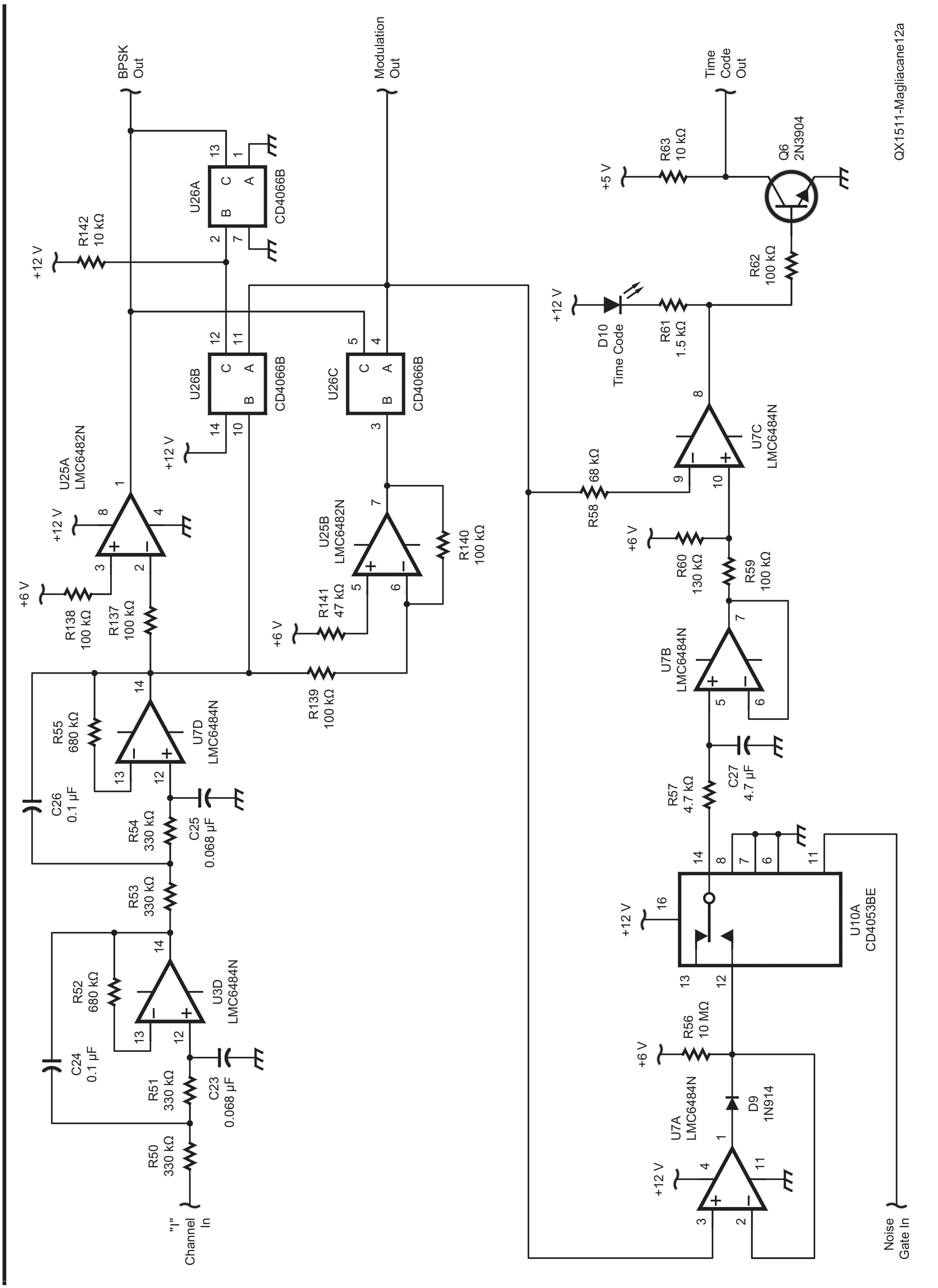

BPSK Out
Modulation Out
Time Code Out
QX1511-Magliacane12a
+12 V
R142 10 kΩ
U26A
CD4066B
+5 V
R63 10 kΩ
Q6 2N3904
R62 100 kΩ
D10 Time Code
R61 1.5 kΩ
U26B
CD4066B
U26C
CD4066B
U25A LMC6482N
U25B LMC6482N
R140 100 kΩ
R141 47 kΩ
+6 V
R138 100 kΩ
R137 100 kΩ
R139 100 kΩ
R58 68 kΩ
U7C LMC6484N
R60 130 kΩ
R59 100 kΩ
U7B LMC6484N
R55 680 kΩ
U7D LMC6484N
C26 0.1 µF
R54 330 kΩ
C25 0.068 µF
R53 330 kΩ
R57 4.7 kΩ
C27 4.7 µF
U10A CD4053BE
R52 680 kΩ
U3D LMC6484N
C24 0.1 µF
R51 330 kΩ
C23 0.068 µF
R50 330 kΩ
"I" Channel In
R56 10 MΩ
D9 1N914
U7A LMC6484N
Noise Gate In

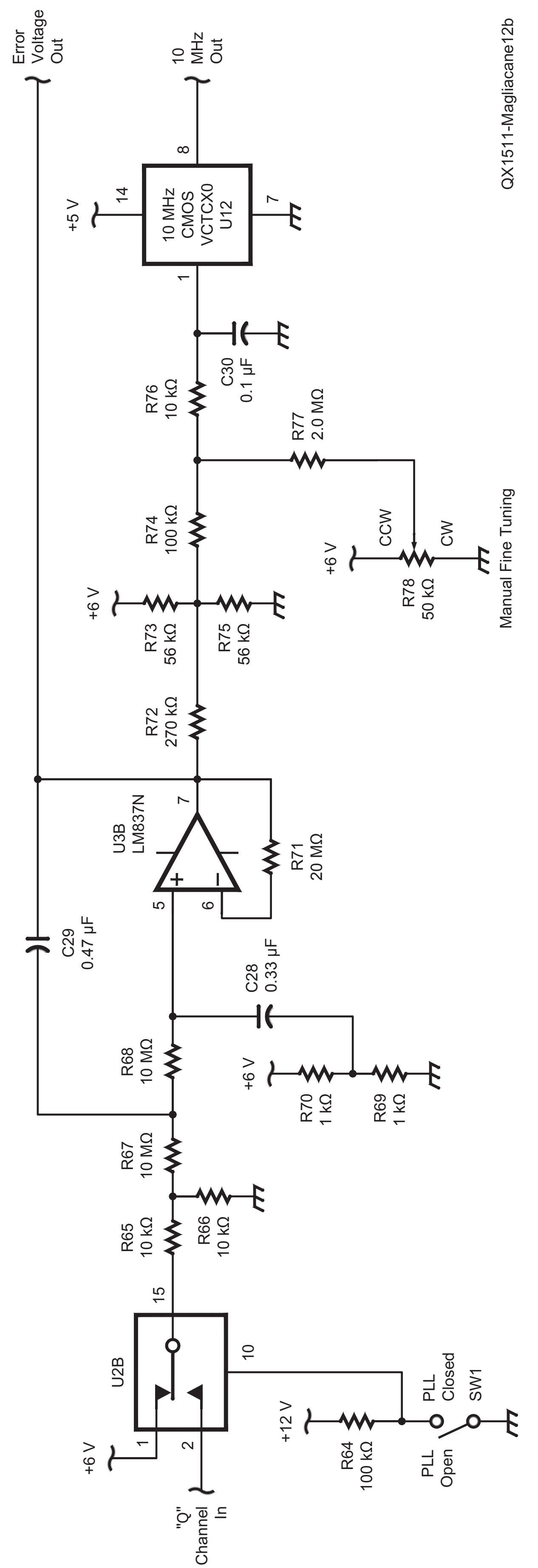

Figure 12 — This schematic diagram shows the details of the I and Q channel filtering and processing. Both amplitude and phase shift keying signals are demodulated from the I channel, while the Q channel develops the tuning voltage that forces the 10 MHz oscillator to track the phase of the WWVB carrier.

Controlling The VCTCXO

After passing through analog switch U2B, the output of the "Q" channel demodulator is fed through a 0.025 Hz wide second order low-pass filter (U3B) before being applied to the 10 MHz VCTCXO. Low leakage, metalized polypropylene film capacitors were employed at C28 and C29.

The resistive network between the low-pass filter and the VCTCXO exhibits 21 dB of attenuation, and controls the VCTCXO tuning sensitivity and the maximum loop gain of the frequency standard. The loop gain setting is fairly critical, since a third-order phase-locked loop (PLL) function is produced by the VCTCXO and the second order low-pass filter that precedes it. Third-order PLLs offer superior noise rejection and lower steady-state errors than second order PLLs, but they do so with a reduced phase margin. Since the VCTCXO will be generally close to its target frequency, acceptable overall loop stability is achieved by simply keeping the PLL loop gain no higher than that necessary to electronically steer the VCTCXO to exactly 10 MHz over a limited tuning range. If greater amounts of steering voltage are required, a front panel mounted 10 turn potentiometer (R78) is available to allow manual fine tuning of the oscillator. Switch SW1 allows manual tuning to take place either with (PLL Closed) or without (PLL Open) there being a tuning influence from WWVB. Changing SW1 to a DPDT switch and adding a red LED and an appropriate current limiting resistor can be advantageous in providing a visual cue to the user that the PLL switch is in the open position.

This frequency standard employs a Bomar Crystal Company model B17025-ADMF-10.000 10 MHz VCTCXO as its master oscillator. The oscillator operates on 5 V, and has a frequency stability of 2.5 ppm. It provides an HCMOS square wave output waveform, and has a measured positive slope tuning sensitivity of 62.8 Hz/V. In addition to being voltage controlled, the oscillator also possesses a trimmer capacitor to permit coarse frequency adjustments to be made independent of the tuning voltage applied to the oscillator. Since this frequency standard operates the oscillator with a nominal tuning voltage close to 3.0 V rather than the 2.5 V ($+V_{cc}/2$) typically expected in a 5 V oscillator, the trimmer allows oscillator adjustment to 10 MHz with this higher tuning voltage applied.

Since the PLL loop gain in this frequency standard is intentionally low, and some dependence on manual tuning is sometimes required, a more stable oscillator would make manual tuning adjustments far less critical when changes in ambient temperature take place.

LO and Standard Frequency Generation

Figure 13 illustrates the circuitry used to buffer the 10 MHz VCTCXO for external applications, and divide it down in frequency for both internal and external use. U18, a Microchip MCP101-460HI/TO active high supervisory circuit, holds the active high CLEAR inputs of every 74HC390 dual decade counter high for approximately 350 ms after the frequency standard is first powered on. In addition, U15A and U15B at the far end of the divider chain are reset independently of the other dividers by the microcontroller in alignment with the beginning of the UTC second, shortly after the frequency standard is first powered on.

Buffered TTL level outputs at 10 MHz, 1 MHz, 100 kHz, 50 kHz, 25 kHz, 10 kHz, 1 kHz, and 100 Hz are available through U17, a 74HC151 multiplexer. Frequency selection takes place through a three bit binary code applied to the multiplexer data select lines. An eight position BCD switch, or simply a three pole eight position rotary switch wired with the appropriate ground connections and pull-up resistors can be used to select the output frequency. Two additional buffered 10 MHz outputs are also provided.

Figure 14 illustrates the circuitry associated with the microcontroller, back-lit LCD alphanumeric display, RS-232 port, and several regulated voltage references and sources used by the frequency standard. The PIC16F88 (U11) accepts the WWVB AM time code, the WWVB BPSK time code, a 10 Hz timing signal from the frequency dividers, filtered PLL error voltage derived from the "Q" demodulator, and a DC reference voltage that is exactly half the +6 V used throughout the frequency standard as a virtual ground.[3] The microcontroller generates the reset pulse that clears 74HC390 decade counters U15A and U15B as previously described. It also generates the signals necessary for driving the legacy ±45° RF phase shift networks in the front end of the frequency standard, the 24 × 2 LCD, and provides serial UTC date and time information to peripheral devices through a Dallas DS232A RS-232 level converter (U9).

Figure 15 illustrates the audio, loss of signal, noise detection, and noise mitigation circuitry. A DC voltage from the "I" channel demodulator that is proportional to the WWVB modulation amplitude is applied to analog switch U2C, where it is modulated at a 1 kHz rate to produce an amplitude modulated audio tone. A narrow bandpass filter following the modulator attenuates the level of harmonics contained in the 1 kHz switching carrier. The resulting sinusoidal waveform is applied to an audio select switch before being made available to an LM380 audio power amplifier.

Noise Detection and Mitigation Circuitry

While the "I" channel contains a DC voltage proportional to the WWVB modulation amplitude, the output of the "Q" channel (after BPSK-correction) is modulation free. Therefore, any rapid modulation of the DC voltage present on the output of the "Q" demodulator is the result of noise energy present at 60 kHz. The circuitry surrounding transistor Q7 forms a 200 Hz wide low-pass filter that rejects any high frequency energy remaining from the "Q" channel demodulation process that might take on the appearance of noise to the circuitry that follows.

The low-pass filter feeds a precision full-wave rectifier designed around op-amps U20A and U20B. The rectifier feeds negative-going noise impulses to U22, an LM555 monostable multivibrator. The triggering threshold for the LM555 is set through potentiometer R97, and is adjusted so that the LM555 triggers only when strong lightning discharges are detected. Once triggered, the LM555 lights D13, an amber colored LED, to indicate noise detection. The 555 also opens the analog switches associated with the AGC (U2A) and peak time code detection (U10A) circuitry to prevent their reaction to the static crash. The rectified noise voltage also drives a front panel meter to provide indications of its relative intensity.

The 200 Hz low-pass filter also provides an audio signal to the LM380 audio amplifier to permit aural monitoring of any 60 kHz background noise that could influence reception quality. U19, an LMC567 tone decoder PLL, monitors the 10 kHz IF and responds to the absence of the WWVB carrier. The LMC567 lights D14, a red colored LED, if a loss of signal condition is detected. It also holds the LM555 in reset mode, and prevents it from lighting the noise LED and opening the noise-gated analog switches under a loss of signal condition, or during the first few seconds after power-up while the AGC becomes fully acclimated to the WWVB signal level.

Multimeter and Sinusoidal Outputs

Figure 16 illustrates the circuitry responsible for providing sinusoidal output signals and analog meter indications. A fourth order 1 kHz bandpass filter designed around op-amps U20C and U20D filter the 1 kHz square wave local oscillator signal into a sinusoidal waveform. This waveform is amplified by U23, an LM386 audio power amplifier that provides sufficient output current to drive a low impedance load.

Op-amp U6D buffers a sample of the 10 kHz IF, U1D buffers a sample of the 60 kHz RF signal, and together these signals are made available for external use. The gain of each buffer has been tailored to produce RF and IF output samples of relatively equal amplitudes.

SW3, a two pole four position rotary switch allows relative measurements of modulation level, peak signal level, center tuning, and ambient radio noise levels to be made through a single 100 µA D'Arsonval panel meter.

The Liquid Crystal Display

The PIC16F88 contains a 10 bit analog-to-digital converter that is used to measure the relative WWVB-derived error voltage fed to the VCTCXO. This voltage is represented as a three digit number between –512 and +511, and is continuously displayed on the bottom center of the LCD. Proper adjustment of the VCTCXO through R78 is achieved when a stable reading close to 000 is made.

The PIC A/D converter has a resolution of 6 V/1024 or 5.86 mV. Since the error voltage is attenuated by a factor of 11.3 (21 dB) before it reaches the VCTCXO, but is read by the PIC prior to this attenuation, the tuning indicator is able to resolve a 518 µV change in the VCTCXO error voltage.

Power Up Procedure

Once powered on, the frequency standard sequences through several modes of operation before it is finally ready for use. The setup process takes several minutes to complete, and the LCD keeps the user informed of the process along the way.

The display illustrated in Figure 17A appears when the frequency standard is first powered on. The microcontroller firmware version is briefly displayed on the first line, while the VCTCXO digital tuning indicator permanently appears in the middle of the line below.

After several minutes have passed and the frequency standard VCTCXO has become locked in phase with that of the WWVB carrier, the microcontroller begins timing the interval between each WWVB amplitude carrier reduction. Carrier reductions occur at the start of each UTC second, and once eight successive properly timed carrier reductions have been detected, the display switches to that illustrated in Figure 17B. When this change occurs, the microcontroller begins looking for the Marker bit sequence, identifying the conclusion of the current time code frame and the beginning of the next.

While waiting for the next frame to begin, the display indicates the phase of the WWVB carrier (+ or –) and the identity of each time code bit (0, 1, or M) received over the previous second. If the bit cannot be identified, a "?" character is displayed.

Since the WWVB carrier level is always "low" for the first 200 ms of every second, and always "high" for the last 200 ms of every second, these intervals carry no time code information and are ignored by the microcontroller bit correlation decoding algorithm. These predictable amplitude levels are instead used to estimate the quality of time code reception, which is displayed as a single digit between 0 (poor) and 8 (excellent) to the right of the time code bit.

Once the beginning of the frame is found, the display switches to that shown in Figure 17C. The microcontroller starts a process

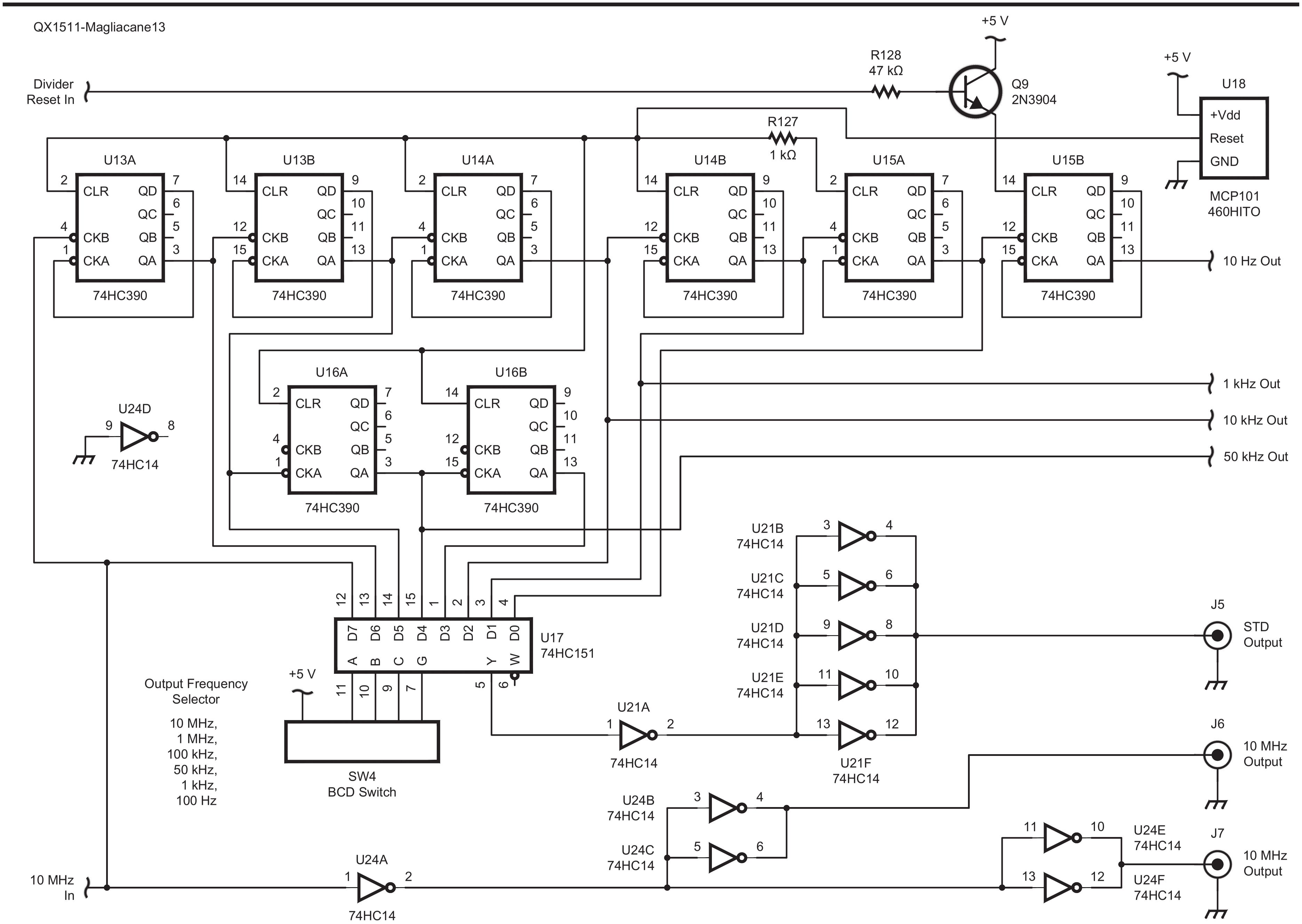

Figure 13 — The 10 MHz VCTCXO is divided and buffered to provide LO injection for every mixer and synchronous demodulator in the frequency standard. A rotary switch allows user selection of 100 Hz, 1 kHz, 10 kHz, 25 kHz, 50 kHz, 100 kHz, 1 MHz, and 10 MHz signals for use in the laboratory.

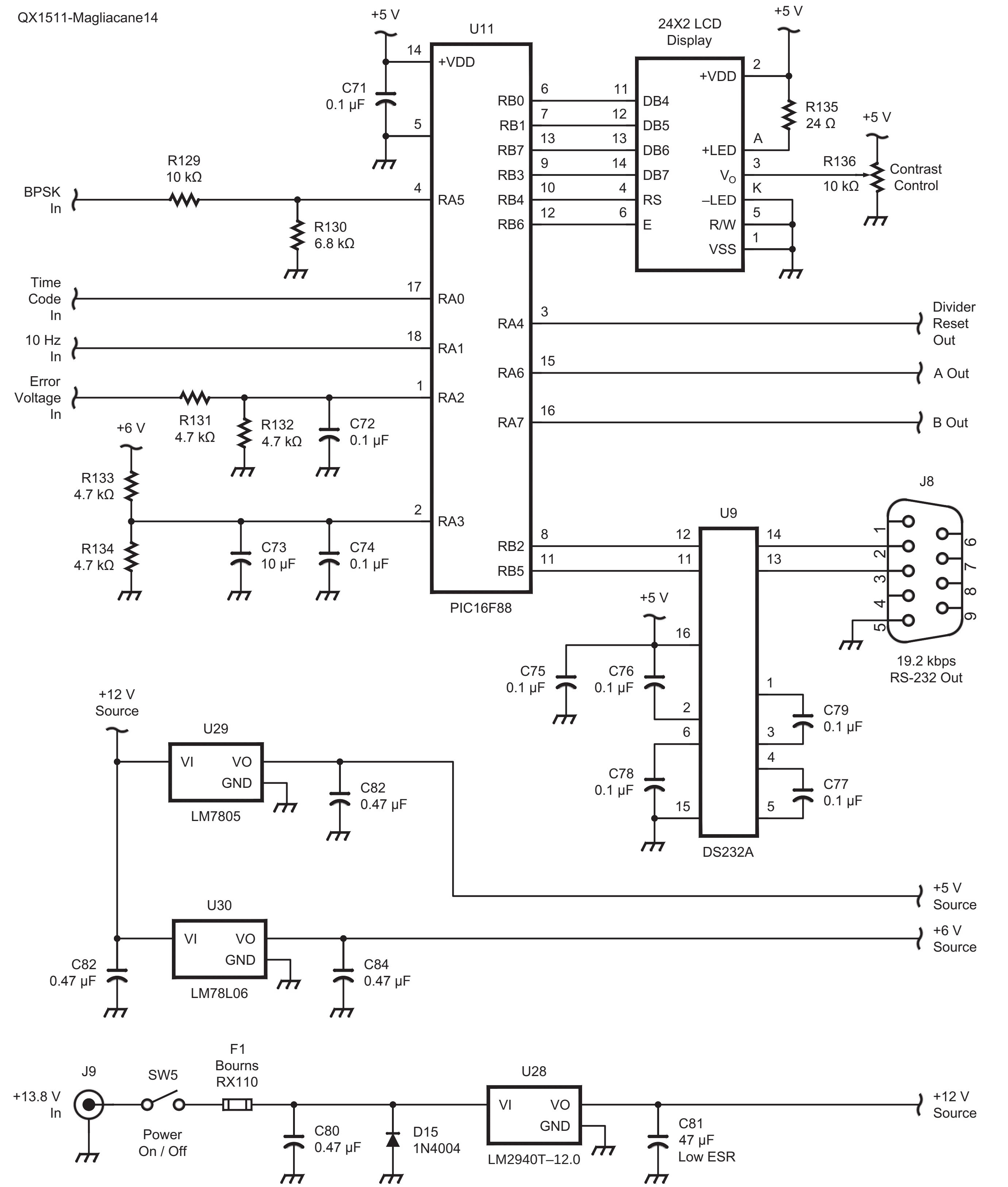

Figure 14 — A PIC microcontroller decodes the WWVB time code, functions as a real-time UTC clock driven by the disciplined oscillator, and provides date and time of day information via the liquid crystal display and RS-232 serial port.

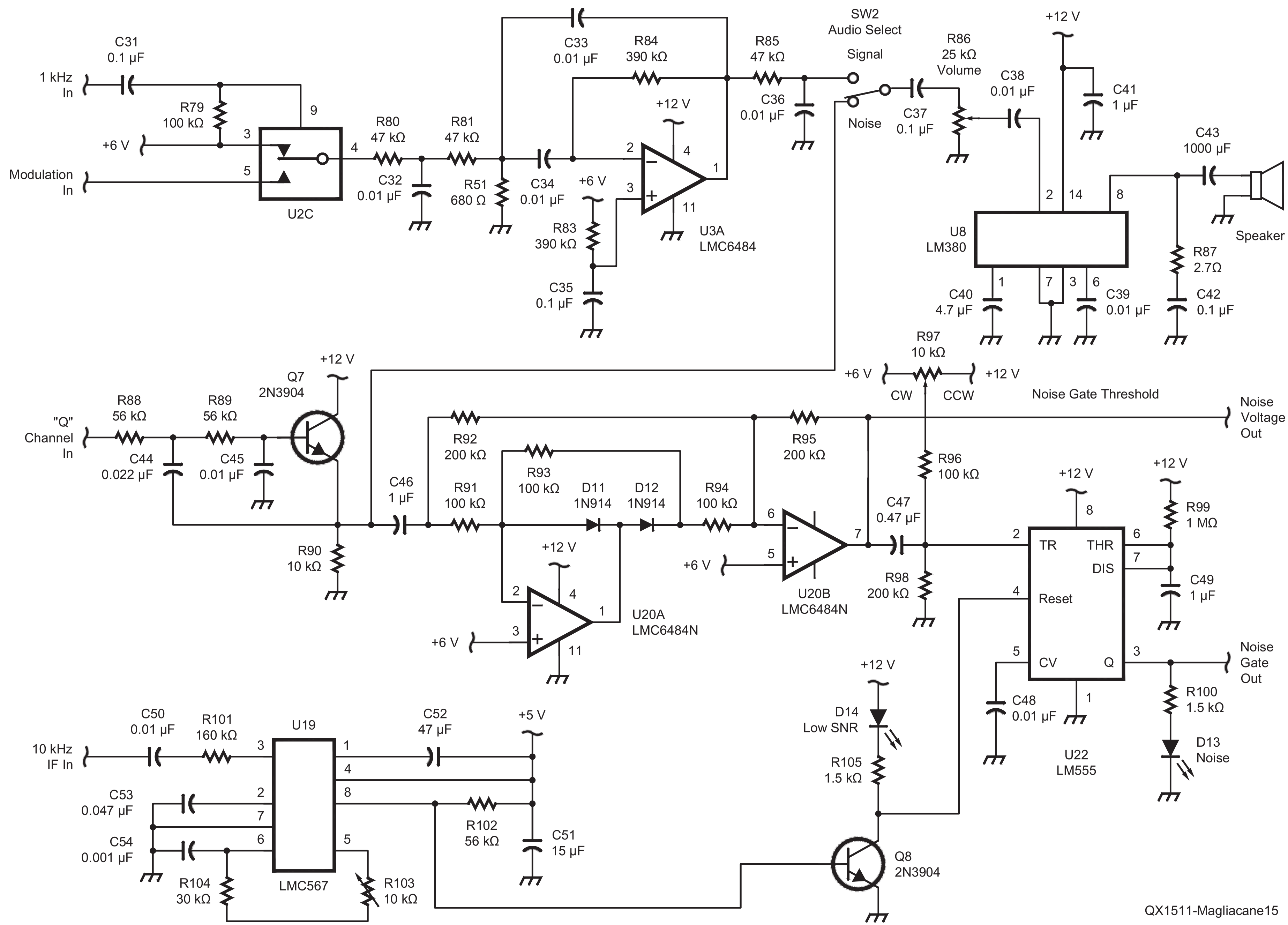

Figure 15 — Here is the schematic diagram for the audio and noise signal processing. Baseband WWVB signals modulate a 1 kHz carrier for aural monitoring of the signal. Noise impulses detected on the Q channel trigger a noise gate that temporarily inhibits AGC action and time code detection. Noise energy can also be monitored through the audio amplifier.

in which it begins decoding the frame and evaluating the integrity of the data being collected. A countdown timer representing the number of seconds until the completion of this process is displayed on the top right hand side of the display. If the data collected looks reasonable, a real-time clock/calendar operating within the firmware of the microcontroller is set to the time and date decoded.

The microcontroller then looks for validation of the information received by examining the next frame of data, and compares the result with that of the real-time clock one minute later (Figure 17D). If the received time and date match that of the clock, then the microcontroller begins displaying the locally running clock and calendar from that point forward. See Figure 17E. If the validation fails, then the process reverts to the point illustrated in Figure 17C, in which the reception and validation routines are repeated until the current time and date are finally confirmed.

Once the validation process is complete, the frequency standard begins sending the current UTC time and date, once every second, to any connected peripherals via the RS-232 port (Figure 18). These peripherals might include a PC with a real-time clock that can be set through appropriate software, or an external digital clock display. While this frequency standard is not intended to serve as an NIST-traceable time source, the date and time reported through both the serial port and the LCD are advanced by 100 ms to compensate for the nearly equal amount of signal processing delay inherent within the electronics in the frequency standard.

Parts and Construction

This frequency standard was developed and tested in discrete stages over a period of several years. Due to this modular design approach, much of the circuitry was built on a series of 95 × 70 mm and 70 × 45 mm perforated circuit boards that have all been interconnected to one another to form a complete unit. Figure 19 is a view inside the cabinet of my unit. With the exception of the DC power supply, antenna, and remote RF preamplifier, all circuitry is housed in a single Ten-Tec model BK-1249 enclosure that measures 12 inches × 4 inches × 9 inches (HWD) Figure 20 is a photo of the front of the unit.

In an effort to enhance frequency stability, thermal effects caused by heat dissipation of the frequency standard electronics are minimized by keeping the DC power supply physically removed from the enclosure, and by mounting both the LM2940T-12.0 and the LM7805 voltage regulators to the enclosure's back panel. The greatest single sources of heat outside of the voltage regulators are the LCD backlight, and interestingly enough, the VCTCXO, itself.

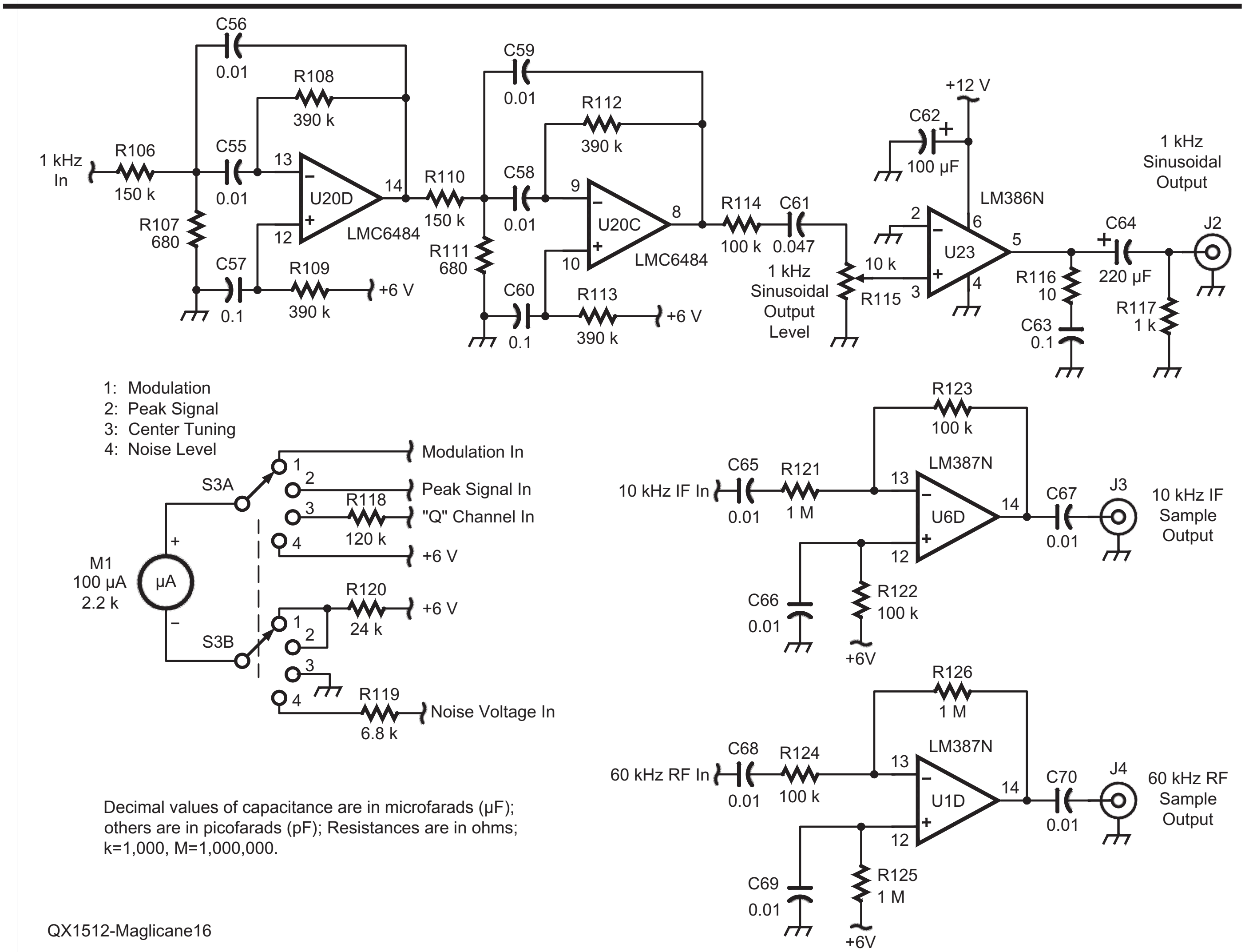

Figure 16 — Metering and various sinusoidal output signals are shown on this schematic diagram. In addition to providing buffered 60 kHz RF and 10 kHz IF samples, a precise 1 kHz sinusoidal waveform capable of driving a small speaker is provided.

Alignment and Testing

The frequency standard may be powered from any 13.8 V DC power source capable of supplying at least 300 mA of current. A Bourns RX110 resettable fuse (F1) located after the power switch is followed by a reverse biased silicon diode to ground (D15). These are used as safety measures to help to protect the circuitry from damage should an over-current or reverse polarity condition ever occur.

The antenna can be adjusted to achieve resonance at 60 kHz by monitoring the output of U1 (AD620 Pin 6) with an oscilloscope while radiating a weak signal at 60 kHz from a nearby function generator and varying the amount of capacitance in parallel with the loop to achieve maximum response. Table 1 provides equations for determining the voltage produced by the loop given its physical dimensions, electrical properties, and local field strength.

Receiver alignment should begin by first adjusting the Manual Fine Tuning Control (R78) until the DC voltage between its wiper and ground reads exactly half that of the +6 V reference.

Next, with the antenna and preamplifier disconnected from the frequency standard, switch SW1 to the "PLL Open" position, and adjust the coarse frequency adjustment capacitor on the VCTCXO until it operates as close to 10 MHz as possible. Being able to obtain a close zero-beat with WWV should be more than adequate at this stage of the alignment.

With the Audio Source Switch (SW2) in the "Noise" position and the 60 kHz function generator off, connect the antenna and preamplifier to the frequency standard. Carefully adjust potentiometers R36 and R39 simultaneously for maximum noise level.

Operation

With the plane of the loop antenna oriented in the direction of Fort Collins, Colorado, final alignment of the VCTCXO can take place. Manual coarse tuning can be achieved by placing SW1 in the "PLL Open" position, and Meter Function Switch (SW3) in the "Center Tuning" position, while slowly adjusting the Manual Fine Tuning control (R78) for a steady, center reading on meter M1.

Table 1

Equations that relate the voltage produced by an electrically small (<0.08 λ) air-core loop antenna to the local field strength given the loop's physical dimensions and electrical properties.

$$E_s = \frac{2\pi eNA}{\lambda}$$

$$e = \frac{E_s \lambda}{2\pi NA}$$

$$Q = \frac{f_r}{bw}$$

$$E_0 = QE_s$$

Where:
E_s = voltage induced into the loop (μV).
E_0 = loop output voltage at resonance (μV).
f_r = loop resonant frequency (Hz).
bw = 3 dB bandwidth (Hz)
Q = the *Q* of the loop.
e = local field strength (mV/m).
N = number of turns.
A = enclosed area of the loop (square meters).
λ = wavelength (meters).

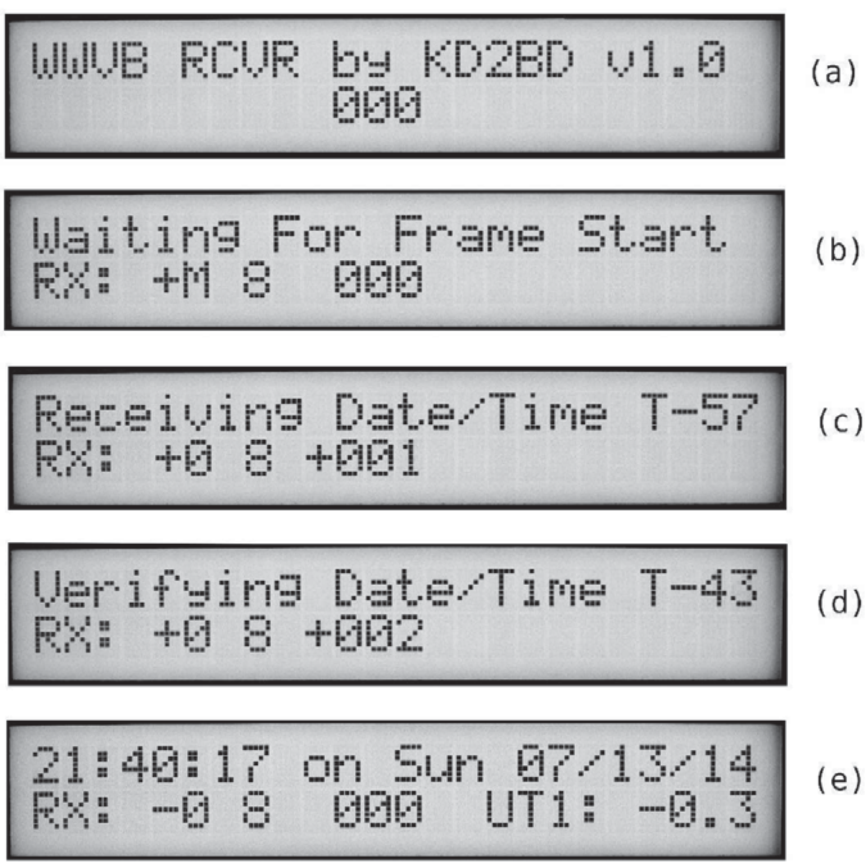

Figure 17 — These images show the various LCD screens depicting each of the five stages of frequency standard operation following power up. The final stage is where the UTC date and time are continuously displayed and made available to peripheral equipment via the RS-232 port.

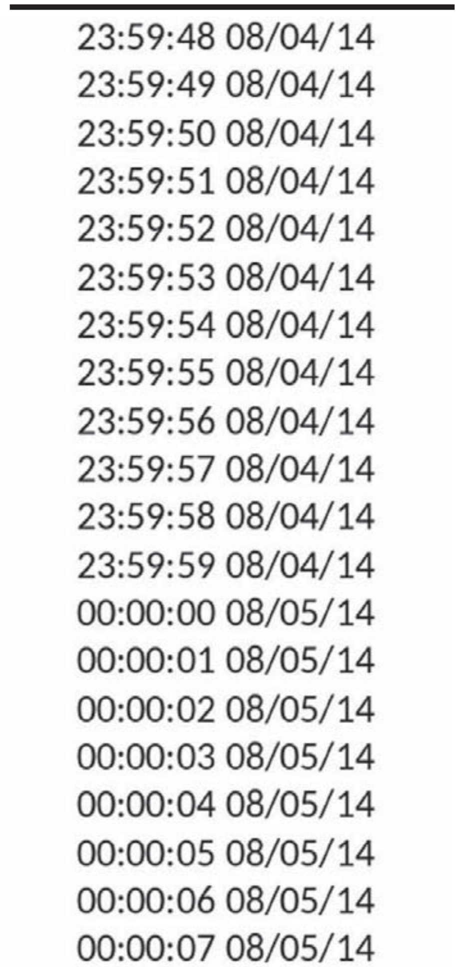

Figure 18 — At the beginning of every second, the 19.2 kbps RS-232 serial port provides the current UTC time and date in the form of HH:MM:SS MM/DD/YY followed by a line feed and carriage return.

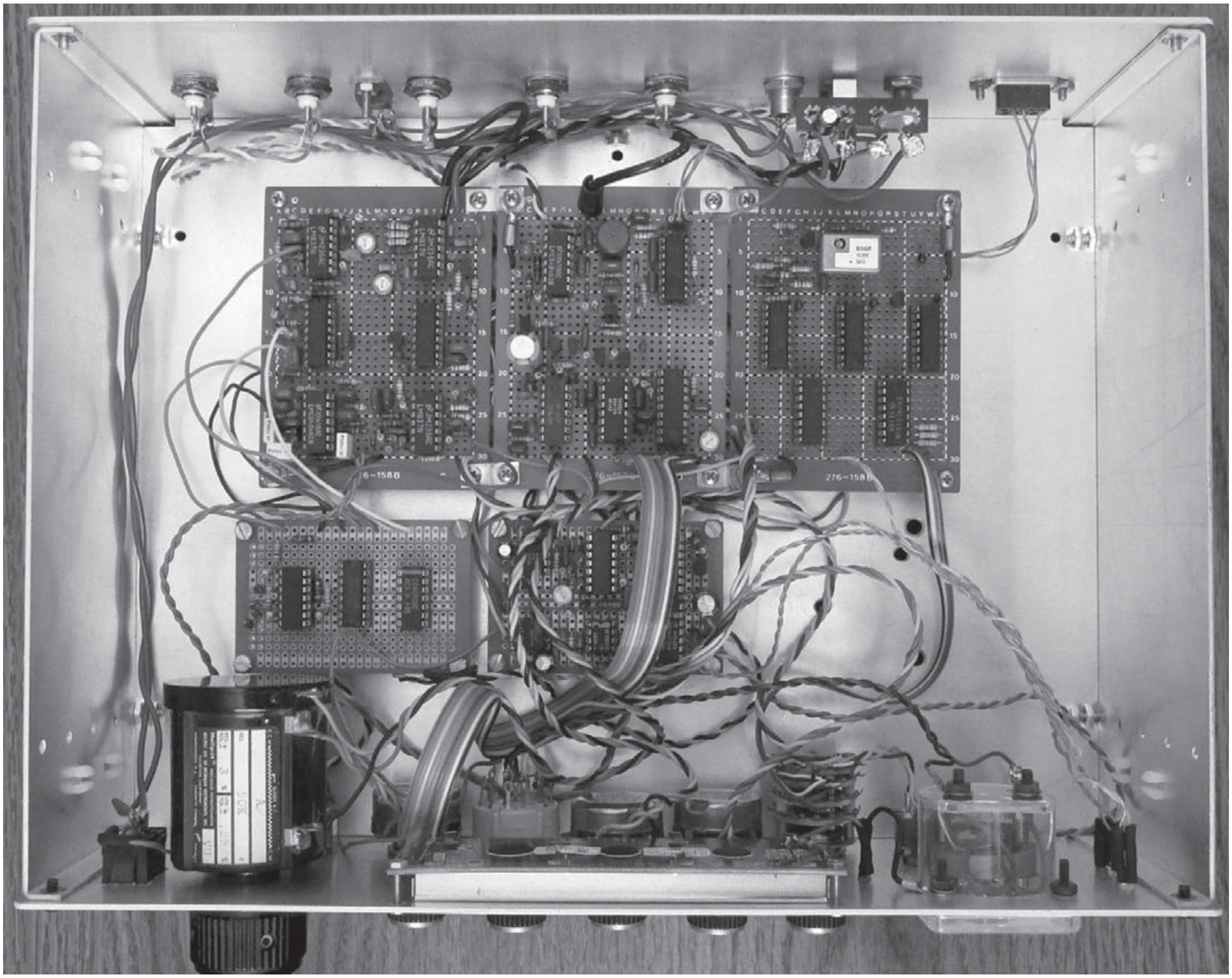

Figure 19 — The frequency standard was designed using a modular approach that employed separate perforated circuit boards for various device functions. This approach provided a convenient way to add circuitry as the design evolved over time.

Figure 20 — Front view of the frequency standard in operation. The large knob on the upper left permits manual fine tuning of the VCTCXO, while the display provides the UTC date and time.

Placing the audio source switch (SW2) in the "Signal" position will help verify that WWVB reception is taking place. If all has gone well, placing SW1 in the "PLL Closed" position should allow the VCTCXO to slowly move into phase alignment with the WWVB carrier. Minor adjustments of the VCTCXO can be made at this point to bring the LCD tuning indicator reading to as close to 000 as possible.

After several minutes of reception have transpired, the LCD sequence illustrated in Figure 17 will begin to take place. If high local noise levels impair reception of the WWVB time code, the antenna may need to be reoriented to place the noise source in one of the two antenna pattern nulls. Placing the Meter Function Switch in the "Noise Level" position will permit the relative ambient noise level to be displayed on the meter. Placing the Audio Source Switch in the "Noise" position will allow the noise level to be monitored through aural means without having to keep an eye on the meter for visual cues.

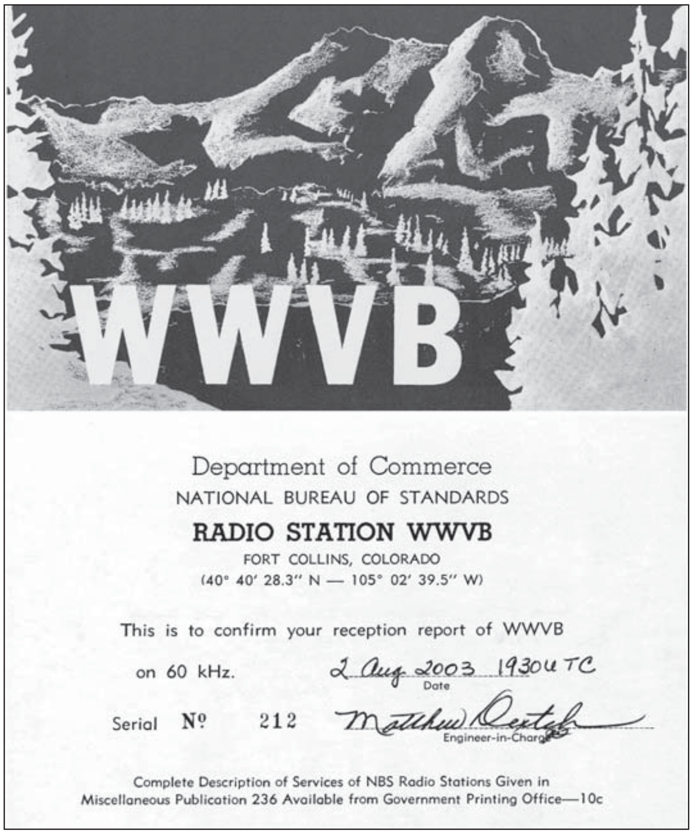

Figure 21 — The ability to receive and successfully identify distant radio signals remains a source of pride for many radio enthusiasts. While formal confirmation of GPS satellite reception may be not be possible, radio station WWVB offers QSL cards to validate reception reports.

Summary

While some may question the merit of employing WWVB as a frequency reference at a time when GPS-disciplined frequency standards are so ubiquitous, similar questions could be raised about the relevance of the Amateur Radio Service in a world dominated by cellphones and the Internet. The frequency standard described here employs a "purely RF" approach toward disciplining a local oscillator against an extremely accurate national atomic standard. It was developed not only to create a laboratory grade frequency standard, but to do so while pursuing a life-long interest and fascination with the underlying radio concepts that make such a process possible. Figure 21 shows a reception QSL that I received from WWVB in 2003.

While not a state-of-the-art device by twenty first century standards, the frequency reference described here will likely provide more than adequate performance for many modern engineering, research, and scientific purposes. For those possessing GPS-disciplined standards, this frequency standard can provide a reliable sanity check as well as a redundant backup.

The recent changes made to the WWVB broadcasts by the National Institute of Standards and Technology have been unsettling for some individuals. What these actions reveal, however, is that while the WWVB primary role is changing, it is changing because its use is growing, and this growth will help ensure there is strong support for keeping WWVB on the air for decades to come. See you in the next FMT!

John A. Magliacane, KD2BD, has held an Advanced Class license for over 31 years and a Commercial FCC Radio License since 1994. John holds Associate Degrees in Electronics Engineering Technology, Computer Science, and Mathematics/Physics, in addition to a Bachelor's Degree in Electronics Engineering Technology.

John is employed at Brookdale Community College, Lincroft, NJ where he has served as a Learning Assistant in the Department of Engineering and Technology for over 27 years, as an advisor to the Brookdale Amateur Radio Club since 1991, and as an Academic Tutor in the Computer Science Department. John has worked as a freelance technical writer for over 20 years, and authored weekly "SpaceNews" newsletters during the 1990s that gained world-wide popularity among the terrestrial packet radio networks and pacsat satellites that carried them.

John has been a Slackware Linux *user for over 20 years, and has created and contributed to a number of open-source software projects. His "*PREDICT*" satellite tracking and "*SPLAT!*" RF propagation analysis applications have not only earned strong followings in the Amateur Radio and commercial telecommunications fields, but have also been adopted for use by scientists and engineers at NASA and the European Space Agency.*

In addition to being a Frequency Measurement Test participant who employs receiving equipment and instrumentation entirely of his own design, John recently published the design of his "TriplePIC SSTV Video Scan Converter" that allows the exploration of vintage 8 second per frame monochrome slow-scan television using twenty first century electronics.

Notes

[1]Michael A. Lombardi, Glenn K. Nelson, "WWVB: A Half Century of Delivering Accurate Frequency and Time by Radio," *Journal of Research of the National Institute of Standards and Technology*, Volume 119, The National Institute of Standards and Technology, March 12, 2014.

[2]J. A. Adcock, VK3ACA, "Propagation of Long Radio Waves," *Amateur Radio*, June to September 1991.

[3]Firmware for the PIC16F88 microcontroller is licensed under the GNU General Public License and is available for download from the ARRL *QEX* files website. Go to **www.arrl.org/qexfiles** and look for the file **11x15_Magliacane.zip**.

Additional References

"NIST Radio Station WWVB," The National Institute of Standards and Technology, **www.nist.gov/pml/div688/grp40/wwvb.cfm**

"ARRL (and non-ARRL) Frequency Measuring Tests", The American Radio Relay League, **www.arrl.org/frequency-measuring-test/**

John A. Magliacane, "KD2BD FMT Methodology," **www.qsl.net/kd2bd/fmt-methodology.html**.

Dr. Ulrich L. Rohde, N1UL

990 Cape Marco Island, FL 34145: **ka2weu@aol.com**

Some Thoughts on Designing Very High Performance VHF Oscillators

Building a very high performance oscillator requires some careful engineering design work.

A *QEX* article by Colin Horrabin about part of the HF7070 receiver retriggered my interest in VHF oscillators / VCOs. (The Development of the Low Phase Noise Double Tank Oscillator, Colin Horrabin, G3SBI, *QEX* Nov/Dec 2014.)[1] He claimed that a type of push-pull oscillator would improve the phase noise roll-off from 20 dB/dec to 40 dB/dec, and he also referred to some receiver measurements made by Rob Sherwood. The data points I reviewed do not support this theory, and the reciprocal mixing tests are not conclusive, because two signal generators were used. The correct comment is that the type 2, high-order phase locked loop inherently has a 40 dB/dec roll off, not the oscillator.

The single resonator oscillator using lumped elements by itself is a good solution. The slope of the radiation resistance of a quarter wave resonator does not change if a half wave resonator will be chosen, so a push-pull oscillator is not better.

The symmetrical oscillator proposed by Horrabin just uses twice the inductance, and the two capacitors, now in series, have half their individual value. In simple terms, Horrabin changed the LC ratio, which cannot have any influence on the phase noise nor the slope. The loading from the transistor may now be different.

The best way to get the phase noise evaluation right is to use a dedicated phase noise system like the Rohde & Schwarz FSUP 26 phase noise tester, spectrum and signal analyzer that the ARRL Lab has to make their measurements. At the same time, it is useful to calculate the best possible phase noise based on physics and using a low flicker noise FET. FETs in oscillators are limited to about 500 MHz because of their cut-off frequency. For higher frequencies SiGe HBT (heterojunction bipolar transistors) are superior, and because modern communications equipment uses PLL systems with sufficiently wide bandwidth, the flicker corner frequency inside the loop bandwidth is of less concern. Outside the loop bandwidth the loaded *Q* of the resonator determines the phase noise. If Colin Horrabin's paper is correct, the roll off has to be 20 dB/decade or 40 dB/decade but not 30 dB/decade, which would be due to flicker noise. A VCO with 1 kHz loop bandwidth was quoted. I will comment on this later.

Only for oscillators using the evanescent mode and distributed elements, like (multiple) coupled lines, the configuration results in an increased operating *Q*, which for lumped circuit components is not possible. Using coupled transmission line structures (distributed components) is a better choice. At VHF, this is prohibitive because of size.

An evanescent wave is a near-field wave with an intensity that exhibits exponential decay without absorption as a function of the distance from the boundary at which the wave was formed. Evanescent waves are solutions of wave equations, and can in principle occur in any context to which a wave equation applies. They are formed at the boundary between two media with different wave motion properties, and are most intense within one third of a wavelength from the surface of formation.

As evidence of how moving from lumped to distributed techniques can improve oscillator performance at frequencies where *LC* tank circuits become problematic, Figure 1 compares the difference in phase-noise performance obtainable using a resonator consisting of an ideal 2 nH inductor and a ¼ λ transmission line (11 Ω, 90° long at 2.6 GHz, attenuation 0.1 dB/meter) with the transistor biased by constant-current and constant-voltage sources for a simulated BJT Colpitts oscillator operating at 2.3 GHz. This is a result of the magnetic coupling, which does not exist for lumped (discrete) inductors.[2] The articles described in Notes 3, 4, 5, and 6 address this topic in practical applications.[3, 4, 5, 6]

The 1 kHz loop bandwidth would be dangerous because mechanically introduced microphonics would then not be suppressed. A 10 kHz loop bandwidth is much more opportune. Better synthesized local oscillators (LOs) use multiple loops and direct digital synthesis (DDS) systems, which allow such wide loop bandwidth. Many modern receivers and transceivers apply this technique.[7, 8] Even better today, software defined radios (SDR) can have excellent phase noise performance. (See the R&S EB-500 9 kHz to 6 GHz receiver: **http://n1ul.com/eb500.htm**.)

[1]Notes appear on page 40

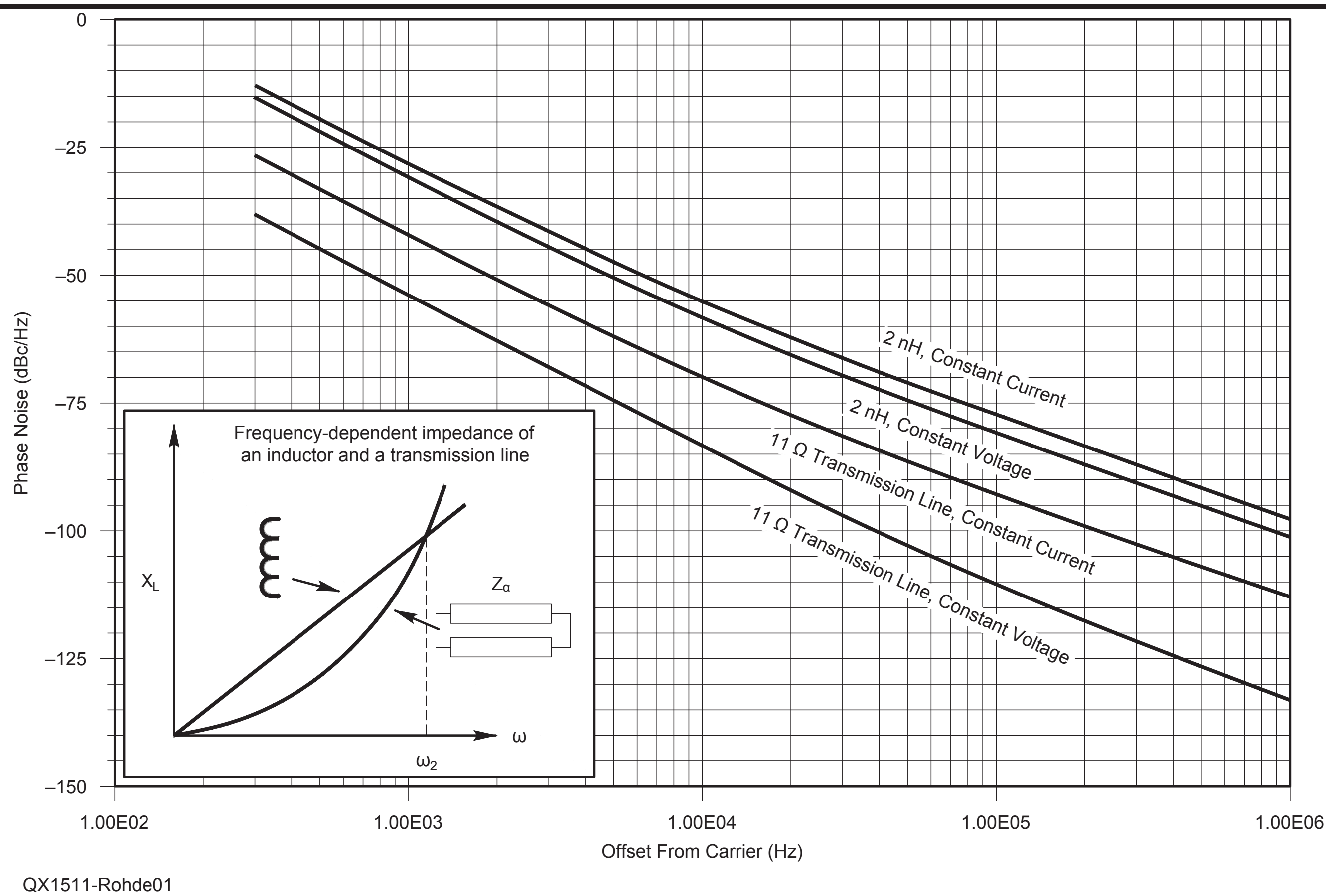

Figure 1 — This graph shows the phase-noise performance of a 2.3 GHz BJT oscillator with a resonator consisting of an inductor (2 nH) and a ¼ λ transmission line (11 Ω, approximating the behavior of a dielectric resonator) with bias from a constant-current source and a low-impedance, resistive constant-voltage source.

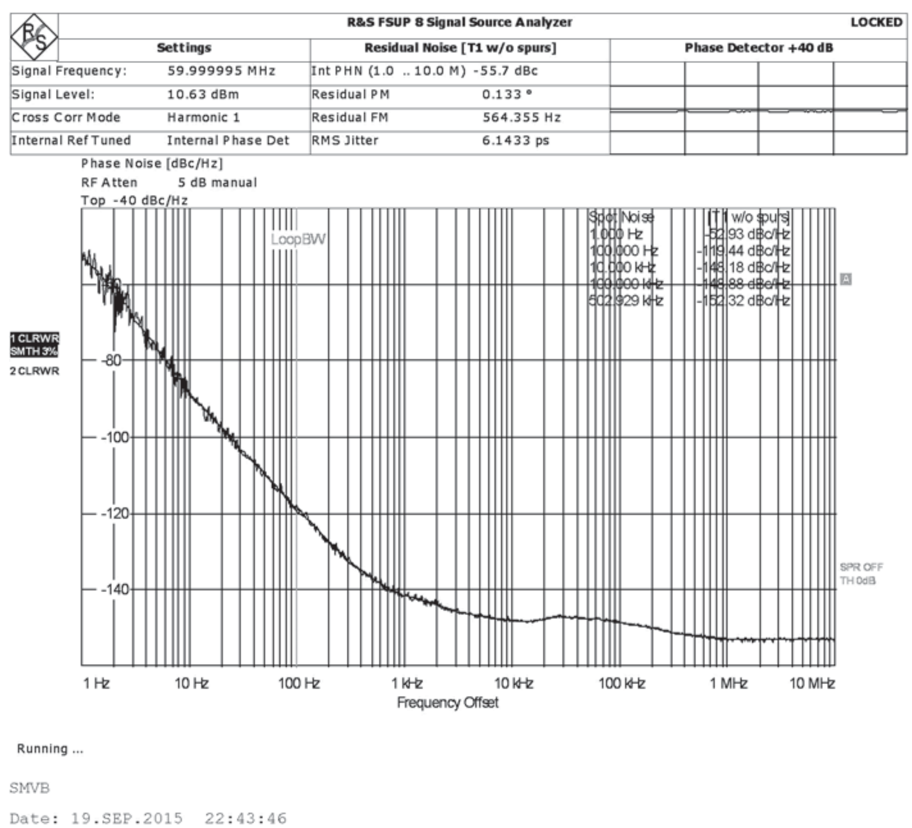

Figure 2 — This screen shot from the Rohde & Schwarz FSUP signal source analyzer shows the measured phase noise of a synthesized 60 MHz LO. The –150 dBc/Hz limit is a result of the buffer amplifier. It requires a special design to obtain better values. Even at +10 dBm output there **is a practical limit of about –175 dBc/Hz for a VCO and buffer. Some additional useful information can be found in the articles of Notes 9 and 10.**

Transceivers with a first IF between 45 to75 MHz, require such VHF oscillators. This paper will try to demystify this topic and will show the correct mathematics, proven schematics and measured data. It is partly based on *RF/Microwave Circuit Design for Wireless Applications* (see Note 2). Figure 2 shows the measured phase noise performance of a modern receiver that uses a 60 MHz LO. This measurement was made using the aforementioned R&S FSUP signal analyzer.

Some Equations

David Leeson was the first to help us understand the mechanics of phase noise, based on a low pass filter approach in 1966.[11] Dieter Scherer and others improved the model further.[9, 10, 12, 13, 14]

Phase noise is defined in terms of the noise spectral density, in units of decibels below the carrier per hertz, and is based on Equation 1 by Leeson, Scherer and Rohde.

$$£\left(f_m\right)=10\log\left[\frac{P_{sideband}\left(f_0+f_m,\ 1\ Hz\right)}{P_{carrier}}\right]=10\log\left[S_\varphi\left(f\right)\right]$$

[Eq 1]

$$£\left(f_m\right)=10\log\left\{\left[1+\frac{f_0^2}{\left(2f_mQ_L\right)^2\left(1-\frac{Q_L}{Q_0}\right)^2}\right]\left(1+\frac{f_c}{f_m}\right)\frac{FkT}{2P_0}+\frac{2kTRK_0^2}{f_m^2}\right\}$$

[Eq 1A]

where:

$£(f_m)$ is the ratio of the sideband power in a 1Hz bandwidth at f_m to total power in dB

f_m is the offset frequency from the carrier

f_0 is the carrier frequency

f_c is the flicker corner frequency

Q_L is the loaded Q of the tuned circuit

Q_0 is the unloaded Q of the tuned circuit

F is the noise factor

k is Boltzmann's constant

T is the temperature in Kelvins

P_0 is the average power at oscillator output

R is the equivalent noise resistance of the tuning diode

K_0 is the oscillator voltage gain.

When adding an isolating amplifier, the noise of an LC oscillator is determined by Equation 2.

$$£\left(f_m\right)=0.5\times10\log\left[\left(S_\varphi\left(f_m\right)\right)\right]$$

$$£\left(f_m\right)=0.5\times10\log\left\{\frac{\left[a_RF_0^4+a_E\left(\frac{F_0}{2Q_L}\right)^2\right]}{f_m^3}+\frac{\left[\left(\frac{2GFkT}{P_0}\right)\left(\frac{F_0}{2Q_L}\right)^2\right]}{f_m^2}+\left(\frac{2a_RQ_LF_0^3}{f_m^2}\right)+\frac{a_E}{f_m}+\frac{2GFkT}{P_0}\right\}$$

[Eq 2]

where,

G = compressed power gain of the loop amplifier

F = noise factor of the loop amplifier

k = Boltzmann's constant

T = temperature in kelvins

P_0 = carrier power level (in watts) at the output of the loop amplifier

F_0 = carrier frequency in Hz

f_m = carrier offset frequency in Hz

$Q_L (= \pi F_0 \tau_g)$ = loaded Q of the resonator in the feedback loop

a_R *and* a_E = flicker noise constants for the resonator and loop amplifier, respectively.

The problem with this design equation, which everyone likes to quote, is that it works after the fact. That means the designer does not know the output power, the flicker corner frequency, and the large signal noise figure, and finally, because the right part of the equation is the noise from the tuning diode, the value of the equivalent noise resistor, *R*!

Influence of the Tuning Diode

It is possible to define an equivalent noise resistor, R_{aeq}, which when inserted into Nyquist's equation, determines an open-circuit noise voltage across the tuning diode.

$$V_n=\sqrt{4kT_0R\Delta f}$$

[Eq 3]

where:

$kT_o = 4.2 \times 10^{-21}$ at about 300 K

R is the equivalent noise resistor

Δf is the bandwidth.

Practical values of R_{aeq} for carefully selected tuning diodes are in the vicinity of 200 Ω to 50 kΩ. We can now determine the noise voltage, V_n.

$$V_n=\sqrt{4\times4.2\times10^{-21}\times10{,}000}=1.296\times10^{-8}V\sqrt{Hz}$$

This noise voltage generated from the tuning diode is now multiplied with the VCO gain, K_o, resulting in the RMS frequency deviation.

$$\left(\Delta f_{rms}\right)=K_0\times\left(1.296\times10^{-8}V\right)\text{in 1 Hz bandwidth}$$

[Eq 4]

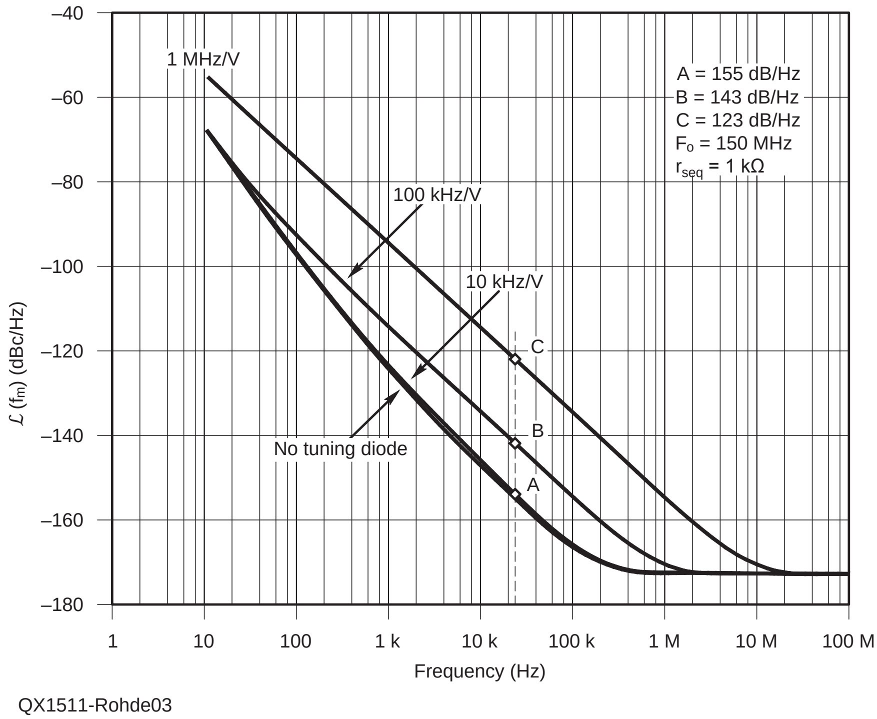

Figure 3 — This graph shows the influence of the diode noise of a VCO at 150 MHz.

To translate this into an equivalent peak phase deviation, we will use Equation 5.

$$\theta_d = \frac{K_0\sqrt{2}}{f_m}\times\left(1.296\times10^{-8}\right)\text{rad in 1 Hz bandwidth} \quad \text{[Eq 5]}$$

Or, for a typical oscillator gain of 100 kHz / V:

$$\theta_d = \frac{0.00183}{f_m}\text{rad in 1 Hz bandwidth} \quad \text{[Eq 6]}$$

For f_m = 2.4 kHz (typical spacing for adjacent-channel measurements for good SSB RF radios), then $\theta_c = 732 \times 10^{-9}$. This can be converted now into the SSB signal-to-noise ratio:

$$£\left(f_m\right) = 20\log_{10}\frac{\theta_c}{2} = -128 \text{ dBc / Hz} \quad \text{[Eq 7]}$$

The tuning diode adds significant noise, so if the above mentioned 1 kHz bandwidth for the PLL is used, at 2.4 kHz, the oscillator dominates.

Figure 3 shows the influence of the diode noise of a VCO at 150 MHz. In the case of lines B and C on the graph, you can see that the tuning diode greatly ruins the overall phase noise regardless of a high loaded *Q*!

The flicker frequency component also has a huge influence on the phase noise. Figure 4 shows the noise contribution of the flicker noise in a circuit with fixed *Q*. At 1 kHz offset, the phase noise deteriorates by 10 dB.

We can calculate the phase noise from circuit parameters, and using large singal parameters, or deriving these with the help from Bessel funtions, we specifically obtain Y21 for a large signal.

The total effect of all the four noise sources can be expressed as Equation 8.

$$£\left(\omega\right) = 10\log\frac{4KT}{\omega L\times Q}\left\{\frac{1}{2}\left[\frac{1}{2\omega_0 C_{eff}}\right]\left[\frac{\omega_0}{\omega}\right]\right\}^2_{\text{Resonator}}$$

$$+4KTr_b\left\{\frac{1}{2}\left[\frac{C_1+C_2}{C_2}\right]\left[\frac{1}{2Q}\right]\left[\frac{\omega_0}{\omega}\right]\right\}^2_{\text{Base Resistance}}$$

$$+\left[2qI_b+\frac{2\pi K_f I_b^{AF}}{\omega}\right]$$

$$\left\{\frac{1}{2}\left[\frac{C_2}{C_1+C_2}\right]\left[\frac{1}{2Q\omega_0 C_{eff}}\right]\left[\frac{\omega_0}{\omega}\right]\right\}^2_{\text{Flicker Base Current}}$$

$$+2qI_c\left\{\frac{1}{2}\left[\frac{C_1}{C_1+C_2}\right]\left[\frac{1}{2\omega_0 Q C_{eff}}\right]\left[\frac{\omega_0}{\omega}\right]\right\}^2_{\text{Collector Current}}$$

[Eq 8]

We will use the example from the 2 Part *Microwave & RF* article, "Large-Signal Approach Yields Low-Noise VHF/UHF Oscillators."[15,]

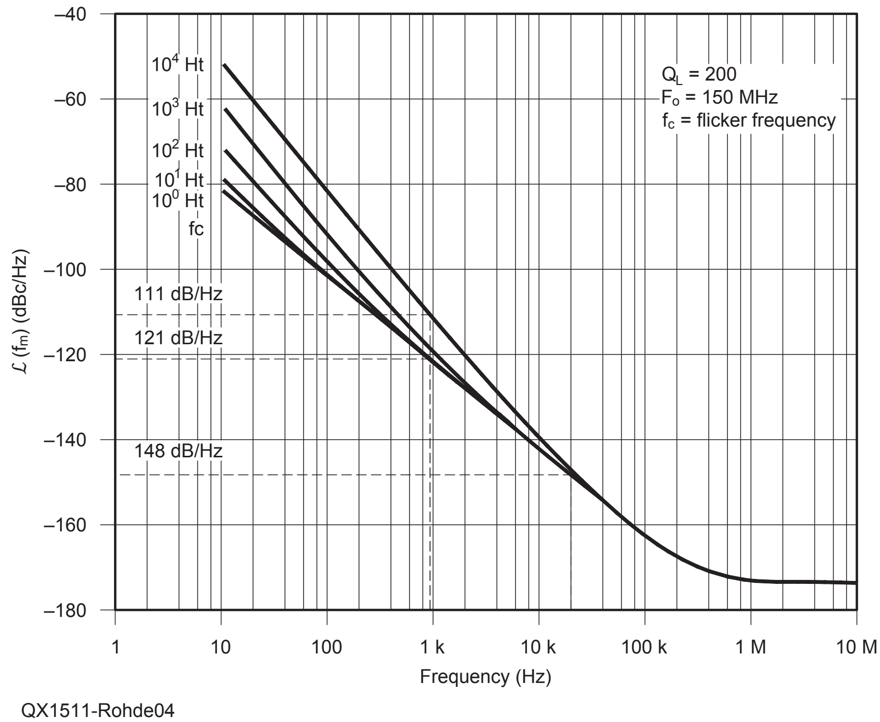

Figure 4 — Here is the phase noise contribution of the flicker noise to the oscillator noise.

[16] The schematic for this circuit is shown at Figure 5, and the measured phase noise of this 144 MHz oscillator is shown in Figure 6.

From the resonator, $R_P = 7056\ \Omega$ ($\omega L \times Q$)

Q of the resonator = 200 (Q of the inductor at 144 MHz)

Resonator inductance = 39 nH

Resonator capacitance = 22 pF

Collector current of the transistor, $I_c = 10$ mA

Base current of the transistor, $I_b = 85\ \mu$A

Flicker noise exponent, $AF = 2$

Flicker noise constant, $K_f = 1 \times 10^{-12}$

Feedback factor, $n = 5$

Phase noise at 10 kHz:

$$PN_{(ibn+ifn)_i}\left(\omega_0 + 10\text{ kHz}\right) \approx -134.2\text{ dBc / Hz}$$

$$PN_{Vbn}\left(\omega_0 + 10\text{ kHz}\right) \approx -151\text{ dBc / Hz}$$

$$PN_{nr}\left(\omega_0 + 10\text{ kHz}\right) \approx -169.6\text{ dBc / Hz}$$

$$PN_{icn}\left(\omega_0 + 10\text{ kHz}\right) \approx -150.6\text{ dBc / Hz}$$

$$P_{out} = 5\text{ dBm}$$

The value for $K_f = 1 \times 10^{-12}$ is vaild for small currents, and in Equation 8 the main phase noise (measured) contribution is the resonator loss. For higher frequencies and higher output power (higher DC current, the flicker and DC current contribuion to the flicker noise will dominate. At 30 mA and higher, a typcal K_f factor of 1×10^{-7} is common.

Going back to the large signal phase noise analysis , the Equation 9 is really the most modern result.

$$\pounds\left(\omega\right) = 10\log\left\{\left[k_o + \left(\frac{k^3 k_1 \left[\frac{Y_{21}^+}{Y_{11}^+}\right]^2 \left[y\right]^{2p}}{\left[Y_{21}^+\right]^3 \left[y\right]^{3q}}\right)\left(\frac{1}{\left(y^2+k\right)}\right)\right]\left[\frac{\left(1+y\right)^2}{y^2}\right]\right\}$$

[Eq 9]

where:

$$k_0 = \frac{kTR}{\omega^2 \omega_0^2 L^2 C_2^2 V_{cc}^2}$$

$$k_1 = \frac{qI_c g_m^2 + \frac{K_f I_b^{AF}}{4\omega} g_m^2}{\omega^2 \omega_0^4 L^2 V_{cc}^2}$$

$$k_2 = \omega_0^4 \left(\beta^+\right)^2$$

$$k_3 = \omega_0^2 g_m^2$$

$$k = \frac{k_3}{k_2^2 C_2^2}$$

where k_1, k_2, and k_3, are constant only for a particular drive level, with $y = C_1 / C_2$, making k_2 and k_3 also dependent on y, as the drive level changes.

This Equation is derived in *Communications Receivers* (see Note 8).

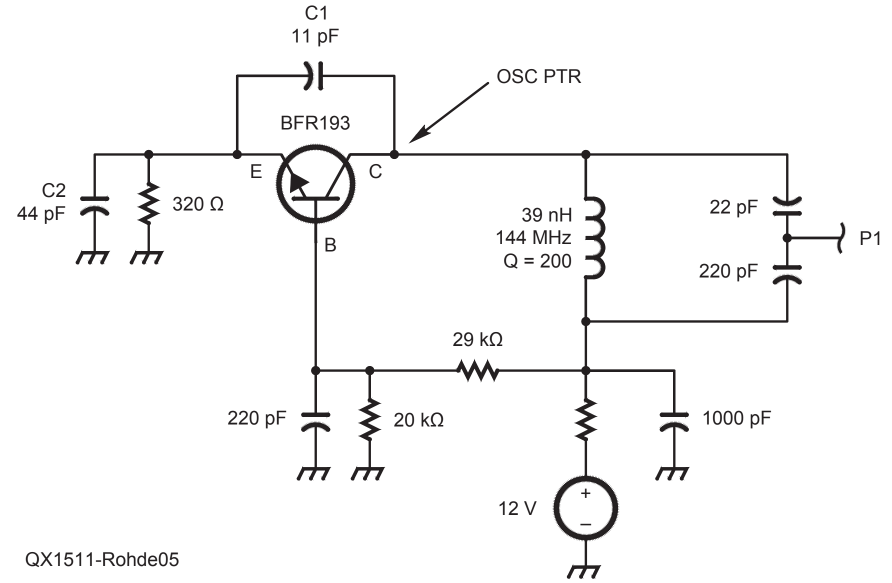

Figure 5 — This schematic shows a 144 MHz oscillator design at 60 MHz. This design is from "Large Signal Approach Yields Low-Noise VHF/UHF Oscillators," published in *Microwaves & RF*. See Notes 15 and 16.

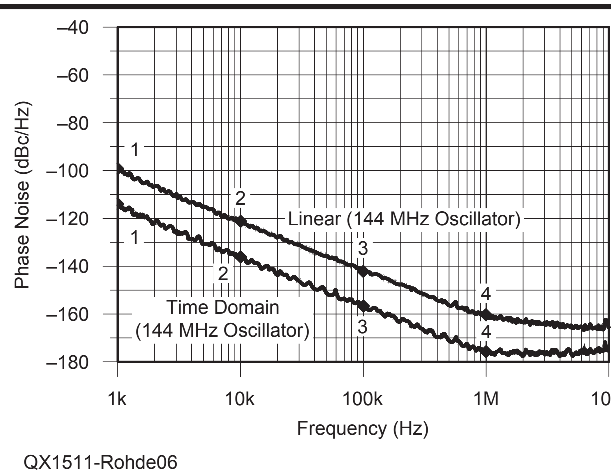

Figure 6 — This is the meassured phase noise of the 144 MHz Oscillator design of Figure 5, based on state of the art linear design, and based on an optimized design using large signal parameters. See Notes 15 and 16.

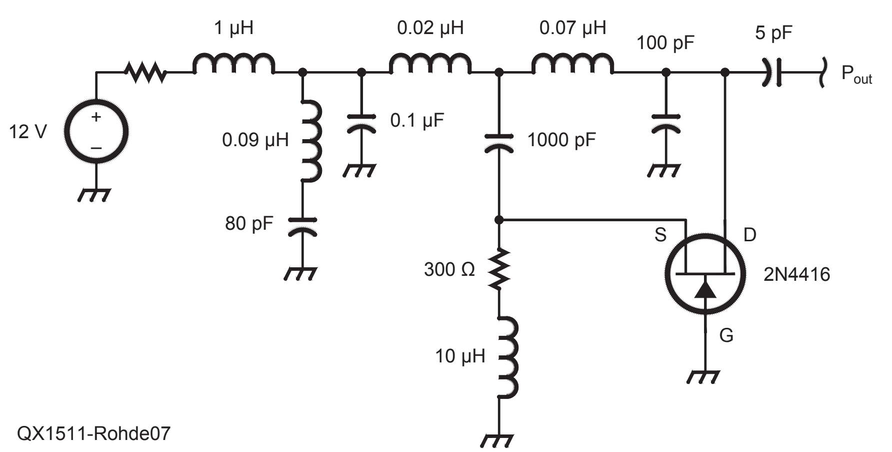

Figure 7 — This circuit is a possible simulation of the 60 MHz oscillator described by Colin Horrabin.

Another phase noise calculation approach is noted by Hajiimiri in "A General Theory of Phase Noise in Electrical Oscillators."[17] It is quoted by academicians frequently because it is an elegant way, but for actual design activities it is useless. It is mentioned here for completeness. Also see *The Design of Modern Microwave Oscillators for Wireless Applications: Theory and Optimization*.[18]

The Circuits

In order to verify the noise quoted by Colin Horrabin, an FET circuit with 2 tuned LC circuits was prepared for simulation using the familiar 2N4416 JFET. Its data was obtained from the non-linear data provided by Philips for CAD applications, such as *SPICE* or *Harmonic Balance* based simulators.[19]

The power supply voltage is applied via a 1 μH RF choke, and in order to validate the claim, the 0.1 μF capacitor in the analysis could be toggled between this value and 0.1 fF = 0.1×10^{-15} F, in practice a value of zero. The result showed no difference in phase noise. There was a discussion about why the simulator did not agree with the expectations, but the phase noise values published by Colin Horrabin did not support the claim either. This topic was addressed in the beginning of this paper. Interestingly enough, if the circuit is made asymmetrical (see the 80 pF and 100 pF capacitors in Figure 7), and the tap is not grounded, a better phase noise results.

The simulation data agree fairly well with the published data, and no correction for the noise of the tuning diode was made. Figure 8 shows the predicted phase noise of the Figure 7 oscillator.

It is now of interest to design a better VCO. This has been achieved with the design shown in Figure 9. The noise improvement comes from the constant current source (5.6 kΩ) in the source; the higher voltage drop is compensated by the positive voltage at the transistor gate.

Figure 10 shows a circuit diagram of an ultra low noise 60 MHz FET oscillator design that uses a 2N4416 FET. The circuit uses a helical resonator, as shown in Figure 11. The original cicuit was modified and is using six aditional diodes for a wider tuning range, and the parallel combination of the diodes, because of no noise correlation, results overall in a lower noise contribution. Figure 12 shows the phase noise simulation for this oscillator circuit, and Figure 13 shows the measured result from the actual circuit.

The diodes make the VCO noisier below 100 khz, but because the loop bandwidth typically is wider, this compensates the noise. If we look at Equation 8, we will find that the major noise contribution is the loaded *Q* of the resonator. If by some magic the loading of the transistor drain impedance could be reduced, the noise would be less. Here, flicker noise is not the dominant cause!

Summary

The design of low noise oscillators is no longer such a mystical task. When I finally got my own R&S FSUP 8 with optimized internal signal sources, I went through the task of measuring my oscillators built 40 years ago, as well as some commercial devices. A good example was the older HP 8640B, and the famous HP 10544A 10 MHz crystal oscillators.

HP products typically were better than promised, something I could not claim for all of my designs, but I was not that far off — and yes some were better than published.

Sadly I found that many VHF crystal oscillators around in the past did not perform as well as we know today, and the same applies to signal generators.

This paper also lists a large number of references and I recommend *RF/Microwave Circuit Design for Wireless Applications* (see Note 2), *Microwave and Wireless Synthesizers: Theory and Design* (see Note 7), and *The Design of Modern Microwave Oscillators for Wireless Applications* (see Note 17) for text books for any readers interested in learning more about synthesizers and oscillators.

Microwave and Wireless Synthesizers: Theory and Design gives a detailed insight into PLL design, but companies now sell

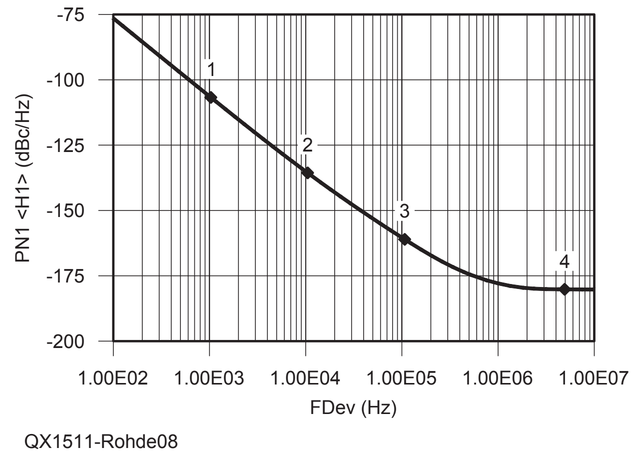

Figure 8 — This graph is the predicted phase noise of the Colin Horrabin oscillator, based on the simulation of Figure 7.

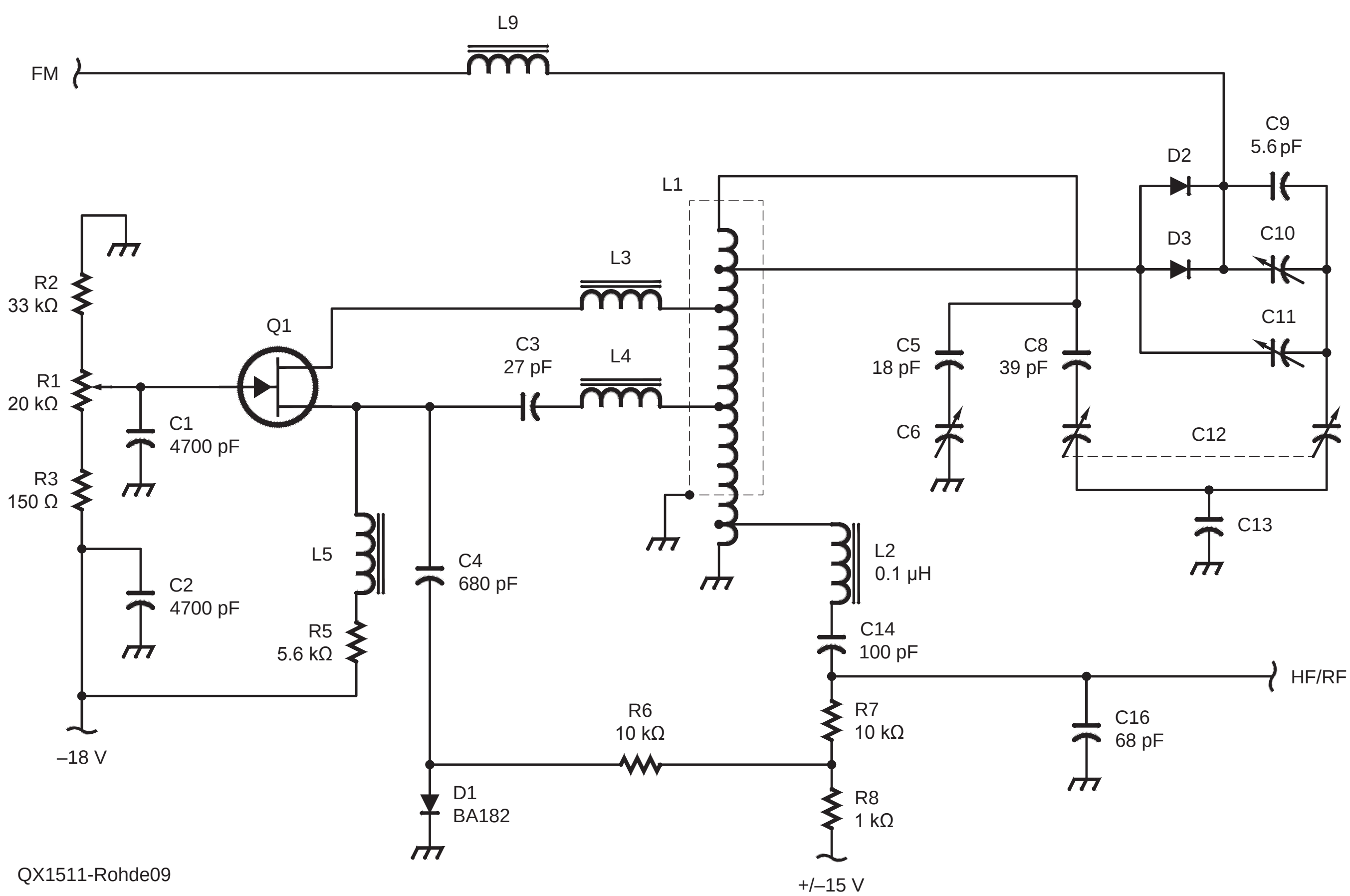

Figure 9 — This schematic diagram shows a 60 MHz VCO optimized for phase noise. It uses the 2N4416 FET and a ±15 V source, which switches the oscillator on and off. L1 is a helical resonator. R&S 1975 Model SMDU radio tester.

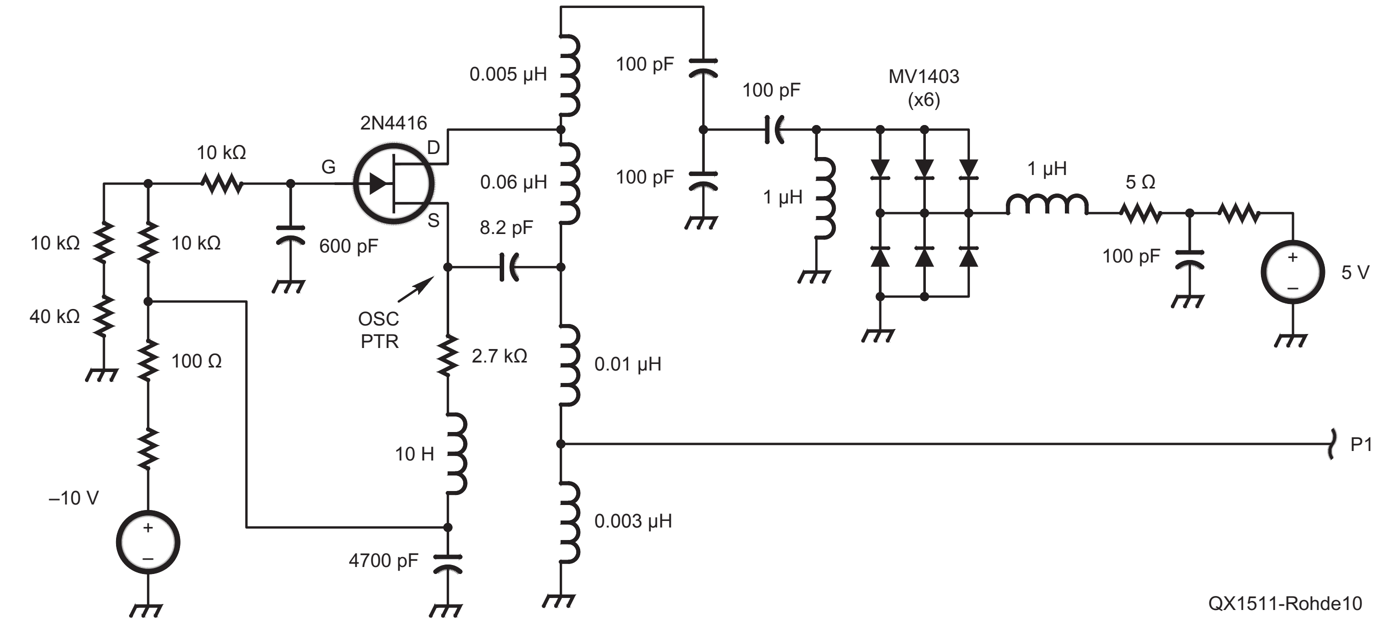

Figure 10 — Here is a typical circuit diagram of the 144 MHz low noise VCO using a 2N4416 FET. Note the six diodes for a wider tuning range of the oscillator. [R&S SMDU]

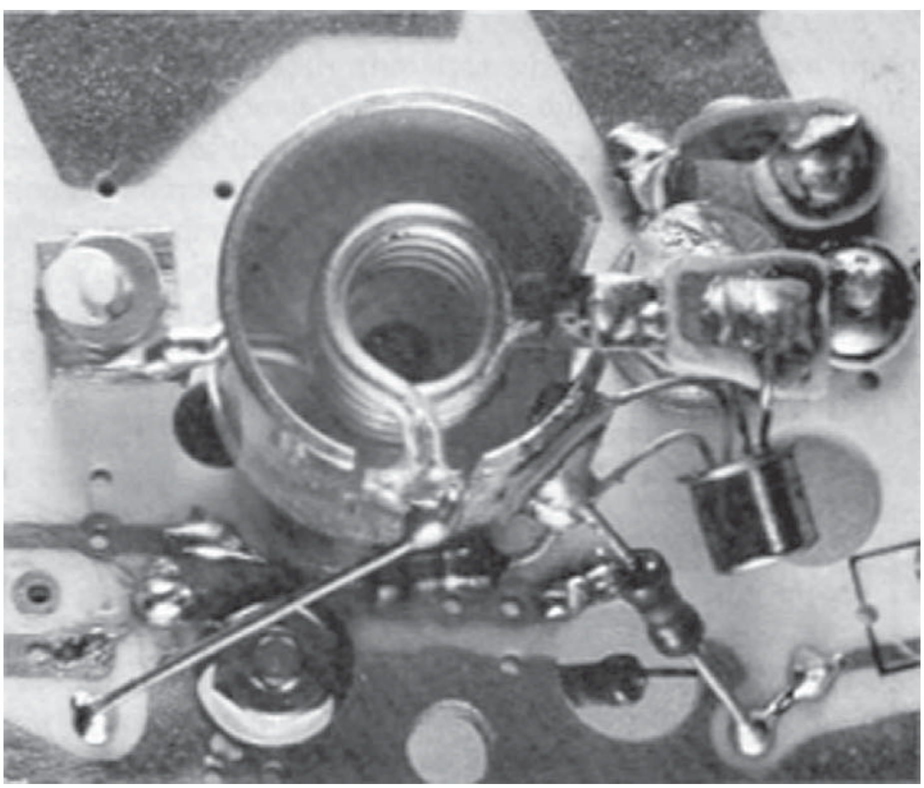

Figure 11 — This photo shows the helical resonator as part of the actual implementation of the oscilltor of Figure 9. Now the phase noise will be interesting. In practice, such an oscillator will have a buffer stage. The buffer stage will make the far off noise worse, so the result will be limited to about –165 dBc/Hz. This oscillator has an output level of 10 dBm (10 mW). The theoretical noise limit is 177 dB + 10 dB ≧ 187 dBc/Hz. The difference is due to the large signal noise figure of the transistor. [R&S SMDU]

complete PLL chips, so the individual designs disappear. Also the crystal chapter written by Roger Clark, then from Vectron, gives very valuable insight into this topic.

RF/Microwave Circuit Design for Wireless Applications, second edition, is a complete desk reference book, which also covers CMOS designs, and spends many pages on oscillators and CAD use.

The Design of Modern Microwave Oscillators for Wireless Applications addresses the very latest of wideband VCO design and push-push oscillators, and provides all the interesting phase noise calculations and design rules.

Based on the mathematics and design rules shown above, and good test equipment to validate the data, the design has become much easier.

As to the Horrabin oscillator, in one of his e-mails he mentioned a *Q* of 70 and the simulation supports that.

The improved oscillator above (no PLL!) at 3 kHz has a phase noise of –135 dBc/Hz while the Horrabin PLL design sits at –120 dBc/Hz. At higher frequencies the measured data published by Colin Horrabin supports a well-designed PLL based oscillator, but *not* any advantage of a symmetrical design. The practical designs above for a 144 MHz bipolar transistor based oscillator and this VCO gives some insight in good designs, both from a mathematical point and from a practical point.

Ulrich L. Rohde, N1UL, studied electrical engineering and radio communications at the Universities of Munich and Darmstadt, Germany. He holds a PhD in electrical engineering (1978) and a ScD (Honorary, 1979) in radio communications, a Dr-Ing (2004), University of Berlin, Germany in oscillator circuits and several honorary doctorates. In 2011 he earned a Dr-Ing Habil. Degree from the University of Cottbus, Germany.

He is President of Communications Consulting Corporation; Chairman of Synergy Microwave Corporation, Paterson, New Jersey; and a partner of Rohde & Schwartz, Munich, Germany. Previously he was President of Compact Software, Inc, Paterson, New Jersey; and Business Area Director for Radio Systems of RCA, Government Systems Division, Camden, New Jersey. He is a Professor of RF Microwave Circuit Design at Cottbus and has held Visiting Professorships at several universities in the United States and Europe.

Dr Rohde holds 25 patents and has published more than 200 scientific papers and has written or contributed to many books.

Dr Rohde is an ARRL Life Member, and is a Fellow of the IEEE, with positions on many IEEE Committees and Societies. In addition to his US call sign, he has held German call signs (DJ2LR/DL1R) since 1956 as well as Swiss call sign HB9AWE.

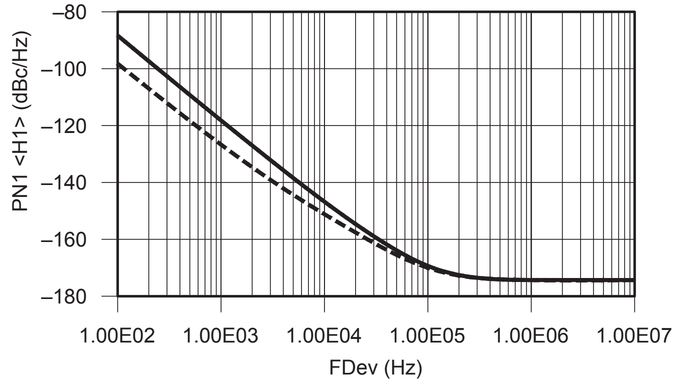

QX1511-Rohde12

Figure 12 — Here is the phase noise simulation of the 60 MHz oscillator, using a helical resonator and tuning diodes.

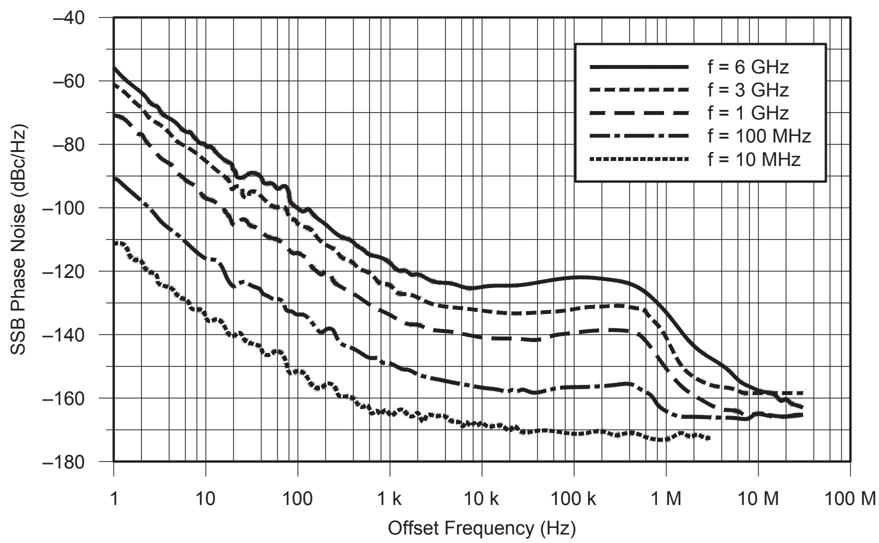

QX1511-Rohde13

Figure 13 — Here is the measured phase noise of the oscillator of Figure 10, imbedded in a PLL system and multiplied up. For 60 MHz, the result would be between the lowest and second measured curve.

Notes

1 Colin Horrabin, G3SBI, “The Development of the Low Phase Noise Double Tank Oscillator,” Nov/Dec 2014 *QEX*, pp 35 – 43.

2 Ulrich L. Rohde, N1UL, and Matthias Rudolph, *RF/Microwave Circuit Design for Wireless Applications*, Second Edition, John Wiley & Sons, 2013, ISBN 978-0-4-470-90181.

3 Ulrich L. Rohde, N1UL, Juergen Schoepf, and Ajay K. Poddar, “Low-Noise VCOs Conquer Wide Bands”, *Microwaves & RF*, pp. 98-106, June 2004.

4 Ulrich L. Rohde, N1UL, and Ajay K. Poddar, “Noise Analysis of Systems of Coupled Oscillators,” Integrated Nonlinear Microwave and Millimeter wave Circuits (INMMIC) workshop, Monte Porzo, Cantone, Italy, November 15-16, 2004.

5 Ulrich L. Rohde, N1UL, and Ajay K. Poddar, “Ultra Low Noise Low Cost Multi Octave Band VCO,” 2005 IEEE Sarnoff Symposium on Advances in Wired and Wireless Communication, 18–19 April 2005, Princeton, USA, pp 05 – 08.

6 Ulrich L. Rohde, N1UL, and Ajay K. Poddar, “Novel Multi-Coupled Line Resonators Replace Traditional Ceramic Resonators in Oscillators/VCOs,” 2006 IEEE International Frequency Control Symposium and Exposition, 5-7 June 2006, Florida, USA, pp 432 – 442.

7 Ulrich L. Rohde, N1UL, *Microwave and Wireless Synthesizers: Theory and Design*, New York: John Wiley & Sons, 1997, ISBN 0-471-52019-5.

8 Ulrich L. Rohde, N1UL, and Jerry Whitaker, *Communications Receivers*, Third Edition, McGraw Hill, New York, NY, January 2001,ISBN 0-07-13621-9.

9 Ulrich L. Rohde, KA2WEU, “All About Phase Noise in Oscillators,” Part 1, Dec 1993 *QEX*, pp 3 – 6, Part 2, Jan 1994, pp 9 – 16, Part 3, Feb 1994, pp 15 – 24.

10 Ulrich L. Rohde, KA2WEU, “Designing Low-Phase-Noise Oscillators,” Oct 1004 *QEX*, pp 3 – 12. This article is available on the ARRL website at: **www.arrl.org/files/file/Technology/ard/rohde94.pdf**.

11 David B. Leeson, W6NL, “A Simple Model of Feedback Oscillator Noise Spectrum,” *Proceedings of the IEEE*, 1966, pp 329 – 330.

12 W. Anzill, F. X. Kärtner, and P. Russer, “Simulation of the Single-Sideband Phase Noise of Oscillators,” Second International Workshop of Integrated Nonlinear Microwave and Millimeterwave Circuits, 1992.

13 Dieter Scherer, “Design Principles and Test Methods for Low Phase Noise RF and Microwave Sources,” RF & Microwave Measurement Symposium and Exhibition, Hewlett-Packard. This paper is available on line at: **www.am1.us/wp-content/Protected_Papers/U11604_Low_Noise_Sources-Scherer.pdf**.

14 Enrico Rubiola, *Phase noise and Frequency Stability in Oscillators*, 2009, Cambridge University Press, ISBN 978-0521-15328-7.

15 Ulrich L. Rohde, N1UL, and Ajay K. Poddar, “Large-Signal Approach Yields Low-Noise VHF/UHF Oscillators,” *Microwaves & RF*, Part 1, April 2008, pp 62 – 76.

16 Ulrich L. Rohde, N1UL, and Ajay K. Poddar, “Large-Signal Approach Yields Low-Noise VHF/UHF Oscillators,” *Microwaves & RF*, Part 2, May 2008, pp 84 – 96.

17 Ali Hajimiri and Thomas H. Lee, A General Theory of Phase Noise in Electrical Oscillators, IEEE Journal of Solid-State Circuits, Feb 1998, pp 179 – 194. This article is available on line at: **http://authors.library.caltech.edu/4917/1/HAJieeejssc98.pdf**.

18 Ulrich L. Rohde, N1UL, Ajay K. Poddar, Georg Böck, *The Design of Modern Microwave Oscillators for Wireless Applications: Theory and Optimization*, John Wiley & Sons, 2005, ISBN: 978-0-471-72342-4.

19 Harmonic Balance Simulator, Model - Serenade, by Ansys Corp., based on V. Rizzoli, F. Mastri, and D. Masotti, “General-Purpose Noise Analysis of forced Nonlinear Microwave Circuits,” Military Microwave, 1992.

In the Next Issue of *QEX*

As we look ahead to 2016, there are some exciting articles in the queue for *QEX*. For the Jan/Feb 2016 issue, you can look forward to Crystal Parameter Measurements Simplified by Chuck Adams, K7QO. In this article, Chuck describes a procedure and test fixture that he developed to measure and calculate various crystal parameters necessary to design and build crystal filters.

David Hershberger, W9GR, has continued his work with “Controlled Envelope Single Sideband,” as described in the Nov/Dec 2014 issue of *QEX*. At that time, David told us that CESSB was best implemented in the radio SSB modulator rather than with an external processor box. Now David is ready to show us how we might be able to generate the audio waveforms in an external processor and then inject them into the SSB modulator. Learn about this exciting development in David’s Jan/Feb 2016 *QEX* article!

UNITED STATES POSTAL SERVICE ®

Statement of Ownership, Management, and Circulation (All Periodicals Publications Except Requester Publications)

1. Publication Title	2. Publication Number	3. Filing Date
QEX	0 8 8 6 – 8 0 9 3	October 1, 2015
4. Issue Frequency	5. Number of Issues Published Annually	6. Annual Subscription Price
Bi-Monthly: Jan/Mar/May/July/Sept/Nov	6	$24.00

7. Complete Mailing Address of Known Office of Publication (Not printer) (Street, city, county, state, and ZIP+4®)
225 Main Street, Newington, Hartford County, CT 06111-1494

Contact Person: Yvette Vinci
Telephone (Include area code): 860.594.0257

8. Complete Mailing Address of Headquarters or General Business Office of Publisher (Not printer)
225 Main Street, Newington, CT 06111-1494

9. Full Names and Complete Mailing Addresses of Publisher, Editor, and Managing Editor (Do not leave blank)

Publisher (Name and complete mailing address)
Harold Kramer, 225 Main Street, Newington, CT 06111-1494

Editor (Name and complete mailing address)
Larry Wolfgang, 225 Main Street, Newington, CT 06111-1494

Managing Editor (Name and complete mailing address)
Larry Wolfgang, 225 Main Street, Newington, CT 06111-1494

10. Owner (Do not leave blank. If the publication is owned by a corporation, give the name and address of the corporation immediately followed by the names and addresses of all stockholders owning or holding 1 percent or more of the total amount of stock. If not owned by a corporation, give the names and addresses of the individual owners. If owned by a partnership or other unincorporated firm, give its name and address as well as those of each individual owner. If the publication is published by a nonprofit organization, give its name and address.)

Full Name	Complete Mailing Address
American Radio Relay League, Inc	225 Main Street, Newington, CT 06111-1494

11. Known Bondholders, Mortgagees, and Other Security Holders Owning or Holding 1 Percent or More of Total Amount of Bonds, Mortgages, or Other Securities. If none, check box → ☒ None

Full Name	Complete Mailing Address

12. Tax Status (For completion by nonprofit organizations authorized to mail at nonprofit rates) (Check one)
The purpose, function, and nonprofit status of this organization and the exempt status for federal income tax purposes:
☒ Has Not Changed During Preceding 12 Months
☐ Has Changed During Preceding 12 Months (Publisher must submit explanation of change with this statement)

PS Form 3526, July 2014 (Page 1 of 4 (see instructions page 4)) PSN: 7530-01-000-9931 PRIVACY NOTICE: See our privacy policy on www.usps.com

13. Publication Title		14. Issue Date for Circulation Data Below	
QEX		Sept/Oct 14 July/Aug 15	Sept/Oct 2015
15. Extent and Nature of Circulation		Average No. Copies Each Issue During Preceding 12 Months	No. Copies of Single Issue Published Nearest to Filing Date
a. Total Number of Copies (Net press run)		7317	7100
b. Paid Circulation (By Mail and Outside the Mail)	(1) Mailed Outside-County Paid Subscriptions Stated on PS Form 3541 (Include paid distribution above nominal rate, advertiser's proof copies, and exchange copies)	4611	4547
	(2) Mailed In-County Paid Subscriptions Stated on PS Form 3541 (Include paid distribution above nominal rate, advertiser's proof copies, and exchange copies)	0	0
	(3) Paid Distribution Outside the Mails Including Sales Through Dealers and Carriers, Street Vendors, Counter Sales, and Other Paid Distribution Outside USPS®	1298	1278
	(4) Paid Distribution by Other Classes of Mail Through the USPS (e.g., First-Class Mail®)	512	455
c. Total Paid Distribution (Sum of 15b (1), (2), (3), and (4))		6421	6280
d. Free or Nominal Rate Distribution (By Mail and Outside the Mail)	(1) Free or Nominal Rate Outside-County Copies included on PS Form 3541	60	58
	(2) Free or Nominal Rate In-County Copies Included on PS Form 3541	0	0
	(3) Free or Nominal Rate Copies Mailed at Other Classes Through the USPS (e.g., First-Class Mail)	69	61
	(4) Free or Nominal Rate Distribution Outside the Mail (Carriers or other means)	68	58
e. Total Free or Nominal Rate Distribution (Sum of 15d (1), (2), (3) and (4))		197	177
f. Total Distribution (Sum of 15c and 15e)		6618	6457
g. Copies not Distributed (See Instructions to Publishers #4 (page #3))		699	643
h. Total (Sum of 15f and g)		7317	7100
i. Percent Paid (15c divided by 15f times 100)		97.03%	97.26

* If you are claiming electronic copies, go to line 16 on page 3. If you are not claiming electronic copies, skip to line 17 on page 3.

PS Form 3526, July 2014 (Page 2 of 4)

UNITED STATES POSTAL SERVICE®

Statement of Ownership, Management, and Circulation (All Periodicals Publications Except Requester Publications)

16. Electronic Copy Circulation	Average No. Copies Each Issue During Preceding 12 Months	No. Copies of Single Issue Published Nearest to Filing Date
a. Paid Electronic Copies		
b. Total Paid Print Copies (Line 15c) + Paid Electronic Copies (Line 16a)		
c. Total Print Distribution (Line 15f) + Paid Electronic Copies (Line 16a)		
d. Percent Paid (Both Print & Electronic Copies) (16b divided by 16c × 100)		

☐ I certify that 50% of all my distributed copies (electronic and print) are paid above a nominal price.

17. Publication of Statement of Ownership

☐ If the publication is a general publication, publication of this statement is required. Will be printed in the Nov/Dec 2015 issue of this publication.

☐ Publication not required.

18. Signature and Title of Editor, Publisher, Business Manager, or Owner

Harold Kramer Publisher

Date: October 1, 2015

I certify that all information furnished on this form is true and complete. I understand that anyone who furnishes false or misleading information on this form or who omits material or information requested on the form may be subject to criminal sanctions (including fines and imprisonment) and/or civil sanctions (including civil penalties).

PS Form 3526, July 2014 (Page 3 of 4) PRIVACY NOTICE: See our privacy policy on www.usps.com.

QEX A Forum for Communications Experimenters **Subscription Order Card**

QEX features technical articles, columns, and other items of interest to radio amateurs and communications professionals. Virtually every part of the magazine is devoted to useful information for the technically savvy.

Subscribe Today: Toll free 1-888-277-5289 • On Line www.arrl.org/QEX

Subscription Rates: 1 year (six issues)

ARRL MEMBER: for ARRL Membership rates and benefits go to www.arrl.org/join
☐ US $24.00 ☐ US via First Class $37.00 ☐ Intl. & Canada by air mail $31.00

NON MEMBER:
☐ US $36.00 ☐ US via First Class $49.00 ☐ Intl. & Canada by air mail $43.00

☐ Renewal ☐ New Subscription

Name: ______________________ Call Sign: ______________

Address: ______________________________________

City: ______________ State: ________ ZIP: __________ Country: __________

☐ Check ☐ Money Order ☐ Credit Card Monies must be in US funds and checks drawn on a US Bank

Charge to: ☐ VISA ☐ MasterCard ☐ American Express Cards ☐ Discover Novus

Account #: ______________________ Exp. Date: __________

Signature: ______________________________________

Published by:
ARRL, 225 Main St,
Newington, CT 06111-1494 USA

Contact **circulation@arrl.org** with any questions or go to www.arrl.org

Web Code: QEC

Project #350

Quicksilver Radio

Test Equipment

USB Microscope

Up to 500X magnification. Captures still images and records live video. Built in LED Lighting. A must for working on suface mount components.

Wireless Relay Switch

200′+ Range. We have single, four, and eight channel models.

GO-PWR Plus™

Portable power to go or backup in the shack. Includes Powerpoles, bright easy to read meter, and lighted switch. For U1 size (35 ah) and group 24 (80 ah) batteries.

Digital Voltmeter/ Ammeter

Two line display shows both current and voltage. Included shunt allows measurement up to 50A and 99V. Snaps into a panel to give your project a professional finish.

LCR and Impedance Meter

Newest Model. Analyzes coils, capacitors, and resistors. Indicates complex impedance and more.

Automatic Passive Component Analyzer

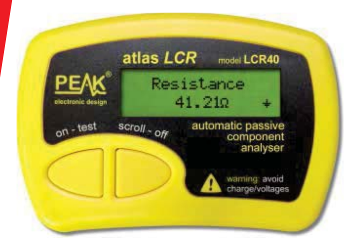

Analyzes coils, capacitors, and resistors.

Advanced Semiconductor Component Analyzer

Analyzes transistors, MOSFETs, JFETs, IGBTs, and more. Graphic display. Enhanced functionality with included PC software.

Semiconductor Component Analyzer

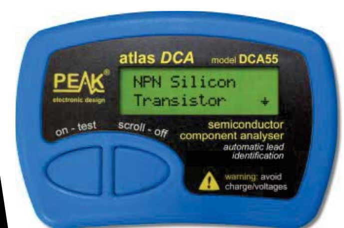

Analyzes transistors, MOSFETs, JFETs and more. Automatically determines component pinout.

Capacitance and ESR Meter

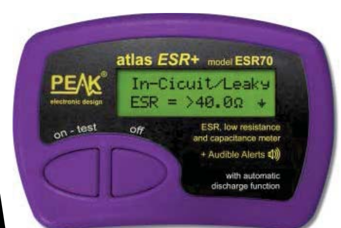

Analyzes capacitors, measures ESR.

Get All Your Ham Shack Essentials at Quicksilver Radio Products. Safe and Secure Ordering at:

www.qsradio.com